A Novel Sensor for Simultaneous Detection of Dihydroxybenzene Isomers

by

Nusrat Tazeen Tonu

A thesis submitted in partial fulfillment of the requirements for the degree of Master of Science in Chemistry

Khulna University of Engineering & Technology
Khulna 9203, Bangladesh.

August 2016

Declaration

This is to certify that the thesis work entitled "**A Novel Sensor for Simultaneous Detection of Dihydroxybenzene Isomers**" has been carried out by **Nusrat Tazeen Tonu** in the Department of Chemistry, Khulna University of Engineering & Technology, Khulna, Bangladesh. The above thesis work has not been submitted anywhere for the award of any degree or diploma.

Signature of Supervisor

Signature of Candidate

Acknowledgement

First of all I am grateful to Almighty Allah for allowing me to complete my thesis successfully.

Then I express my deepest sense and sincere appreciation to my respected supervisor, Dr. Mohammad Abu Yousuf, Professor, Department of Chemistry, Khulna University of Engineering & Technology, for his heartily co-operative and constant supervision, constructive guidance, never ending encouragement and patience which greatly inspired me during the entire period of my thesis.

I am thankful to Professor Dr. Md. Abdul Aziz, Professor Dr. Md. Abdul Motin, Department of Chemistry, Khulna University of Engineering & Technology, Dr. Md. Mizanur Rahman Badal, Associate Professor, Department of Chemistry, Khulna University of Engineering & Technology, Dr. Abu Bin Hasan Susan, Professor, Department of Chemistry, University of Dhaka and Dr. Md. Mominul Islam, Associate Professor, Department of Chemistry, University of Dhaka for their necessary advice and help for thesis correction.

I would also like to express my heartfelt thank Dr. A.B.M. Mamun Jamal, Assistant Professor, Department of Chemistry, Khulna University of Engineering & Technology, for his excellent support and advice throughout the M.Sc. research.

I also want to express my thanks to all my friends and well-wishers for their co-operation and blessings during the period of study.

Nusrat Tazeen Tonu
Department of Chemistry
KUET

Abstract

A novel, facile and low-cost electrochemical technique for the detection of dihydroxybenzene isomers (DHBIs), catechol (CC), hydroquinone (HQ) and resorcinol (RS), in aqueous system was developed. An attempt was made for the analyses of HQ, CC and RS in the same aqueous system by UV-Vis spectroscopy. UV-Vis spectrum of CC, HQ and RS exhibited absorbance maxima in PBS supported aqueous solution at 275.4, 288.6 and 273.2 nm respectively. But in the possible binary and ternary mixture of CC, HQ and RS, UV-Vis spectra showed single absorption peak instead of two and three separate peaks respectively. So, simultaneous detection of DHBIs was impossible by UV-Vis spectroscopy.

Three electrodes electrochemical system was employed which was controlled by computer supported auto potentiostat. Cyclic voltammetry (CV) and differential pulse voltammetry (DPV) were adopted as detection techniques. 2B pencil collected from the local stationary shop was used for fabricating working electrode termed as pencil graphite electrode (PGE) in the experiment. PGE electrode was characterized by Scanning Electron Microscopy (SEM) and Energy-dispersive X-ray Spectroscopy (EDX). From the SEM it was seen that surface morphology of PGE was not smooth as conventional glassy carbon electrode (GCE) instead contained huge grooves as well. It indicates that the graphite rod of the pencil was not pure crystalline. From EDX it was seen that PGE surface are impure as propped up by SEM. Results showed that it is composed of 79.39% carbon, 10.03% Si, 3.06% O_2, 3.49% Al, 2.68% Fe and trace amount of Mg and Ca. So a lot of defects and few foreign materials were present in the surface of PGE confirmed by both SEM and EDX.

PGE was first modified electrochemically by ionic liquid (IL), [1-Hexylpyridinium hexafluorophosphate (HIL) or 1-Butyl-3-Methylimidazolium hexafluorophosphate (BIL)] and then used in detection analyte by CV and DPV. Modified electrodes were termed as HIL-PGE and BIL-PGE in total working process. Modified electrodes showed excellent electroanalytical activity effect on the redox reaction of DHBIs. Total analyses and detection processes were performed in phosphate buffer solution (PBS) at pH 7.0 which was used as supporting electrolyte. The influences of scan rate and concentration on the redox behavior of HQ, CC and RS in both HIL-PGE and BIL-PGE were discussed. The anodic peak current versus the concentration of HQ, CC and RS showed a

linear relationship. The variation of peak current was also plotted with Square root of scan rate. The electrochemical processes were diffusion controlled. Variation of peak potential separation was plotted with scan rate. The anodic peak potential shift was positive, which was due to IR drop. HIL-PGE showed splendid selectivity and strong anti-interference for detection of HQ, CC and RS simultaneously in aqueous media with excellent results.

The limit of detection (LOD) was calculated by signal-to-noise ratio (S/N = 3). In simultaneous detection, the LOD for HQ, CC and RS at HIL-PGE were 6.38 μML^{-1}, 4.56 μML^{-1} and 19.6 μML^{-1} respectively and those were 9.09 μML^{-1}, 8.15 μML^{-1} and 26.78 μML^{-1} respectively at BIL-PGE. The sensitivity for HQ, CC and RS is 448.49 $\mu A/mM/cm^2$, 627.35 $\mu A/mM/cm^2$ and 146.10 $\mu A/mM/cm^2$ respectively at HIL-PGE and 525.21 $\mu A/mM/cm^2$, 585.68 $\mu A/mM/cm^2$ and 178.0 $\mu A/mM/cm^2$ respectively at BIL-PGE in simultaneous detection.

Contents

List of Tables

List of Figures

Nomenclature

Name	Description
HQ	Hydroquinone
CC	Catechol
RS	Resorcinol
PBS	Phosphate Buffer Solution
CV	Cyclic Voltammetry
DPV	Differential Pulse Voltammetry
SEM	Scanning Electron Microscopy
EDX	Energy Disperse X-ray
UV	Ultra Violet
IL	Ionic Liquid
HIL	1-Hexylpyridinium hexafluorophosphate
BIL	1-Butyl-3-methylimidazolium hexafluorophosphate
PGE	Pencil Graphite Electrode
GCE	Glassy Carbon Electrode
DHBIs	Dihydroxybenzene Isomers
GCE	Glassy Carbon Electrode

CHAPTER I

Introduction

1.1 General

Electroanalytical chemistry is the study of the separation, identification and quantification of the chemical components of natural and artificial materials. This is divided into two categories. First one, qualitative analysis that gives the indication of the identity of the chemical species in the sample and the second one, quantitative analysis that determines the amount of certain components in the substance. It is the branch of physical chemistry that studies chemical reactions which take place at the interface of an electrode, usually a solid metal or a semiconductor, and an ionic conductor, the electrolyte. These reactions involve electric charges moving between the electrodes and the electrolyte (or ionic species in a solution), the interaction between electrical energy and chemical change.

When a chemical reaction is caused by an externally supplied current, as in electrolysis, or if an electric current is produced by a spontaneous chemical reaction as in a battery, it is called an electrochemical reaction. Chemical reactions where electrons are transferred directly between molecules and/or atoms are called oxidation-reduction or (redox) reactions. In general, electrochemistry describes the overall reactions when individual redox reactions are separate but connected by an external electric circuit and an intervening electrolyte.

Electroanalytical methods are a class of techniques in analytical chemistry which study an analyte by measuring the potential (volts) and/or current (amperes) in an electrochemical cell containing the analyte. These methods can be broken down into several categories depending on which aspects of the cell are controlled and which are measured. The three main categories are potentiometry (the difference in electrode potentials is measured), coulometry (the cell's current is measured over time), and voltammetry (the cell's current is measured while actively altering the cell's potential).

Electroanalytical chemistry can play a very important role in the protection of our environment. In particular, electrochemical sensors and detectors are very attractive for on-site monitoring of priority pollutants, as well as for addressing other environmental needs. Such devices satisfy many of the requirements for on-site environmental analysis. They are inherently sensitive and selective towards electroactive species, fast and accurate, compact, portable and inexpensive. Such capabilities have already made a significant impact on decentralized clinical analysis. Yet, despite their great potential for environmental monitoring, broad applications of electrochemical sensors for pollution control are still in their infancy.

Several electrochemical devices, such as pH or oxygen electrodes, have been used routinely for years in environmental analysis. Recent advances in electrochemical sensor technology will certainly expand the scope of these devices towards a wide range of organic and inorganic contaminants and will facilitate their role in field analysis. These advances include the introduction of modified or ultramicroelectrodes, the design of highly selective chemical or biological recognition layers, of molecular devices or sensor arrays, and developments in the areas of microfabrication, computerized instrumentation and flow detectors [1-5].

1.2 Principle of Electrochemical Sensors

In electrochemical sensors, the analytical information is obtained from the electrical signal that results from the interaction of the target analyte and the recognition layer. Different electrochemical devices can be used for the task of environmental monitoring (depending on the nature of the analyte, the character of the sample matrix, and sensitivity or selectivity requirements). Most of these devices fall into two major categories (in accordance to the nature of the electrical signal): amperometric and potentiometric.

Amperometric sensors are based on the detection of electroactive species involved in the chemical or biological recognition process. The signal transduction process is accomplished by controlling the potential of the working electrode at a fixed value (relative to a reference electrode) and monitoring the current as a function of time. The applied potential serves as the driving force for the electron transfer reaction of the electroactive species. The resulting current is a direct measure of the rate of the electron

transfer reaction. It is thus reflecting the rate of the recognition event and is proportional to the concentration of the target analyte.

In potentiometric sensors, the analytical information is obtained by converting the recognition process into a potential signal, which is proportional (in a logarithmic fashion) to the concentration (activity) of species generated or consumed in the recognition event. Such devices rely on the use of ion selective electrodes for obtaining the potential signal. A permselective ion-conductive membrane (placed at the tip of the electrode) is designed to yield a potential signal that is primarily due to the target ion. Such response is measured under conditions of essentially zero current. Potentiometric sensors are very attractive for field operations because of their high selectivity, simplicity and low cost. They are, however, less sensitive and often slower than their amperometric counter parts. In the past, potentiometric devices have been more widely used, but the increasing amount of research on amperometric probes should gradually shift this balance [6-10].

1.3 Chemically Modified Electrodes for Environmental Monitoring

Chemical layers can be used for imparting a high degree of selectivity to electrochemical transducers. While conventional amperometric electrodes serve mainly for carrying the electrical current, powerful sensing devices can be designed by a deliberate modification of their surfaces. Basically, the modification of an electrode involves immobilization (on its surface) of reagents that change the electrochemical characteristics of the bare surface. Inclusion of reagents within the electrode matrix (e.g. carbon paste) is another attractive approach for modifying electrodes. Such manipulation of the molecular composition of the electrode thus allows one to tailor the response to meet specific sensing needs. While sensors based on modified electrodes are still in the early stages of their lifetime, such preparation of structured interfaces holds great promise for the task of environmental monitoring. There are different directions by which the resulting modified electrodes can benefit environmental analysis, including acceleration of electron-transfer reactions, preferential accumulation or permselective transport**.**

Electrocatalys is involves electron transfer mediation between the target analyte and the surface byan immobilized catalyst (Figure 1.1). Such catalytic action results in faster

electrode reactions at lower operating potentials. Various catalytic surfaces have thus been
successfully employed for facilitating the detection of environmentally-relevant analytes (with otherwise slow electron-transfer kinetics). These include the electrocatalytic determination of hydrazines [11] or nitrosamines [12] at electrodes coated with mixed-valent ruthenium films, monitoring of aliphatic aldehydes at palladium-modifiedcarbon paste, [13] sensing of nitrite at a glassy carbon electrode coated with an osmium-based redox polymer, [14]of nitrate at a copper modified screen printed carbon electrode, [15] monitoring of organic peroxides at cobalt-phthalocyanine containing carbon pastes, [16] and of hydrogen peroxide at a copper heptacyano nitrosyl ferrate-coated electrode [17].

Preconcentrating modified electrodes can also be useful for environmental sensing. In this case animmobilized reagent (e.g. ligand, ion-exchanger) offers preferential uptake of target analytes. This approach enjoys high sensitivity because it is a preconcentration procedure. A second major advantage lies in the addeddimension of selectivity, which is provided by the chemical requirement of the modifier-analyte interactions. Such improvements have been documented for the measurement of nickel, mercury, or aluminumions at dimethylglyoxine, [18] crown-ether, [19] or alizarin [20]containing carbon pastes, respectively, monitoring ofnitrite, chromium, or uranyl ions at ion-exchangermodified electrodes, [21-23] and of copper at analgae modified electrode [24] Covalent reactions can beused for analogous collection/determination of organicanalytes, e.g. monitoring of aromatic aldehydes atamine-containing carbon pastes [25]. Routine environmental applications of these preconcentratingelectrodes would require attention to competition for thesurface site and the regeneration of an ‘analyte-free’surface.

Another promising avenue is to cover the sensingsurface with an appropriate permselective film. Discriminative coatings based on different transport mechanisms (based on analyte size, charge, or polarity)can thus be used for addressing the limited selectivity of controlled-potential probes in complex environmental matrices. The size-exclusion sieving properties of various polymer-coated electrodes offer highly selective detection of small hydrogen peroxide or hydrazinemolecules [26-27]. In addition, surface passivation (due to adsorption of macromolecules present in natural waters) can be prevented via the protective action of these films.

More powerful sensing devices may result from the coupling of several functions (permselectivity,pre-concentration or catalysis) onto the same surface. Additional advantages can be achieved by designing arrays of independent modified electrodes, each coatedwith a different modifier and hence tuned toward aparticular group of analytes. The resulting array response offers a unique fingerprint pattern of the individual analytes, as well as multicomponent analysis(in connection with statistical, pattern-recognition procedures). Use of different permselective coatings orcatalytic surfaces thus holds great promise formultiparameter pollution monitoring. Related to this are new molecular devicesbased on the coverage of interdigitated microarrays with conducting polymers [28-29]. Eventually we expect to see molecular devices in which the individual componentsare formed by discrete molecules. Modification of miniaturized screen-printed sensor strips can also beaccomplished via the inclusion of the desired reagent(e.g. ligand, catalyst) in the ink used for the microfabricationprocess.

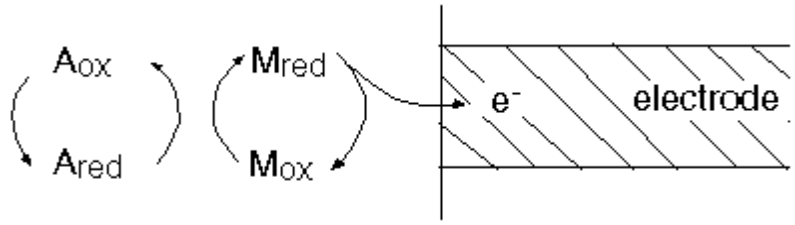

Figure 1.1: Electrocatalysis at modified electrodes; electron transfer mediated reaction between the target analyte and surface-bound catalyst.

1.4 General methods of modification of electrodes

The concept of chemically modified electrodes (CMEs) is one of the exciting developments inthe field of electroanalytical chemistry. Many different strategies have been employed for themodification of the electrode surface. The motivations behind the modifications of the electrodesurface are: (i) improved electrocatalysis, (ii) freedom from surface fouling and (iii) prevention of undesirable reactions competing kinetically with the desired electrode process [30].The simultaneous determination of isomers is an interesting subject in electroanalysis [31-35]. Theincreasing demand for it has led to the development of a rapid, simple and non-separation method for the simultaneous determination of isomers where the CMEs have emerged as an efficient and versatile approach, and have attracted considerable attention over the past decades due to its advantages interms of reduced costs, automatic and fast analysis, high sensitivity and

selectivity [36-38]. There are numerous techniques that may be used to modify electrode surfaces.Among various CMEs, polymer-modified electrodes (PMEs) are promising approach to determination of isomers. Some modification processes are-

Covalent Bonding: This method employs a linking agent (e.g. an organosilane) to covalently attach one of several monomolecular layers of the chemical modifier to the electrode surface [39].

Drop-Dry Coating (or solvent evaporation): A few drops of the polymer, modifier or catalyst solution are dropped onto the electrode surface and left to stand to allow the solvent to dry out[40].

Dry-Dip Coating: The electrode is immersed in a solution of the polymer, modifier or catalyst for a period sufficient for spontaneous film formation to occur by adsorption.The electrode is then removed from solution and the solvent is allowed to dry out [41].

Composite: The chemical modifier is simply mixed with an electrode matrix material, as in the case of an electron-transfer mediator (electrocatalyst) combined with the carbon particles (plus binder) of a carbon paste electrode. Alternatively, intercalation matrices such as certain Langmuir-Blodgett films, zeolites, clays and molecular sieves can be used to contain the modifier [42].

Spin-Coating (or Spin-Casting): also called spin casting, a droplet of a dilute solution of the polymer is applied to the surface of a rotating electrode. Excess solution is spun off the surface and the remaining thin polymer film is allowed to dry. Multiple layers are applied in the same way until the desired thickness is obtained. This procedure typically produces pinhole-free thin films for example, oxide xerogel film electrodesprepared by spin-coating a viscous gel on an indium oxide substrate[43].

Electrodeposition: In this technique the electrode is immersed in a concentrated solution(~10^{-3} $molL^{-1}$) of the polymer, modifier or catalyst followed by repetitive voltammetric scans.The first and second scans are similar, subsequent scans decrease with the peak current.For example, electrochemical deposition of poly(o-toluidine) on activated carbon fibre [44].

Electropolymerisation: A solution of monomer is oxidized or reduced to an activated form that polymerizes to form a polymer film directly on the electrode surface. This procedure results in few pinholes since polymerization would be accentuated at exposed

(pinhole) sites at the electrode surface. Unless the polymer film itself is redox active, electrode passivation occurs and further film growth is prevented.

In this technique the electrode is immersed in a polymer, modifier or catalyst solution and layers of the electropolimerized material builds on the electrode surface. Generally, the peak current increases with each voltammetric scan such that there is a noticeable difference between the first and final scans indicating the presence of the polymerized material.For example, electropolymerization of aniline on platinum electrode.

1.5 Simultaneous Detection

Simultaneous detection of isomers is an interesting subject in electroanalytical chemistry. The increasing demand for it has led to the development of a rapid, simple and non-separation method for the simultaneous detection of isomers where the chemically modified electrodes (CMEs) have emerged as an efficient and versatile approach and have attracted considerable attention over the past decades due to its advantages in terms of reduced costs, automatic and fast analysis, high sensitivity and selectivity [45-47].CC, HQ and RS are isomers of dihydoxybenzene. All of them are phenolic compounds and often coexist as isomers in environmental samples. The simultaneous detection of CC, HQ and RS is highly desirable due to their coexistence as isomers and highly toxic environmental pollutants in environmental samples [48]. The established methods for the detection of CC, HQ and RS are commonly performed after pretreatment and separation.This sample pretreatment and separation, as well as the significant operating complexity, the long times required and the large volumes of reagents consumed by established techniques, make it important to develop a new method capable of simultaneous detection without the need for prior separation of these compounds.

CC, HQ and RS (i.e., isomers of dihydroxybenzenes) are widely used for photographic chemicals, pesticides and medicines[49].CC is a significant environmental pollutant with high toxicity and it exists with HQ and RS in environmental samples[50]. CC even in low concentration in foods and cigarette smokes may cause mutagenesis and cancerous alteration [51-53]. Moreover, CC is readily absorbed from the gastrointestinal tract, causing renal tube degeneration and liver function decrease [54]. Because of its high toxicological potential, the accurate determination of CC in presence of HQ and RS is very important. Accordingly, it is crucial to develop a selective and simple method to

determine CC, HQ or RS quantitatively in presence of other isomers without prior treatment or separation [55-56].

1.6 Prospect of Modified Electrodes in Simultaneous Detection

HQ, CC and RS have a basic quinone structures that might be electrochemically oxidized at a platinum or carbon electrodes [57]. The oxidation process to quinone has been widely studied from electrochemical point of view [58-59]. But so many difficulties were existed to simultaneously determine HQ, CC and RS. The major difficulty is that the voltammetric peaks corresponding to oxidation/reduction of three phenol isomers are, in many cases, highly overlapped. Moreover, the competition of the phenolic isomers by electrode surface makes the relationship between the voltammetric response and the isomers concentrations, in the mixtures, non-linear [65].Again at bare Glassy Carbon and other available electrodes CC, HQ and RS are detectable quantitatively if they are investigated individually. But when investigated simultaneously one in presence of other, in spite of giving corresponding peaks they give a broad overlapped peak resulting from all the isomers. This is why modification of electrode is necessaryto get corresponding, non-overlapped peaks. Recently, an enormous amount of research has been devoted to the development of new chemically modified electrodes for monitoring HQ or CC[61]. Among various chemically modified electrodes, polymer-modified electrodes (PMEs) are promising approach to detect isomers. Polymer-modified electrodes prepared by electropolymerization have received extensive interest in the detection of analytes because of their selectivity, sensitivity and homogeneity in electrochemical deposition, strong adherence to electrode surface and chemical stability of the films. Selectivity of PMEs as a sensor can be attained by different mechanisms such as size exclusion, ion exchange, hydrophobicity interaction and electrostatic interaction [62-66].

1.7.1 Ionic liquid

Ionic liquids are salts of organic cations with melting points generally below 100 °C and are being widely investigated as replacements for volatile organic solvents in industrial and laboratory processes because they are thought to be "environmentally benign." Although some efforts have begun to study their potential for ecotoxicity, limited vertebrate or genetic toxicity testing has been done. Three ionic liquids, 1-butyl-3-methylimidazolium chloride ([bmim]Cl), 1-butyl-1-methylpyrrolidinium chloride

([bmpy]Cl), and N-butylpyridinium chloride ([NBuPy]Cl), were nominated to the National Toxicology Program (NTP) for toxicological testing based on their widespread interest as possible alternatives to organic solvents. These chlorides are representative of the three most common cation classes of ionic liquids being investigated: imidazolium, pyridinium, and pyrrolidinium. The chlorides, soluble in water and polar organic liquids, are generally prepared from approximately equimolar amounts of the appropriately substituted heterocyclic compound and butyl chloride, often under both heat and pressure.

The types of organic cations used in ionic liquids include:

1. mono-, di-, and trisubstituted imidazoliums, and substituted pyridiniums and pyrrolidiniums [the free electron pairs of one of the two nitrogen atoms in the five-membered imidazoline ring and of the sole nitrogen atom in the five-membered pyrrolidine or six-membered pyridine ring have been donated to univalent alkyl groups to produce an N^+ cation]
2. tetraalkylammoniums (R_4N^+)
3. guanidiniums [$(NH_2)_3C^+$ and derivatives]
4. isouroniums and thioisouroniums [urea and thiourea derivatives of general formula $(NH_2)_2(RX)C^+$ where X = O or S and R = alkyl]
5. tetraalkylphosphoniums (R_4P^+)

Solubility and other physical-chemical properties suitable for a particular application can be designed by appropriate combinations of the cations and anions. For example, in general, chlorides are water-soluble while hexafluorophosphates are water-insoluble. As reaction solvents, ionic liquids have been shown to increase reaction rates, selectivities, and yields . By changing substitution patterns on the organic cation and changing anions, researchers can fine-tune reaction rates and selectivities for a particular catalyzed synthetic reaction. Because of their resistance to oxidation and reduction, they are suitable for electrochemical applications such as batteries, capacitors, electrochemical sensors, and photovoltaic devices.

A typical IL has a bulky organic cation (e.g., N alkylpyridinium, N-N_-dialkylimidazolium) that is weakly coordinated to an organic or inorganic anion, such as BF_4^-, Cl^-, I^-, $CF_3SO_3^-$, and $AlCl_4^-$. The big difference in the size of a bulky cation and a

small anion does not allow packing of lattice, which happens in many inorganic salts; instead, the ions are disorganized. This results in that some of these salts remain liquid at the room temperature.

Traditional salts like sodium chloride are able to efficiently pack to form a crystal lattice.

With ionic liquids, the cations are asymmetrically substituted with different length groups to prevent the packing of the cations/anions into a crystal lattice.

Figure 1.2 (a) Crystal lattice of NaCl, (b) Crystal lattice of imidazolium chloride.

Since the electrochemical window of the pure ILs depends on the electrochemical stability of the cation and/or anion, understanding the ion behavior at the electrode surface leads to improvement and implementation of the IL to the desired system. The presence of an abundance of charge carriers means that when ILs are used as solvents, no supporting electrolyte is required for electrochemical experiments and this minimizes waste towards greener site.

ILs posses several advantages over conventional organic solvents, which make them environmentally compatible.

(i) A diverse range of organic, inorganic, and organometallic compounds are soluble in ILs. The solubility of gases such as O_2, benzene, nitrous oxide, ethylene, ethane, and carbon monooxide is also good, which makes them attractive solvent system for catalytic hydrogenations, carbonylations, hydroformylation, and aerobic oxidations.

(ii) Due to the large electrochemical window, they are especially suitable as reaction media for electrochemical (and also chemically induced) polymerization processes leading to conducting polymers.

(iii) ILs are highly polar.

(iv) ILs consist of loosely coordinating bulky ions.

(v) Most of ILs have a liquid window of up to 200◦C which enables wide kinetic control.

(vi) ILs have high thermal conductivity.

(vii) ILs are immiscible with many organic solvents.

(viii) ILs are nonaqueous polar alternatives for phase transfer processes.

(ix) The solvent properties of ILs can be tuned for a specific application by varying the anion cation combinations.

(x) ILs tend to have good thermal stability and can be liquid over a range of 300◦C. This wide liquid range is distinct advantages over traditional solvent system that have a much narrower liquid range; for example, water has a liquid range of 100◦C or toluene 206◦C.

(xi) The majority of ILs have low volatility. This property makes them easy to contain, use, and transfer and in addition they can be used under high vacuum conditions. This is an important feature that reduces chronic exposure to solvent vapors.

(xii) ILs can be recycled. Recovery and recycling of the catalyst are also possible with the ILs, thus keeping production of waste and loss of valuable catalysts to a minimum.

Properties such as nonflammability, high ionic conductivity, and electrochemical and thermal stability of ILs make them ideal electrolytes in electrochemical devices like in batteries, capacitors, fuel cells, photovoltaics, actuators and electrochemical sensors.

Recently, ILs have captured the attention of the analysts to use them in different analytical applications as well. ILs can improve separation of complex mixtures of both polar and nonpolar compounds when used either as stationary phase or as additives in gas-liquid chromatography, liquid chromatography, and capillary electrophoresis. They are also used in optical sensors and also to enhance the analytical performance of the matrix-assisted laser desorption ionizationmass spectrometry (MALDI-MS).The use of ILs in different applications is determined by their intrinsic properties [67-70].

1.7.2 1-Hexylpyridinium hexafluorophosphate

It is an ionic liquid has molecular formula $C_{11}H_{18}F_6NP$, formula weight 309.23g, synthesized in laboratory, low solubility in water and strongly hygroscopic. It has a white powder like appearance. It has a slight pungent smell.

1.7.3 1-Butyl-3-methylimidazolium hexafluorophosphate

It is also known as BMIM-PF_6, has molecular formula $C_8H_{15}F_6N_2P$, molar mass 284.19 $g \cdot mol^{-1}$, has density 1.38 g/mL (20 °C). It is a viscous, colorless, hydrophobic and non-water-soluble ionic liquid with a melting point of -8°C. It is one of the most widely studied ionic liquids. It is known to very slowly decompose in the presence of water.

a b

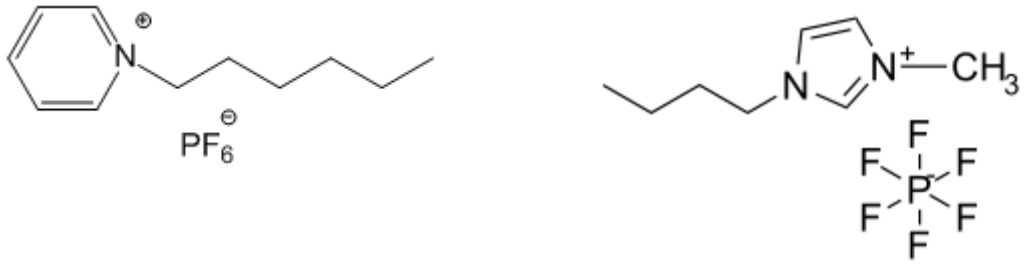

Figure 1.3: (a) Structure of 1-Hexylpyridinium hexafluorophosphate, (b) Structure of 1-Butyl-3-methylimidazolium hexafluorophosphate.

1.8 Wooden Pencil graphite electrode

The chemical reactivity of the working electrode (where the reaction of interest occurs) has significant impact on the function of electrochemical sensors. Currently, GCE is the most commonly employed working electrode material due to the ability of carbon to react with diverse classes of analyte. In the field of the detection of DHBIs, GCEs have been widely used. However, despite their widespread usage, GCEs are prone to electrode fouling, are relatively costly (approximately $190 to $1200 each, depending on the exact specifications and supplier), and require labour-intensive and time-consuming cleaning procedures.

Numerous modifications and novel electrode materials have been proposed to overcome the limitations of traditional glassy carbon-based sensors, including metallization, derivatization and doping. In particular, however, interest has turned to the development of pencil-graphite electrodes (PGEs), due to their disposability, simplicity and low cost [71-72].

1.9 Catechol

CC (also known as pyrocatechol or 1,2-dihydroxybenzene), is an organic compound with the molecular formula $C_6H_4(OH)_2$shown in (Figure 1.4). It is the ortho isomer of the three isomeric benzenediols. This colourless compound occurs naturally in trace amounts. About 20M kg are produced annually, mainly as a precursor to pesticides, flavors and fragrances. CC occurs as feathery white crystals which are very rapidly soluble in water.

1.9.1 Natural Occurrence of Catechol

Small amounts of CC occur naturally in fruits and vegetables, along with the enzyme polyphenol oxidase (also known as catecholase, or catechol oxidase). Upon mixing the enzyme with the substrate and exposure to oxygen (as when a potato or apple is cut and left out), the colorless CC oxidizes to reddish-brown melanoid pigments, derivatives of benzoquinone. The enzyme is inactivated by adding an acid, such as lemon juice, and slowed with cooling. Excluding oxygen also prevents the browning reaction. Benzoquinone is said to be antimicrobial, which slows the spoilage of wounded fruits and other plant parts**.** CC moieites are also found widely within the natural world. Arthropodcuticle consists of chitin linked by a catechol moiety to protein. The cuticle may be strengthened by cross-linking (tanning and sclerotization), particularly in insects, and of course by biomineralization[73].

1.9.2 Uses of Catechol

Approximately 50% of synthetic CC is consumed in the production of pesticides, the remainder being used as a precursor to fine chemicals such as perfumes and pharmaceuticals [74]. It is a common building block in organic synthesis [75]**.** Several industrially significant flavors and fragrances are prepared starting from CC [76].Guaiacol is prepared by methylation of CC and is then converted to vanillin on a scale of about 10M kg per year (1990). The related monoethyl ether of CC, guethol, is converted to ethylvanillin, a component of chocolate confectionaries. 3-trans-Isocamphylcyclohexanol, widely used as a replacement for sandalwood oil, is prepared from CC via guaiacol and camphor. Piperonal, a flowery scent, is prepared from the methylene diether of CC followed by condensation withglyoxal and decarboxylation[77].

CC is used as a black-and-white photographic developer, but except for some special purpose applications, its use until recently was largely historical. Modern CC developingwas pioneered by noted photographer Sandy King. His "PyroCat" formulation enjoys widespread popularity among modern black and white film photographers.

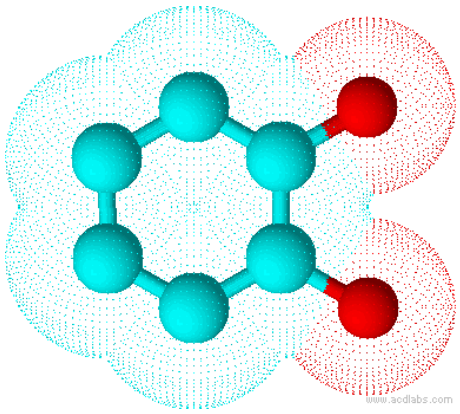

Figure 1.4: Molecular structure of catechol.

1.10 Hydroquinone

HQ (Benzene-1, 4-diol or quinol), is an aromatic organic compound that is a type of phenol, having the chemicalformula$C_6H_4(OH)_2$. Its chemical structure has two hydroxyl groups bonded to a benzene ring in a *para* position (Figure 1.5). It is a white granular solid. Substituted derivatives of this parent compound are also referred to as HQ.

1.10.1 Natural Occurrence of Hydroquinone

HQ is one of the two primary reagents in the defensive glands of bombardierbeetles, along with hydrogenperoxide (and perhaps other compounds, depending on the species), which collect in a reservoir. The reservoir opens through a muscle-controlled valve onto a thick-walled reaction chamber. This chamber is lined with cells that secrete catalases and peroxidases. When the contents of the reservoir are forced into the reaction chamber, the catalases and peroxidases rapidly break down the hydrogen peroxide and catalyze the oxidation of the HQ into p-quinone. These reactions release free oxygen and generate enough heat to bring the mixture to the boiling point and vaporize about a fifth of it, producing a hot spray from the beetle's abdomen.Farnesyl HQ derivatives are the principal irritants exuded by the poodle-dogbush, which can cause severe

contactdermatitis in humans. HQ is thought to be the active toxin in *Agaricushondensis* mushrooms [78].

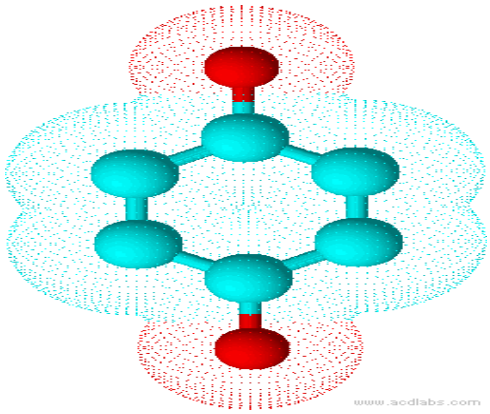

Figure 1.5: Molecular structure of hydroquinone.

1.10.2 Uses of Hydroquinone

HQ has a variety of uses principally associated with its reducing power. It is a major component in most photographic developers where, with the compound metol (monomethyl-p-aminophenol hemisulfate), it reduces silver halides to elemental silver. As a polymerization inhibitor, HQ prevents polymerization of acrylic acid, methyl methacrylate, and other monomers that are susceptible to radical-initiated polymerization. This application exploits the antioxidant properties of HQ. It is also used as a raw material for the production of diverse industrial chemicals.

In human medicine, HQ is used as a topical application in skin whitening to reduce the color of skin as it does not have the same predisposition to cause dermatitis as metol does. This use is banned in some countries, including the member states of the European Union.

In 2006, the United States Food and Drug Administration revoked its previous approval of HQ and proposed a ban on all over-the-counter preparations [79]. The FDA stated that HQ cannot be ruled out as a potential carcinogen. This conclusion was reached based on the extent of absorption in humans and the incidence of neoplasms in rats in several studies where adult rats were found to have increased rates of tumours, including thyroid follicular cell hyperplasias, anisokaryosis, mononuclear cell leukemia, hepatocellular adenomas and renal tubule cellademonas. The Campaign for Safe Cosmetics has also

highlighted concerns. Numerous studies have revealed that HQ can cause exogenous ochronosis, a disfiguring disease in which blue-black pigments are deposited onto the skin [80].

1.11 Resorcinol

RS (known as pyrocatechol or 1,3-dihydroxybenzene), is an organic compound with the molecular formula $C_6H_4(OH)_2$ shown in (Figure 1.6). It is the meta isomer of the three isomeric benzenediols. This colourless compound occurs naturally in trace amounts. It is produced when any of a large number of resins (e.g. galbanum, asafoetida, etc.) are melted with potassium hydroxide, or by the distillation of Brazilwood extract. It may be prepared synthetically by melting 3-iodophenol, phenol-3-sulfonic acid or benzene-1,3-disulfonic acid with potassium carbonate; by the action of nitrous acid on 3-aminophenol; or by the action of 10% hydrochloric acid on 1,3-diaminobenzene [81]. Many ortho- and para-compounds of the aromatic series (for example, the bromophenols, benzene-para-disulfonic acid) also yield RS on fusion with potassium hydroxide.

1.11.1 Natural Occurrence of Resorcinol

Parts of a molecule of catechin, another natural compound which is present in tea, has the RS skeleton structure in it.

1.11.2 Uses of Resorcinol

Medical: Used externally it is an antiseptic and disinfectant, and is used 5 to 10% in ointments in the treatment of chronic skin diseases such as psoriasis, hidradenitissuppurativa and eczema of a sub-acute character. It is present in over-the-counter topical acne treatments at 2% or less concentration, and in prescription treatments at higher concentrations. Weak, watery solutions of RS (25 to 35 g/kg) are useful in allaying the itching in erythematous eczema. A 2% solution used as a spray has been used with marked effect in hay fever and in whooping cough. In the latter disease 0.6 mL of the 2% solution has been given internally. It can be included as an anti-dandruff agent in shampoo or in sunscreen cosmetics. It has also been employed in the treatment of gastric ulcers in doses of 125 to 250 mg in pills, and is said to be analgesic and haemostatic in its action. In large doses it is a poison causing giddiness, deafness, salivation, sweating and convulsions. It is also worked up in certain medicated soaps.

Monoacetylresorcinol, $C_6H_4(OH)(O\text{-}COCH_3)$, is used under the name of euresol. RS is one of the main active ingredients in products like Resinol and Vagisil.

Chemical: RS is also used as a chemical intermediate for the synthesis of pharmaceuticals and other organic compounds. It is used in the production of diazo dyes and plasticizers and as a UV absorber in resins.An emerging use of RS is as a template molecule in supramolecular chemistry. The -OH groups on RS form hydrogen bonds to target molecules holding them in the proper orientation for a reaction. Many such reactions are able to be carried out in the solid state thereby reducing or eliminating the use of solvents that may be harmful to the environment. RS is an analytical reagent for the qualitative determination of ketoses (Seliwanoff's test).It is the starting material for resorcinarene molecules and the initiating explosive lead styphnate[83]. RS reacts with formaldehyde to form a thermoset resin, which can form the basis of an aerogel.

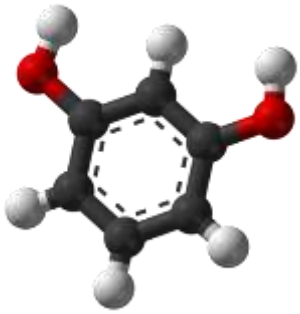

Figure 1.6: Molecular structure of resorcinol.

Table 1.1: Comparison among physical properties of CC, HQ and RS [77]

Properties	Catechol	Hydroquinone	Resorcinol
Molecular formula	$C_6H_6O_2$	$C_6H_6O_2$	$C_6H_6O_2$
Molar Mass	110.1 g/mol	110.1 g/mol	110.1 g/mol
Exact Mass	110.036779 u	110.036779 u	110.036779 u
Appearance	white solid	white solid	White solid
Density	1.344 g/cm³, solid	1.3 g/cm^3, solid	1.28 g/cm^3, solid
Melting Point	105 °C	172 °C	110 °C
Boiling Point	245.5 °C	287 °C	277 °C
Solubility in Water	43 g/100 mL	5.9 g/100 ml	110 g/100 mL
Acidity (pKa)	9.85	10.35	9.15

1.12 Electrochemistry as an analytical tool

Electrochemistry has become a powerful tool to study widely for solving the different problem in the arena of organic chemistry, biochemistry, material science, environmental science etc. Many natural and biochemical processes have redox nature. Their redox mechanisms can be easily established based on the experiment in voltammetry. For example, cyclic voltammetry is the most widely used modern electro-analytical method available for the mechanistic probing study of redox system.

In our present study we have investigated the redox behavior of CC, HQ and RS in various supporting electrolytes and tried to develop a method which is simple and effective process to determine CC, HQ and RS selectively in presence of others.

Various electrochemical techniques such as CV, DPV along with UV-visible Spectrophotometry were used for investigation.

1.13 Mass transfer process in voltammetry

The movement of the electro-active substance through solution is called mass transfer at the electrode surface. There are different types of mass transport by which a substance may be carried to the electrode surface from bulk solution. Depending on the experimental conditions, any of these, or more than one might be operating in a given experiment.
In general, there are three types of mass transfer processes by which a reacting species may be brought to an electrode surface [83]. These are,

a) Migration of charged ions in an electric field
b) Diffusion under the influence of a concentration gradient
c) Convection due to the motion of the solution or the electrode

1.13.1 Migration

Migration refers to movement of a charged particle in a potential field. In most voltammetric experiments, migration is undesirable but can be eliminated by the addition of a large excess of supporting electrolytes.Ions in the electrolysis solution, being charged them, will move towards the charged electrons, *i.e.* cation to the cathode and anions to the anode. This motion of charged particle through solution, induced by the charges on the electrodes is called migration [84]**.** The fraction of the current carried by a given cation

and anion is known as its transference number. Migration of charged electro-active substances and intermediates may be effectively eliminated by addition to the solution of an electrochemically inactive salt, called supporting electrolyte which does not undergo an electrochemical reaction at the cathode. When the potential is applied, supporting electrolyte remains unchanged and gives diffusion current.

Generally metal ion (cation) of the sample is migrated towards the cathode due to the electrostatic attraction, where they are reduced. When the cations are migrated towards the cathode a special type of current is produced. This current is called migration current. In cyclic voltammetry the effect of migration is usually eliminated by adding a 50 or 100 fold excess of an inert supporting electrolyte such as KC1, KNO_3.

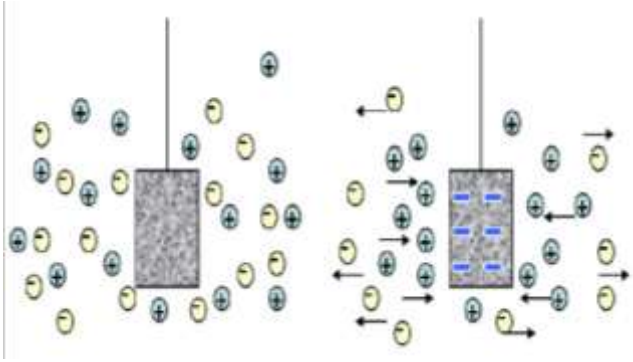

Figure 1.7: Movement of charged particles in a potential field.

1.13.2 Diffusion

The movement of a substance through solution by random thermal motion is known as diffusion. Whereas a concentration gradient exists in a solution, that is the concentration of a substance, is not uniform throughout the solution. There is a driving force for diffusion of the substance from regions of high concentration to regions of lower concentration. In any experiment in which the electrode potential is such that the electron transfer rate is very high, the region adjacent to the electrode surface will become depleted of the electro-active species, setting up a concentration in which this species will constantly be arriving at the electrode surface by diffusion from points further away.

An electrochemical cell in cyclic voltammetry in which the only mode of mass transfer is diffusion to an electrode surface. Since 50-100 fold excess supporting electrolyte is

present in the solution, therefore the electrical force on the reducible in is nullified. When the potential is applied, the metal ions are reduced at the cathode and the concentration of the investigated substance is decrease at the cathode region. Hence a concentration gradient is produced. Under this condition, the reducible ions are diffused from the bulk of the solution and diffusion current is produced.

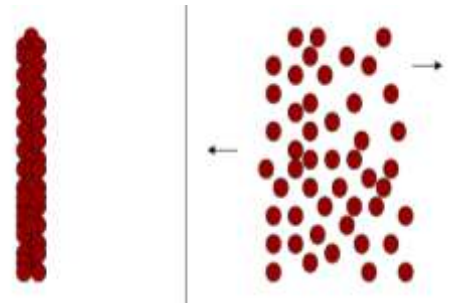

Figure 1.8: Spontaneous movement of particles.

1.13.3 Convection

Convection or hydrodynamic transport is the movement of a substance through solution by stirring. When the electrolyte is stirred or heated the ions are transported from one space to another. At the same time a type of current is produced. This current is called convection current. Removing the stirring and heating can eliminate this current. Convection is a far more efficient means of mass transport than diffusion. Therefore mass transport limited electrolysis currents are much higher for stirred solution than unstirred solution, where diffusion is the only means of mass transport. So, for minimizing convection unstirred vibration free solutions are required. Under such condition, the current is controlled unequally by diffusion of the reacting species through the concentration gradient adjacent to the electrode

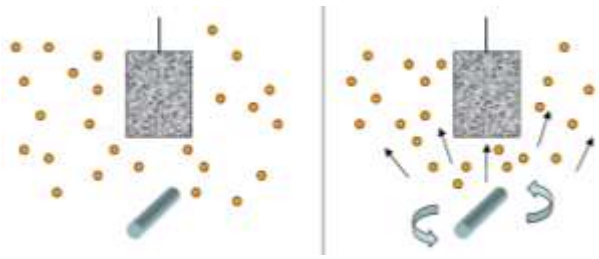

Figure 1.9: Movement of particles by stirring.

1.14 Cyclic Voltammetry

There are several well established electrochemical techniques for the study of electrochemical reactions. We chose the CV technique to study and analyze the redox reactions occurring at the polarizable electrode surface. This technique helps us to understand the mechanism of electron transfer reaction of the compounds as well as the nature of adsorption of reactants or products on the electrode surface.

CV is perhaps the most effective and versatile electroanalytical technique available for the mechanistic study of redox systems. It enables the electrode potential to be rapidly scanned in search of redox couples. Once located, a couple can then be characterized from the potentials of peaks on the cyclic voltammogram and from changes caused by variation of the scan rate. CV is often the first experiment performed in an electrochemical study. CV consists of imposing an excitation potential nature on an electrode immersed in an unstirred solution and measuring the current and its potential ranges varies from a few millivolts to hundreds of millivolts per second in a cycle. This variation of anodic and cathodic current with imposed potential is termed as voltammogram.

The technique involves under the diffusion controlled mass transfer condition at a stationary electrode utilizing symmetrical triangular scan rate ranging from 1 mV/s to hundreds millivolts per second.

The cyclic voltammetric technique reveals information about the following important phenomena:

i) reversibility of a reaction and a very rapid means of analysis of various systems

ii) direct investigation of reactive intermediate

iii) investigation of stepwise electrochemical and chemical reaction

iv) redox characteristic of oxidizing-reducing couple

v)investigation of charge transfer reaction at the electrode-solution interface and determination of charge transfer rate constant

1.15 Differential Pulse Voltammetry

Differential Pulse Voltammetry (DPV) or Differential Pulse Polarography (DPP) is often used to make electrochemical measurements. It can be considered as a derivative of linear sweep voltammetry or staircase voltammetry, with a series of regular voltage

pulses superimposed on the potential linear sweep or stair steps[85]. The current is measured immediately before each potential change, and the current difference is plotted as a function of potential. By sampling the current just before the potential is changed, the effect of the charging current can be decreased.

1.15.1 Uses of DPV

DPV is a very important analytical tool for quantitative determination in trace level. Thistechnique can be used to study the redox properties of extremely small amounts of chemicals because of the following two features[86]:

(i) In these measurements, the effect of the charging current can be minimized, so high sensitivityis achieved.
(ii) Faradaic current is extracted, so electrode reactions can be analyzed more precisely.

1.16 UV-Vis Spectrophotometry

In spectrometric analysis a source of radiation is used that extends into the ultraviolet region of the spectrum. From this definite wavelength of radiation are chosen possessing bandwidth of less than 1nm. This process necessities the use of more complicated and consequently more expensive instrument. The instrument employed for this purpose is a spectrophotometer.

An optical spectrometer is an instrument possessing an optical system which can produce dispersion of incident electromagnetic radiation, and with which measurements can be made of the quantity of transmitted radiation at selected wavelength of the spectral range. A photometer is a device for measuring the intensity of transmitted radiation. When combined in the spectrophotometer the spectrometer and photometer are employed conjointly to produce a signal corresponding to the difference between the transmitted radiation of a reference material and that of a sample of selected wavelengths.

The essential parts of spectrophotometer are:

1. A source of radiant energy
2. A monochromator
3. Glass or silica cells for holding the solvent and for the solution under test

4. A device to receive of measure the beam or beam of radiant energy passing through the solvent or solution.

1.17 Scanning Electron Microscopy

The scanning electron microscope (SEM) is one of the most versatile instruments available for the examination and analysis of the microstructure morphology and chemical composition characterizations. SEM uses a focused beam of high-energy electrons to generate a variety of signals at the surface of solid specimens. The signals that derive from electron-sample interactions reveal information about the sample including external morphology (texture), chemical composition, and crystalline structure and orientation of materials making up the sample. In most applications, data are collected over a selected area of the surface of the sample, and a 2-dimensional image is generated that displays spatial variations in these properties. Areas ranging from approximately 1 cm to 5 microns in width can be imaged in a scanning mode using conventional SEM techniques (magnification ranging from 20X to approximately 30,000X, spatial resolution of 50 to 100 nm). The SEM is also capable of performing analyses of selected point locations on the sample; this approach is especially useful in qualitatively or semi-quantitatively determining chemical compositions (using EDS), crystalline structure, and crystal orientations (using EBSD) [87]. SEM is used to characterize the electrode surface both before and after modification.

1.18 Energy Dispersive X-ray Microanalysis

Energy Dispersive X-ray microanalysis (EDX) makes use of the X-ray spectrum emitted by a solid sample bombarded with a focused beam of electrons to obtain a localized chemical analysis. All elements from atomic number 4 (Be) to 92 (U) can be detected in principle, though not all instruments are equipped for 'light' elements ($Z < 10$). Qualitative analysis involves the identification of the lines in the spectrum and is fairly straightforward owing to the simplicity of X-ray spectra. Quantitative analysis (determination of the concentrations of the elements present) entails measuring line intensities for each element in the sample and for the same elements in calibration Standards of known composition. EDX was used for element determination at the surface of bare PGE.

CHAPTER II

Literature Review

Extensive efforts have been made to develop new electrochemical sensors for the determination of DHBIs. Some literatures have been reviewed and are summarized below:

Yang *et al.*, 2007, fabricated a novel modified electrode by electro polymerization of acid chrome blue K at a multi-walled carbon nanotubes modified GCE. The electrode developed was used for simultaneous determination of the DHBIs in environmental samples using first order linear sweep derivative voltammetry with background sub-traction. A linear relationship between peak current and concentration of HQ, CC and RS was obtained in the range of 1×10^{-6} – 1×10^{-4} mol L^{-1} , and the detection limits were estimated to be 1×10^{-7} ,1×10^{-7} and 9×10^{-8} mol L^{-1} respectively. The constructed electrode showed excellent reproducibility and stability. Real water samples were analyzed and satisfactory results were obtained. This method provides a new way of constructing electrodes for environmental and biological analysis [88].

Wang *et al*., 2007, developed a simple and highly selective electrochemical method for the simultaneous determination of HQ and CC at a GCE covalently modified with penicillamine. The electrode is used for the simultaneous electrochemical determination of HQ and CC and shows an excellent electrocatalytical effect on the oxidation of HQ and CC upon CV in acetate buffer solution of pH 5.0. In DPV measurements, the modified electrode was able to separate the oxidation peak potentials of HQ and CC present in binary mixtures by about 103 mV although the bare electrode gave a single broad response. The determination limit of HQ in the presence of 0.1 mM L^{-1} CC was 1.0×10^{-6} mol^{-1} and the determination limit of CC in the presence of 0.1 mM L-1 HQ was 6.0×10^{-7} mol^{-1}. The method was applied to the simultaneous determination of HQ and CC in a water sample. It is simple and highly selective [89].

Wang *et al.*, 2007, made a GCE that is covalently modified with aspartic acid. The modified electrode is used for the simultaneous electrochemical determination of HQ and CC and shows an excellent electrocatalytical effect on the oxidation of HQ and CC by

CV in 0.1 M/L acetate buffer solution (pH 4.5). In DPV measurements, the modified electrode could separate the oxidation peak potentials of HQ and CC present in binary mixtures by about 101 mV though the bare electrode gave a single broad response. A successful elimination of the fouling effect by the oxidized product of HQ on the response of CC has been achieved at the modified electrode. The determination limit of HQ in the presence of 0.1 mM/L CC was 9.0×10^{-7} M/L and the determination limit of CC in the presence of 0.1 mM/L HQ was 5.0×10^{-7} M/L. The proposed method has been applied to the simultaneous determination of HQ and CC in a water sample with simplicity and high selectivity [90].

Bai *et al.*, 2009, studied the voltammetric behaviors of DHBIs at an ordered mesoporous carbon-modified GCE. Compared to the bare electrode, the electrocatalytic activity of the modified electrode toward DHBIs is evidenced by the increase of the peak current and the decrease of the peak separation in 0.1 M pH 5.0 PBS. Furthermore, at the OMC/GC-modified electrode, the three isomers could be separated entirely. The oxidation peak potential difference between HQ and CC is 154 mV, whereas that difference between CC, and RS is 370 mV. In the amperometric detection, the peak currents of dihydroxybenzene increased linearly with increasing dihydroxybenzene contents. The detection limits were 7.6×10^{-8} M, 1.0×10^{-7} M, 9.0×10^{-8} M for HQ, CC and RS, respectively, which are the lowest values ever reported for DHBIs. These make OMC/GC electrode a promising candidate for the simultaneous determination of isomers [91].

Naranchimeg *et al.*, 2011, developed Poly-ethylenedioxypyrrole (PEDOP) coated thiolated multiwall carbon nanotubes palladium nanoparticles (MWCNTs-Pd) modified GCE [PEDOP/MWCNTs-Pd/GCE] for the determination of HQ and it's isomer CC and were synthesized and compared with bare GCE and thiolated multiwall carbon nanotubes (MWCNTs-SH/GCE). The modification could be made by simple processes on a GCE with MWCNTs-Pd covered by PEDOP in a 0.05 M tetrabutylammonium perchlorate (TBAP)/MeCN solution system. A well-defined peak potential evaluation of the oxidation of HQ to quinone at 0.05 V (vs. Ag/AgCl), and electrochemical reduction back to HQ were found by CV in PBS at pH 7.4. Peak current values increased linearly with increasing HQ contents. The peak separation between the anodic and cathodic peaks at the PEDOP/MWCNTs-Pd/GCE was $\Delta Ep = 40$ mV for HQ and $\Delta Ep = 70$ mV for CA, resulting in a higher electron transfer rate. Moreover, good reproducibility, excellent

storage stability, a wide linear range (0.1 μM - 5 mM for HQ and 0.01 μM - 6 mM for CC), and low detection limits (2.9×10^{-8} M for HQ and 2.6×10^{-8} M for CC; S/N = 3) were determined using DPV and amperometric responses; this makes it a promising candidate as a sensor for determination of HQ and CC [92].

Ahammad *et al.*, 2011, developed simple and highly sensitive electrochemical method for the simultaneous and quantitative detection of HQ and CC, based on a poly(thionine)-modified GCE. The modified electrode showed excellent electrocatalytic activity and reversibility towards the oxidation of both HQ and CC in 0.1M PBS (pH 7.0). The peak-to-peak separations between oxidation and reduction waves in CV were decreased significantly from 262 and 204 mV at the bare GCE, to 63 and 56mV, respectively for HQ and CC at the poly(thionine) modified GCE. Furthermore, the redox responses from the mixture of HQ and CC were easily resolved in both CV and DPV due to a difference in the catalytic activity of the modified GCE to each component. The peak potential separation of 0.1V was large enough for the simultaneous determination of HQ and CC electrochemically. The oxidation peak currents of HQ and CC were linear over the range from 1 to 120 μM in the presence of 100 and 200μM of HQ and CC, respectively. The modified electrode showed very high sensitivity of 1.8 and 1.2 μA μM^{-1} cm^{-2} for HQ and CC, respectively. The detection limits (S/N=3) for HQ and CC were 30 and 25nM, respectively. The developed sensor was successfully examined for real sample analysis with tap water and revealed stable and reliable recovery data [93].

Ghoreishi *et al.*, 2012, made a multi-walled carbon nanotubes (MWCNTs) film coated GCE and the electrochemical oxidation of RS was studied in Britton–Robinson (BR) buffer (pH 6.0) using CV, SWV, and DPV. The results revealed that the modified electrode shows an electrocatalytic activity toward the oxidation of RS by a marked enhancement in the current response in buffered solution. The oxidation of RS at this nano-structured film coated electrode was irreversible and diffusion-controlled. Under the optimum conditions, the anodic peak current showed a linear relation versus RS concentration in the range of 1.2×10^{-6} to 1.9×10^{-4} M with detection limits of 4.9×10^{-7} and 1.1×10^{-6} M (S/N = 3) for SWV and DPV, respectively. Moreover, the modified electrode demonstrated good reproducibility (RSD = 2.4%, n= 10) and long-term stability. This method has been applied to the determination of RS in wastewater, and the recoveries were from 93% to 104% [94].

Li *et al.*, 2012, made graphene-modified GCE which was applied in a sensor for highly sensitive and selective voltammetric determination of HQ. Graphene was prepared by electrochemical reduction of exfoliated graphite oxide at cathodic potentials and used to fabricate a modified electrode. As compared to a bare GCE, the redox peak current for HQ in pH 5.7 acetate buffer solution is significantly increased, indicating that graphene possesses electrocatalytic activity towards HQ. In addition, the peak-to-peak separation is significantly improved. The modified electrode enables sensing of HQ without interference by CC or RS. Under optimal conditions, the sensor exhibits excellent performance for detecting HQ with a detection limit of 0.8μM, a reproducibility of 2.5% (expressed as the RSD), and a recoveries from 98.4 to 101.2% [95].

Wang *et al.*, 2012, investigated simultaneous determination of CC and HQ by voltammetry based on GCE modified by poly (diallyldimethylammonium chloride) (PDDA) functionalized graphene (PDDA-G). The modified electrode showed excellent sensitivity and selectivity properties for the two DHBIs. In 0.1 M/L PBS (pH 7.0), the oxidation peak potential difference between CC and HQ was 108 mV and the peaks on the PDDA-G/GCE were three times as high as the ones on graphene-modified GCE. Under optimized conditions, the PDDA-G/GCE showed wide linear behaviors in the range of 1×10^{-6} -4×10^{-4} M/L for CC and 1×10^{-6} -5×10^{-4} M/L for HQ, with the detection limits 2.0×10^{-7} M/L for CC and 2.5×10^{-7} M/L for HQ (S/N=3) in mixture, respectively. Some kinetic parameters, such as the electron transfer number (n), charge transfer coefficient (α), and the apparent heterogeneous electron transfer rate constant (ks), were calculated. The proposed method was applied to simultaneous determine CC and HQ in real water samples of Yellow river with satisfactory results [96].

Zhou *et al.*, 2012, developed an over-oxidized poly(HQ) electrode for selective determination of HQ in the presence of CC. The electrochemical polymerization of HQ was carried out by potentiostatic method on a GCE. The resulting PHQ was over-oxidized in 0.10 M/L NaOH solution and thus poly (p-benzoquinone) was obtained. Two DHBIs, HQ and CC, show different voltammetric behavior at the over-oxidized PHQ electrode. The peak current of HQ is much larger than that of CC with the same concentration, which is attributed to the different position of the hydroxyl groups in benzene ring of the two isomers. The results from electrochemical impedance spectroscopy also demonstrates that the over-oxidized PHQ electrode has a stronger affinity for HQ over CC [97].

Huang *et al.*, 2013, reported on the modification of a GCE with a composite consisting of silver nanoparticles (AgNPs), polydopamine, and graphene to give an electrochemical sensor for CC. The composite was characterized by transmission electron microscopy, and the electrochemical behavior of CC at the modified electrode was studied by CV. The electrochemical response is greatly enhanced and thought to result from a combination of beneficial effects including the good conductivity and large surface area of the AgNPs, the high conductivity of graphene, the synergistic effects of the composite and the increased quantity of CC that is adsorbed on the surface of the electrode. DPV responses are proportional to the concentration of CC between 0.5 and 240μM levels of CC, and the detection limit is 0.1μM (S/N=3). The performance of the sensor was evaluated with CC-spiked water samples, and recoveries range from 96.5% to 103.1%. The results indicated that the composite presented here is a promising substrate for use in electrochemical sensing [98].

Selvakumar *et al.*, 2014, demonstrated the simultaneous and selective electrochemical determination of DHBIs at a reduced graphene oxide (RGO) and copper nanoparticles (Cu-NPs) composite modified electrode. The RGO/Cu-NPs composite was prepared by a single-step electrochemical reduction method. The synthesized RGO/Cu-NPs composite was characterized using SEM and elemental analysis. Linear sweep voltammetry was employed for the simultaneous determination of HQ, CC and RS. A well defined and more enhanced oxidation peak response is observed for HQ, CC and RC at the RGO/Cu-NPs composite electrode compared to other modified electrodes, which indicate fast electron transfer from DHBIs at the RGO/Cu-NPs composite electrode. The composite modified electrode shows high electrocatalytic activity towards the oxidation of HQ, CC and RC. The electrochemical sensor shows a wide linear response in the concentration range of 3μM to 350μM, 3 to 350μM and 12μM to 200μM for HQ, CC and RC respectively with a detection limit of 0.032μM, 0.025μM and 0.088μM (S/N=3). In addition, the proposed sensor shows good selectivity and stability along with good precision and consistency. The obtained results clearly demonstrate that the RGO/Cu-NPs composite can be an advanced electrode material for the real time sensing of DHBIs [99].

Cui *et al.*, 2014, successfully realized the simultaneous determination of DHBIs in neutral condition by a simple and easy prepared modified electrode without previous chemical or physical separations. The multi-walled carbon nanotubes modified GCE

(MWCNTs/GCE), which was prepared by the drop-coating method, was characterized by FE-SEM and TEM. Then, the electrochemical behavior of DHBIs at MWCNTs/GCE was systematically studied at different temperature and pH conditions. The oxidation peak potentials were separated in neutral condition with 105 mV to HQ and CC and 390 mV to CC and RS . And in neutral condition, the amperometric current were found to be linear with concentration of HQ, CC, and RS (20–140μM) with the presence of 100μM other isomers. Furthermore, excellent anti-interference, stability, and reproducibility were also presented by this modified electrode [100].

Liu *et al.*, 2014, prepared the nitrogen doped porous carbon nanopolyhedrons (N-PCNPs)-multi-walled carbon nanotubes (MWCNTs) hybrid materials for the first time. Combining the excellent catalytic activities,good electrical conductivities and high surface areas of N-PCNPs and MWCNTs, the simultaneous determination of HQ, CC and RS with good analytical performance was achieved at the N-PCNPs-MWCNTs modified electrode. The linear response ranges for HQ, CC and RS are 0.2-455 μM, 0.7-440 μM and 3.0-365 μM respectively, and the detection limits (S/N = 3) are 0.03 μM, 0.11 μM and 0.38 μM respectively. These results are much better than that obtained on some graphene or CNTs-based materials modified electrodes. Furthermore, the developed sensor was successfully applied to simultaneously detect HQ, CC and RS in the local river water samples [101].

Liu *et al.*, 2014, investigated the simultaneous determination of DHBIs [HQ, CC, and RS] by using CV and DPV at thionine functionalized multiwalled carbon nanotube (TH-MWCNTs) modified GCE. CV and DPV results showed that the TH-MWCNTs modified electrode exhibited excellent recognition ability toward the three isomers of dihydroxybenzene. Their oxidize peak currents were linear over ranges from 9.0×10^{-7} to 3.6×10^{-4} M for HQ, from 3.3×10^{-6} to 8.1×10^{-4} M for CC and from 4.3×10^{-6} to 9.0×10^{-4} M for RS, with the detection limits of 2.7×10^{-7} , 1.0×10^{-6} , and 1.1×10^{-6} M, respectively. The proposed method would potentially be applied to multi-component analysis in environmental control and chemical industry [102].

Li *et al.*, 2014, modified a GCE with poly(sulfosalicylic acid) and poly(diallyldimethy-lammonium chloride)-graphene (PDDA-GN) was prepared by a simple self-assembly method. The formation of films was ascribed to the electrostatic force between negatively charged PSA and positively charged PDDA-GN as well as the π–π stacking

interaction between PSA and PDDA-GN. The as prepared films were characterized by SEM, Raman spectroscopy and electrochemical methods. Under the optimized condition, the modified GCE showed two well-defined redox waves for CC and HQ in CV with a peak potential separation of 111 mV, which ensured the anti-interference ability of the electro-chemical sensor and made simultaneous determination of DHBIs possible in real samples. The corresponding oxidation currents increased remarkably compared with those obtained at the bare GCE, PSA/GCE and PDDA-GN/GCE, respectively. DPV was used for the simultaneous determination of CC and HQ. The anodic peak current of CC was linear in the concentration from 1×10^{-6} to 4×10^{-4} M in the presence of 3×10^{-5} M HQ, and the detection limit was 2.2×10^{-7} M (S/N=3). At the same time, the anodic peak current of HQ was linear in the concentration from 2×10^{-6} to 4×10^{-4} M in the presence of 2×10^{-5} M CC, and the detection limit was 3.9×10^{-7} M (S/N=3). The proposed method was applied to simultaneous determination of CC and HQ in tap water with satisfactory results. These results indicated that PSA/PDDA-GN is a promising modified material with great potential in electrocatalysis and electrochemical sensing [103].

Wang *et al.*, 2014, developed a three dimensionally ordered macroporous (3DOM) polycysteine (PCE) film and it was electropolymerized on the GCE using polystyrene spheres as template. The electrochemical behaviors of HQ and CC were studied, and two independent oxidation peaks were observed. Compared with the bare GCE and GCE modifiedwith PCE without using template, this electrode displays larger peak currents which may be attributed to the structure of PCE and the large surface area of the nanopore array structure. As a result, a novel electrochemical method was developed for the simultaneous determination of HQ and CC. Under the optimized conditions, the peak currents were linear to concentrations in the wider ranges of 9 to 700 μM for HQ and from 3 to 700 μM for CC. The method was successfully applied to the simultaneous determination of HQ and CC in spiked water samples, and the results are satisfactory [104].

Alshahrani *et al.*, 2014, modified GCE with a copper(II) complex [Cu(Sal-β-Ala) (3,5-DMPz)2] (Sal = salicylaldehyde, β-Ala = β-alanine, 3,5-DMPz = 3,5-dimethylpyrazole) and single-walled carbon nanotubes (SWCNTs). The modified electrode was used to detect CC and HQ and exhibited good electrocatalytic activities toward the oxidation of CC and HQ. The peak currents were linear with the CC and HQ concentrations over the range of 5–215 μML^{-1} and 5–370 μML^{-1} with orresponding detection limits of 3.5

μML^{-1} and 1.46 μML^{-1} (S/N = 3) respectively. Moreover, the modified electrode exhibited good sensitivity, stability and reproducibility for the determination of CC and HQ, indicating the promising applications of the modified electrode in real sample analysis [105].

Hua *et al.*, 2014, developed A Poly (arginine acid)/GCE modified electrode was prepared by electrochemical polymerization method, which showed an excellent electrocatalytical activity effect on the redox reaction of CC and HQ, significantly increased the reversible electrochemical reaction. The electrochemical behavior of CC and HQ at the modified electrode was studied by CV and DPV. The influences of scan rate and acidity factors on catalytic oxidation of HQ in modified electrode were discussed. The results suggest that the modified electrode was controlled and pH = 7 is the optimum acidity condition for the selective determination and of CC and HQ. The anodic peak current versus the concentration of HQ showed a linear relation over the range of 6.0×10^{-6} ~4.5×10^{-4} M/L with a detection limit of 8.0×10^{-7} M/L, R^2=0.997. The anodic peak current versus the concentration of CC also showed a linear relation over the range of 1.0×10^{-6}~4.8×10^{-4} M/L, the detection limit was 5.0×10^{-7} M/L, R^2=0.997. The modified electrode showed good selectivity and strong anti-interference applied to the determination of a water sample with satisfactory results [106].

Zhang *et al.*, 2015, prepared substrate-selective flower-like Pd nanoparticles by using a simple electrodeposition method. The flower-like Pd–graphene nanocomposites showed excellent electrochemical properties, as proven by electrochemical impedance and cyclic voltammetry. Developed to serve as a sensor for simultaneous determination of CC and HQ, the Pd–grapheme nanocomposite-modified GCE (Pd–graphene/GCE) displayed good electrochemical catalytic activity toward CC and HQ, which was attributed to the flower-like composite structure, i.e. high electrical conductivity and larger surface area of Pd–graphene nanocomposites. Several kinetic parameters were calculated, including the electron transfer number (n), proton transfer number (m), charge transfer coefficient (c), and apparent heterogeneous electron transfer rate constant (ks). Under optimized conditions, the oxidation peak current was linear over a range from 0.075 to 5 mM. The detection limits were 1.25×10^{-6} M/L for HQ and 1.0×10^{-6} M/L for CT (S/N=3). The proposed Pd–graphene/GCE was applied to the simultaneous determination of HQ and CT in Songshan Lake water samples [107].

Foroughi *et al.*, 2015, used a decorated GCE with functionalized multi-walled carbon nanotube (CNTs) and ruthenium red (RR) for simultaneous determination of HQ and CC. The electrocatalytic behaviors of the GC/CNTs–RR were studied in acetate buffer solution with pH 4.5 by DPV and chronoamperometry techniques. Due to the excellent electrocatalytic activity and enhanced electrical conductivity of the CNTs–RR, the simultaneous determination of HQ and CC with two well-defined peaks was achieved at the GC/CNTs–RR modi-fied electrode. The catalytic peak currents linearly depend on the HQ and CC concentrations in the range of 1.3– 433.3 μM with the sensitivity of 5.0 μA μM^{-1} cm^{-2} and 7.45 μA μM^{-1} cm^{-2}, respectively. The detection limits for HQ and CC were obtained 0.21 and 0.18 μM. The diffusion coefficient for the oxidation of HQ and CC at the modified electrode was calculated as $1.06 \pm 0.05 \times 10^{-6}$ and $1.76 \pm 0.07 \times 10^{-5}$ cm^2 s^{-1}, respectively. The proposed sensor was successfully examined for real water samples analysis and revealed stable and reliable recovery data [108].

Zhang *et al.*, 2015, developed a simple and highly sensitive electrochemical method for the simultaneous detection of HQ, CC and RS based on a carbon dot/reduced graphene oxide composite on a GCE. The electron communication between reduced graphene oxide (r-GO) and CDs can be further strengthened viahydrogen bonding and p–p stacking forces. The electrochemical behavior of the CD/r-GO/GCE sensor toward HQ, CC and RC was probed by CV and DPV. The results showed that the calibration curves were in the range of 0.5 to 1000μM, 1.0 to 950μM and 5.0 to 600μM, respectively. The detection limits for HQ, CC and RC were 0.17μM, 0.28μM and 1.0μM (S/N=3), respectively. Moreover, the sensor has been successfully applied in detecting tapwater, river water and industrial sewage [109].

Hu *et al.*, 2015, synthesized a novel sandwiched film of cadmium sulphide/reduced graphene oxide (CdS/r-GO) via one step hydro-thermal reaction and electrodes modified with this composite were successfully used to simultaneously determine HQ, CC and RS. Additionally, some kinetic parameters, such as the charge transfer coefficient (a) and the electron transfer rate constant (ks) were calculated. DPV was used for the simultaneous determination of HQ, CC and RS in their ternary mixture. The calibration curves of HQ, CC and RC were obtained in the ranges of 0.2 to 2300μM, 0.5 to 1350μM and 1.0 to 500μM, respectively. The detection limits for HQ, CC and RS were 0.054μM, 0.09μM and 0.23μM, respectively (S/N=3). The modified electrode was then used to analyze tap

water, well water and river water and the results show its significance for practical applications in the aquatic environment [110].

Meng *et al*., 2015, fabricated a novel TiO_2/multi-walled carbon nanotubes (MWCNTs) composite film-modified electrode to develop an electrochemical sensor for the simultaneous determination of HQ and CC. The prepared electrode not only separated the peaks of HQ and CC on the CV with oxidation potential difference of 116 mV but also lowered the over potential significantly and increased the reversible process and the peak currents of HQ and CC. In 0.1 M PBS (pH=7.0). The oxidation peak current was linearly proportional to the concentration of CC and HQ in two broad linear ranges with the detection limit of 0.8μM. The present electrochemical sensor for the simultaneous determination of CC and HQ showed high sensitivity and low detection limit [111].

Wang *et al.,* 2015, made an electrochemical sensor for simultaneous determination of HQ and CC. A GCE was modified with gold nanoparticles, L-cysteine, and ZnS/NiS@ZnS quantum dots using a layer-by-layer technique. The materials were characterized by X-ray diffractometry, field emission SEM, and electrochemical impedance and Fourier transform infrared spectroscopy. CV and DPV revealed this modified GCE to represent a highly sensitive sensor for the simultaneous determination of HQ and CC. The anodic peak current for HQ at a working voltage of 80mV (vs. Ag/AgCl) is related to its concentration in the 0.1 to 300 μM range (even in the presence of 0.1 mM of CC). The anodic peak current for CC at a working voltage of 184 mV is related to its concentration in the 0.5 to 400 μM range (even in the presence of 0.1 mM of HQ). The detection limits (at an S/N ratio of 3) are 24 and 71 nM for HQ and CC, respectively. The modified GCE was successfully applied to the determination of HQ and CC in aqueous solutions and gave satisfactory results [112].

Wang *et al*., 2016, applied a very simple and reliable strategy to modify a GCE by pre-electrolyzing GCE in ammonium carbamate aqueous solution was employed for the simultaneous determination of HQ and CC. Compared with bare GCE, the incorporation of nitrogen into the GCE surface structure improved the electrocatalytic properties of GCE towards the electro-oxidation of HQ and CC. The nitrogen-introduced GCE (N-GCE) was evaluated for the simultaneous detection of HQ and CC and the linear ranges for HQ and CC were both from 5 to 260 μM. Their detection limits were both evaluated to be 0.2 μM (S/N = 3). The present method was applied for the determination of HQ and

CC in real river water samples with recoveries of 95.0–102.1%. In addition, a possible detection mechanism of HQ and CC was discussed [113].

Hossain *et al.*, 2015, fabricated a modified GCE. CV and DPV were performed with the GCE modified with poly glutamic acid (PGA) on the three DHBIs, CC, HQ and RS. At bare GCE, these isomers exhibited voltammograms with highly overlapped redox peaks that impeded their simultaneous detection in binary and ternary mixtures. On the contrary, at PGA modified GCE binary and ternary mixtures of the DHBIs showed well-resolved redox peaks in both CV and DPV experiments. This resolving ability of PGA modified GCE proves its potential to be exploited as an electrochemical sensor for the simultaneous detection of these isomers [114].

Wang and Huang, 2014, used a sensitive voltammetric method for trace measurements of HQ in the sewage water is described. The poly-L-histidine is prepared to modify the GCE in order to improve the electrochemical catalysis of interesting substances such as HQ. The influence of the base solution, pH value, and scanning speed on the tracing of HQ is discussed, and the experimental procedures and conditions are optimized. The laboratory results show that it is possible to construct a linear calibration curve between the peak current of HQ on modified electrode and its concentration at the level of 0.00001M/L. The potential limitation of the method is suggested by a linear peaking shift model as well. The method was successfully applied to the determination of HQ in the actual sample of industrial waste water [115].

Xu *et al*., 2015, investigated electrochemical characteristics of HQ, CC and RS at GCE modified with poly(3-thiophenemalonic acid) by CV. The effect of key parameters on the detection of three substances was evaluated at the modified electrode, such as immerging time, scanning rate and so on. Under optimum conditions, the catalytic oxidation currents increased linearly with increasing the concentration of HQ, CC and RS in the ranges of 7.81～500 μM, 3.91～500 μM and 15.6～500 μM with detection limits of 7.81 μM, 3.91μM and 15.6 μM, respectively, by DPV. In addition, the modified electrodes exhibited good sensitivity, selectivity, reproducibility and stability. The modified electrode can be used for the selective detecting the HQ, CC and RS [116].

Song *et al.*, 2016, developed a rapid and highly sensitive miniaturized sensor for determination of HQ and CC based on a carbon fiber electrode modified by poly(3,4-ethylenedioxythiophene) by DPV and amperometric. This lowcost diphenol microsensor was constructed by several simple steps and displayed excellent electrochemical activity toward the oxidation of HQ and CC in 0.1 M PBS (pH 7.0). Furthermore, the microsensor had the virtues of good stability and high sensitivity. Under the optimal working conditions, linear relationships between the amperometric current response and the concentration of substrates were obtained in the ranges of 5.3 × 10-7 M to 8.6 × 10^{-4} M for HQ and 5.2 ×10^{-7} M to 4.9 × 10^{-3} M for CC, with the detection limits (S/N = 3) of 4.2 × 10^{-7} M and 1.6 × 10^{-6} M, respectively. The proposed microsensor was applied to the determination of the mixture of HQ and CC, and satisfying results were obtained [117].

Huo *et al.*, 2011, made a highly sensitive electrochemical sensor by electrodeposition of gold nanoparticles onto carbon nanofiber film precast on an Au electrode for the simultaneous determination of CC and HQ. Both CC and HQ cause a pair of quasi-reversible and well-defined redox peaks at the modified electrode in pH 7.0 solution. Simultaneously, the oxidation peak potentials of CC and HQ become separated by 112 mV. When simultaneously changing the concentrations of both CC and HQ, the response is linear between 9.0μM and 1.50 mM. In the presence of 0.15 mM of the respective isomer, the electrode gives a linear response in the range from 5.0 to 350 μM, and from 9.0 to 500μM for CC and HQ, respectively, and detection limits are 0.36 and 0.86μM. The method was successfully examined for real sample analysis with high selectivity and sensitivity [118].

Yao *et al.*, 2014, investigated the simultaneous determnination of DHBIs CC, RS and HQ using a simple, inexpensive, water-stable, and conducting poly(3,4-ethylenedioxythiophene):poly-(styrenesulfonate) (PEDOT:PSS) composite sensing electrode by linear sweep voltammetry. The sensing electrode was prepared by dip-coating a mixture of PEDOT:PSS, Nafion, and carboxylic acid-functionalized single-walled carbon nanotubes on a gold electrode, then modifying by electrochemical doping in a hydrophobic ionic liquid. Nafion was selected as a binding agent to improve the adhesion and binding force between films and electrode interface, and ionic liquid was employed to improve the conductivity and water resistance of the composite electrode. The as proposed sensing electrode displayed excellent electrochemical catalytic activities

towards CC, RS, and HQ. Large peak separations were obtained between HQ and CC as well as CC and RS, i.e., up to 109 and 496 mV, respectively. The calibration curves for CC, RS and HQ were obtained in the ranges of 0.56–70, 0.18–50, and 0.56–50μM, with detection limits (S/N=3) of 0.19, 0.08, and 0.20μM, respectively. Finally, the sensing electrode was applied to river water sample analysis with reliable recovery. Satisfactory results revealed that the PEDOT:PSS composite can provide a promising platform for the design and application of sensing devices [119].

Li *et al.*, 2015, compared the electrochemical performance of various reduced graphene oxides (RGOs), including chemically reduced graphene oxide (CRGO), thermally reduced graphene oxide (TRGO), and electrochemically reduced graphene oxide (ERGO) under different reduction potentials, using aromatic species of HQ and CC as analytes. Strong adsorption of analytes on RGOs surface is found due to π-π interaction between RGOs and aromatic species. Analytical parameters of electron transfer rate, detection sensitivity, and linear response range were considered. CRGO showed the fastest heterogeneous electron transfer rate and the most wide linear range but among the poorest detection sensitivity. The different restoration extent of graphitic network, such as ERGO prepared under different reduction potentials, will also affect the sensing performance. These results will enhance our understanding of the applicability of RGOs in biosensing [120].

Wang *et al.*, 2010, developed a cheap, sensitive, and rapid method for the electrochemical determination of HQ and CC in aqueous pH 6.0 buffer solution without previous separation. By employing both anodically pretreated screen-printed carbon electrodes (SPCE) and square wave voltammetric techniques, a direct and simultaneous determination of the two positional isomers was achieved. The oxidation peak potentials for HQ and CC were completely separated at the SPCE, exhibiting well defined and reversible redox peaks and showing greatly enhanced activity. Under optimized conditions, the linear calibration ranges for HQ and CC were in the ranges of 0.1-50 and 0.1-70 μM, with detection limits (S/N = 3) of 0.05 and 0.05 μM, respectively. This method was applied to the direct determination of HQ and CC in river water with satisfactory recovery results [121].

Yu *et al.*, 2009, investigated the simultaneous determination of DHBIs at a multi-wall carbon nanotubes (MWCNTs)/b-cyclodextrin composite modified carbon ionic liquid

electrode in PBS (pH 7.0) in the presence of cationic surfactant cetylpyridinium bromide (CPB). With the great enhancement of surfactant CPB, the voltammetric responses of DHBIs were more sensitive and selective. The oxidation peak potential of HQ was about 0.024 V, CC was about 0.140 V and RS was about 0.520 V in DPV measurements, which indicated that the DHBIs could be separated entirely. The electrode showed wide linear behaviors in the range of 1.2×10^{-7} –2.2×10^{-3}, 7.0×10^{-7} –1.0×10^{-3}, 2.6×10^{-6} – 9.0×10^{-4} M/L for HQ, CC and RS, respectively. And the detection limits of the three DHBIs were 4.0×10^{-8}, 8.0×10^{-8}, 9.0×10^{-7} M/L, respectively. The proposed method could be applied to the determination of DHBIs in artificial wastewater, and the recovery was from 97.4% to 104.2% [122].

She *et al.*, 2010, fabricated three types of carbon paste electrodes (CPEs) with different liquid binders and their electrochemical behavior was characterized via a potassium hexacyanoferrate(II) probe. 1-octyl-3-methylimidazolium hexafluorophosphate IL as a hydrophobic conductive pasting binder showed better electrochemical performance compared with the commonly employed binder. The IL-contained CPEs demonstrated excellent electroactivity for oxidation of HQ. A diffusion control mechanism was confirmed and the diffusion coefficient (D) of 5.05×10^{-4} cm^2 s^{-1} was obtained. The hydrophobic IL-CPE is promising for the determination of HQ in terms of high sensitivity, easy operation, and good durability [123].

Sun *et al.*, 2011, developed an ionogel electrode by using an IL 1-butyl-3-methylimidazolium hexafluorophosphate ($BMIMPF_6$) for the sensitive voltammetric sensing of HQ in this paper. Due to the specific characteristics of the prepared working electrode, HQ exhibited an enhanced electrochemical response on CIE with a pair of well-defined redox peaks appeared in pH 2.5 PBS. The electrochemical behaviors of HQ on CIE were investigated by different electrochemical methods such as CV and DPV with the electrochemical parameters calculated. Under the optimal conditions the oxidation peak currents exhibited good linear relationship with the HQ concentration in the range from 0.13 to 100.0l M/L with the detection limit of 0.07 μM/L (3r). The CIE showed separated electrochemical response to HQ and CC in the mixture solution. The proposed method was successfully applied to HQ detection in artificial wastewater with the recovery in the range from 98.9% to 102.0% [124].

Dong *et al.*, 2012, made hydrophobic IL-functionalized SBA-15 modified carbon paste electrode (CPSPE) and its electrochemical performance was investigated by CV, electrochemical impedance spectra, and chronocoulometry in $K_3Fe(CN)_6/K_4Fe(CN)_6$ solution. Compared with carbon paste electrode (CPE) and SBA-15 modified carbon paste electrode (CSPE), the electron transfer ability was in the sequence as: CPSPE>CSPE>CPE. Meanwhile, the electrocatalytic activity of CPSPE to CC and HQ was evaluated by CV, and then, the linear concentration ranges were obtained by the amperometric detection from 2.0×10^{-5} to 3.2×10^{-4} M for CC and 5.0×10^{-5} to 5.5×10^{-4} M for HQ, with the detection limits of 5.0×10^{-7} and 6.0×10^{-7} M respectively. The advantages of both ionic liquids and heterogeneous supports made CPSPE exhibit high electrocatalytic activity towards the redox of CC and HQ by significantly improving their reversibility and enhancing their peak currents. In addition, the present method was applied to the determination of CC and HQ in artificial waste water sample, and the results were satisfactory [125].

Hua *et al.*, 2012, used an IL 1-ethyl-3-mmethylimidazolium tetrafluoroborate ($EMIMBF_4$) to make a modified carbon paste electrode. Then a gold nanoparticle (Au-NPs) and graphene composite film was co-electrodeposited on the carbon IL electrode (CILE) surface by immersing CILE in the graphite oxide and tetrachloroauric acid dispersion solution with CV reduction. The fabricated Au-NPs–GN/CILE exhibited good electrochemical performances with higher conductivity and lower electron transfer resistance. Electrochemical behaviors of HQ were further investigated on the modified electrode by CV and DPV. A pair of well-defined redox peaks appeared with the peak-to-peak separation (Ep) as 0.077 V in 0.1 M/L pH 2.5 PBS, indicating a fast quasi-reversible electron transfer process. The result could be attributed to the presence of high conductive Au-NPs–GN nanocomposites on the electrode surface. The electrochemical parameters of HQ on the Au-NPs–GN/CILE were calculated and the experimental conditions were optimized. Under the optimal conditions, the linear relationship between the oxidation peak current of HQ and its concentration can be obtained in the range from 0.06 μM/L to 800.0 μM/L with the detection limit as 0.018 μM/L (3σ). The coexisting CC exhibited no interference and Au-NPs–GN/CILE was applied to the detection of HQ in synthetic wastewater samples with satisfactory results [126].

Ma and Zhao, 2012, prepared a new composite electrode with doping graphene into the paste consisting graphite and IL, n-octylpyridinum hexafluorophosphate (OPFP). This

electrode shows an excellent electrochemical activity for the redox of HQ, CC and RS. In comparison with bare paste electrode, the redox peaks of three isomers of dihydroxybenzene can be obviously, simultaneously observed at graphene doping paste electrode. Under the optimized condition, the simultaneous determination of HQ, CC and RS in their ternary mixture can be carried out with a DPV technique. The peak currents are linear to the concentration of HQ, CC and RS in the range from 1×10^{-5} to 4×10^{-4}, 1×10^{-5} to 3×10^{-4} and 1×10^{-6} to 1.7×10^{-4} M/L respectively. The limits of detection are 1.8×10^{-6} M/L for HQ, 7.4×10^{-7} M/L for CC and 3.6×10^{-7} M/L for RS, respectively [127].

Liu *et al*., 2012, developed a simple sensor based on bare carbon ionic liquid electrode for simultaneous determination of DHBIs in 0.1 mol L^{-1} PBS (pH 6.0). The oxidation peak potential of HQ was about 0.136 V, CC was about 0.240 V, and RS 0.632 V by DPV measurements, which indicated that the DHBIs could be separated absolutely. The sensor showed wide linear behaviors in the range of 5.0×10^{-7} – 2.0×10^{-4} M/L for HQ and CC, 3.5×10^{-6} – 1.535×10^{-4} M/L for RS, respectively. And the detection limits of the three DHBIs were 5.0×10^{-8}, 2.0×10^{-7}, 5.0×10^{-7} M/L,respectively(S/N=3). The proposed method could be applied to the determination of DHBIs in artificial wastewater and the recovery was from 93.9% to 104.6% [128].

2.1 Aim of the present work

CC, HQ and RS are isomers of dihydoxybenzene. All of them are phenolic compounds and often coexist as isomers in environmental samples. The simultaneous detection of CC, HQ and RS is highly desirable due to their coexistence as isomers and highly toxic environmental pollutants in the environment [129]. The established methods for the detection of CC, HQ and RS are commonly performed after pretreatment and separation. The pretreatment and separation as well as the significant operating complexity, the long detection times and the large volumes of reagents consumption by the present techniques come forward them on challenges.

From the literature, it is seen that most of the work for the simultaneous detection has been done by modified GCE, where some can successfully detect the three isomers and some can detect only two. But in order to detect three isomers simultaneously in most cases glassy carbon is modified by graphene and carbon nanotube which are very costly.

For simultaneous detection, carbon paste electrode has a great effect and the lowest detection limits. Only n-octylpyridinium hexafluorophosphate modified carbon paste electrode can detect three isomers simultaneously; 1-hexylpyridinium hexafluorophosphate and 1-butyl-3-methyl imidazolium hexafluorophosphate modified carbon paste electrode can only detect HQ with very low detection limit but they didn't used for simultaneous detection. But the fabrication of carbon paste electrode is very difficult and it needs very much specialization to make it and use it. The carbon paste is made by ionic liquid which is also expensive and rare to purchase. A huge amount of ionic liquid is waste in this way because the experiment needs new active surface for every time. Therefore it is still important to develop a new facile, cheap method capable of simultaneous *in situ* detection of the phenolic isomers. Pencil graphite is very cheap and available material and ionic liquid is not only a carbon particle binder but also an organic salt can be used as the raw materials for fabricating the new sensor of developed techniques, the aim of our research. Keeping all these fact the main aims of the present work are-

(i) to establish the complete redox behaviors of CC, HQ and RS in aqueous media at bare PGE.

(ii) to modify the electrode with two ionic liquids (1-Hexylpyridinium hexafluorophosphate and 1-Butyl-3-Methylimidazolium hexafluorophosphate) for the improvement of the selectivity of these electrodes towards CC, HQ and RS.

(iii) to compare the redox behavior of the three isomers at bare PGE and IL modified PGE.

(iv) to compare the behavior of the three isomers at two different IL modified PGE.

(v) to detect the isomers simultaneously (one in presence of other) in aqueous solution at two different IL modified PGE.

CHAPTER III

Experimental

The redox behavior of different isomers of dihydroxybenzene, mechanism of electrochemical reactions in aqueous medium has been observed using CV at PGE. The selectivity of electrode reactions has been improved by modifying the electrodes with 1-hexylpyridinium hexafluorophosphate (HIL) and 1-butyl-3-methylimidazolium hexafluorophosphate (BIL). The modified electrodes have been characterized by SEM. DPV has been employed for the quantitative estimation of the isomers simultaneously. The modification of the electrodes has also been evaluated with the response of the isomers in UV-Vis Spectroscopy. Details of the instrumentations are given in the following sections. The sources of different chemicals, the instruments and brief description of the methods are given below.

3.1 Chemicals

All the Chemicals used in this research work were analytical grade obtained from British Drug House (BDH) of England, Tokyo Chemical Industry (TCI) and Sigma-Aldrich Chemical Company. The used chemicals were-

(i) Catechol (BDH, England)
(ii) Hydroquinone (BDH, England)
(iii) Resorcinol (BDH, England)
(iv) Sodium dihydrogen phosphate, NaH_2PO_4 (Sigma-Aldrich)
(v) Disodium hydrogen phosphate, Na_2HPO_4 (Sigma-Aldrich)
(vi) 1-Hexylpyridinium hexafluorophosphate (TCI, Japan)
(vii) 1-Butyl-3-methylimidazolium hexafluorophosphate (TCI, Japan)
(viii) Alumina (0.5μm) (CH Instrument, USA)
(ix) For cleaning and all other purposes double distilled water was used

3.2 Equipments

During this research work some instruments were used. The electrochemical studies (CV and DPV) were performed with a PC controlled potentiostat (μ-stat 8000,

DropSens, Spain). Graphite pencil, grade 2B (Local market) was used as working electrode. Ag/AgCl was reference electrode. Coil of Pt wire was counter electrode Magnetic stirrer (Glassgo, India) with a Teflon coated magnetic bar. pH meter (Hanna Instruments) was employed for maintaining the pH of the solutions. Solutions were prepared using ordinary laboratory glassware. An electronic balance (Model: HR-200, Japan) was used to weigh required amount of compounds. Scanning Electron Microscopy (Manufactured by Jeol, USA) was used for the electrode surface characterization. UV-Vis Spectrophotometer (Model: Heλios γ, Thermo Scientific, USA) was used spectroscopic analysis. Anti-cutter, offset paper, polishing pads etc were also used as accessories.

3.3 Cyclic Voltammetry

There are several well established electrochemical techniques for the study of electrochemical reactions. Here three electrode system CV technique was employed to study and analyze the redox reactions occurring at the electrode surface. This technique helps us to understand the mechanism of electron transfer reaction of the compounds as well as the nature of reactants or products on the electrode surface. The useful parameters derived from the data obtained from the CV experiments are cathodic peak current (i_{pc}), anodic peak current (i_{pa}), cathodic peak potential (E_{pc}), anodic peak potential (E_{pa}). These parameters along with controlled outputs including scan rates are used to diagnose the reaction pattern and the behavior of the reaction.

CV is the most effective and versatile electroanalytical technique available for the electrochemical study of any redox systems. It enables the electrode potential to be rapidly scanned in search of redox couples. Once located, a couple can then be characterized from the potentials of peaks on the cyclic voltammogram and from changes caused by variation of the scan rate. CV consists of imposing an excitation potential nature on an electrode immersed in solution and measuring the current. The potential ranges vary from a few millivolts to hundreds of millivolts per second in a cycle. This variation of anodic and cathodic current with imposed potential is termed as voltammogram [130].

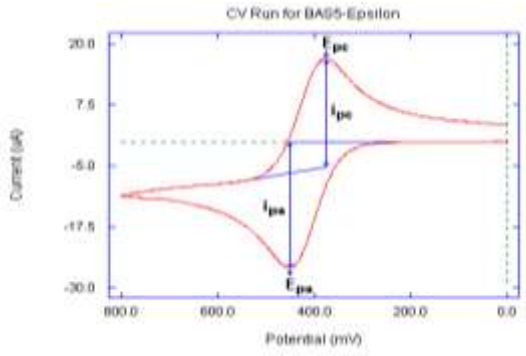

Figure 3.1: A typical CV and its various parameters.

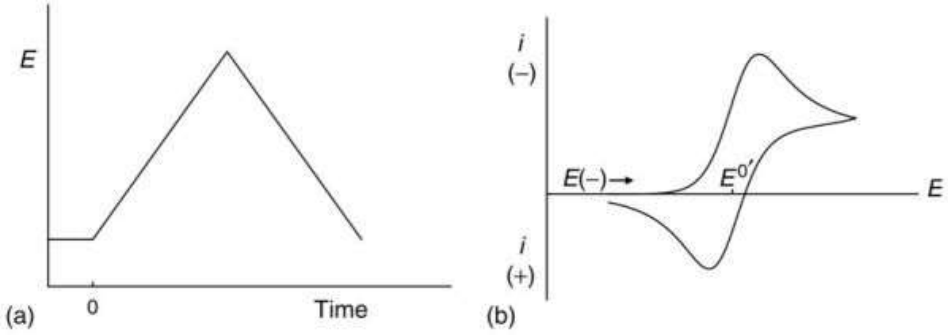

Figure 3.2: (a) A typical excitation signal in CV (b) corresponding voltammogram.

The technique involves under the diffusion controlled mass transfer condition at a stationary electrode utilizing symmetrical triangular scan rate ranging from 1mV/s to hundreds millivolts per second.

In CV the current function can be measured as a function of scan rate. The potential of the working electrode is controlled vs. a reference electrode such as Ag/AgCl electrode. The electrode potential is ramped linearly to a more negative potential and then ramped in reversed back to the starting voltage. The forward scan produces a current peak for any analyte that can be reduced through the range of potential scan. The current will increase as the current reaches to the reduction potential of the analyte [131].

The current at the working electrode is monitored as a triangular excitation potential is applied to the electrode. The resulting voltammogram can be analyzed for fundamental information regarding the redox reaction. The potential at the working electrode is controlled vs a surface electrode, Ag/AgCl(s)/Cl^- electrode. The excitation signal varies linearly with time. First scan positively and then the potential is scanned in reverse, causing a negative scan back to the original potential to complete the cycle. Signal on multiple cycles can be used on the scan surface. A cyclic voltammogram is plot of

response current at working electrode to the applied excitation potential. The cyclic voltammetric technique reveals information about the following important phenomena:

i) reversibility of a reaction and a very rapid means of analysis of various systems
ii) direct investigation of reactive intermediate
iii) investigation of stepwise electrochemical and chemical reaction
iv) redox characteristic of oxidizing-reducing couple
v) investigation of charge transfer reaction at the electrode-solution interface and determination of charge transfer rate constant.

3.4 Important Features of Cyclic Voltammetry

An electrochemical system containing species 'O' capable of being reversibly reduced to 'R' at the electrode is given by,

$$O + ne = R \qquad (1)$$

Nernst equation for the system is

$$E = E^{O} + \frac{0.059}{n} \log \frac{C_0^S}{C_R^S} \qquad (2)$$

where,

E = Potential applied to the electrode, E^o = Standard reduction potential of the couple versus reference electrode, n = Number of electrons in Eq. (1), C_0^S = Surface concentration of species 'O', C_0^S = Surface concentration of species 'R'.

A redox couple that changes electrons rapidly with the working electrode is termed as electrochemically reverse couple. For Eq. (2), the relation gives the cathodic peak current $i_{pc,}$

$$i_{pc} = 0.4463\ nFA\ (D\alpha)^{1/2}C \qquad (3)$$

$$\alpha = \left(\frac{nFv}{RT}\right) = \left(\frac{nv}{0.026}\right)$$

where,

i_{pc} = cathodic peak current in amperes, F = Faraday's constant (approximately 96500), A = Area of the working electrode in cm^2, V = Scan rate in volt/sec, C = Concentration of the bulk species in mol/L, D = Diffusion coefficient in cm^2/sec.

In terms of adjustable parameters, the cathodic peak current is given by the Randless-Sevcik equation,

$$i_{pc} = 2.69 \times 10^5 x n^{3/2} A D^{1/2} C v^{1/2} \quad (4)$$

The cathodic peak potential E_{pc} for reversible process is related to the half wave potential $E_{1/2,}$ by the expression,

$$E_{pc} = E_{1/2} - 1.11\left(\frac{RT}{nF}\right) \qquad \text{at } 25^oC \quad (5)$$

$$E_{pc} = E_{1/2} - \left(\frac{0.0285}{n}\right) \quad (6)$$

The relation relates the half wave potential to the standard electrode potential

$$E_{1/2} = E^0 - \frac{RT}{nF} \ln \frac{f_{red}}{f_{ox}} \left(\frac{D_{ox}}{D_{ox}}\right)^{1/2}$$

$$E_{1/2} = E^0 - \frac{RT}{nF} \ln \left(\frac{D_{ox}}{D_{red}}\right)^{1/2} \quad (7)$$

Assuming that the activity coefficient f_{ox} and f_{red} are equal for the oxidized and reduced species involved in the electrochemical reaction.

From equation (6), we have,

$$E_{pa} - E_{pc} = 2.22\left(\frac{RT}{nF}\right) \qquad \text{at } 25^0C \quad (8)$$

$$\text{or,} \quad E_{pa} - E_{pc} = \frac{0.059}{n} \qquad \text{at } 25^0C \quad (9)$$

This is a good criterion for the reversibility of electrode process. The value of i_{pa} and i_{pc} should be close for a simple reversible couple,

$$i_{pa}/i_{pc} \approx 1 \quad (10)$$

And such a system $E_{1/2}$ can be given by,

$$E_{1/2} = \left(\frac{E_{pa} + E_{pc}}{2}\right)$$

For irreversible processes (those with sluggish electron exchange), the individual peaks are reduced in size and widely separated. Totally irreversible systems are characterized by a shift of the peak potential with the scan rate [132]:

$$E_p = E° - (RT/\alpha n_a F)[0.78 - \ln(k^o/(D)^{1/2}) + \ln (\alpha n_a F\alpha/RT)^{1/2}]$$

Where α is the transfer coefficient and n_a is the number of electrons involved in the charge-transfer step. Thus, E_p occurs at potentials higher than E°, with the over potential related to k° (standard rate constant) and α. Independent of the value k°, such peak displacement can be compensated by an appropriate change of the scan rate. The peak potential and the half-peak potential (at 25°C) will differ by 48/αn mV. Hence, the voltammogram becomes more drawn-out as αn decreases.

The peak current, given by

$$\boldsymbol{i}_p = (2.99x10^5)n(\alpha n_a)^{1/2}ACD^{1/2}v^{1/2}$$

is still proportional to the bulk concentration, but will be lower in height (depending upon the value of α). Assuming α = 0.5, the ratio of the reversible-to-irreversible current peaks is 1.27 (*i.e.* the peak current for the irreversible process is about 80% of the peak for a reversible one). For quasi-reversible systems (with $10^{-1} > k° > 10^{-5}$ cm/s) the current is controlled by both the charge transfer and mass transport. The shape of the cyclic voltammogram is a function of the ratio $k°/(\pi vnFD/RT)^{1/2}$. As the ratio increases, the process approaches the reversible case. For small values of it, the system exhibits an irreversible behavior. Overall, the voltammograms of a quasi-reversible system are more drawn out and exhibit a larger separation in peak potentials compared to a reversible system.

Unlike the reversible process in which the current is purely mass transport controlled, currents due to quasi-reversible process are controlled by a mixture of mass transport and charge transfer kinetics [133-134]. The process occurs when the relative rate of electron transfer with respect to that of mass transport is insufficient to maintain Nernst equilibrium at the electrode surface.

3.5 Differential Pulse Voltammetry

DPV is often used to make electrochemical measurements. It can be considered as a derivative of linear sweep voltammetry or staircase voltammetry, with a series of regular voltage pulses superimposed on the potential linear sweep or stair steps. The current is measured immediately before each potential change, and the current difference is plotted

as a function of potential. By sampling the current just before the potential is changed, the effect of the charging current can be decreased.

By contrast, in normal pulse voltammetry the current resulting from a series of ever larger potential pulses is compared with the current at a constant 'baseline' voltage. Another type of pulse voltammetry is squarewave voltammetry, which can be considered a special type of DPV in which equal time is spent at the potential of the ramped baseline and potential of the superimposed pulse. The potential wave form for DPV is shown in (Figure 3.3). The potential wave form consists of small pulses (of constant amplitude) superimposed upon a staircase wave form [135]. Unlike NPV, the current is sampled twice in each Pulse Period (once before the pulse, and at the end of the pulse), and the difference between these two current values is recorded and displayed.

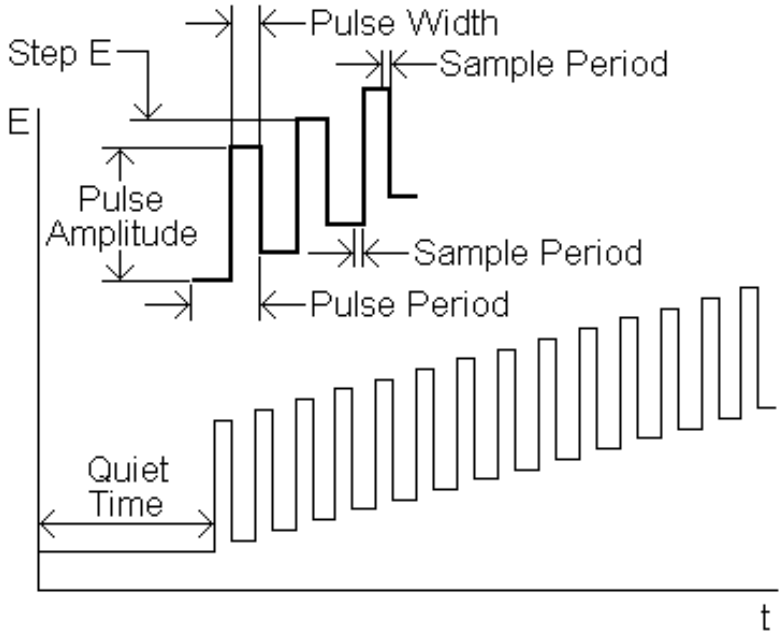

Figure 3.3: Excitation signal and potential wave form for DPV.

3.6 Important features of differential pulse voltammetry

DPV has these characteristics:

i) Reversible reactions show symmetrical peaks, and irreversible reactions show asymmetrical peaks.

ii) The peak potential is equal to $E_{1/2}^{r}$-ΔE in reversible reactions, and the peak current is proportional to the concentration.

iii) The detection limit is about 10^{-8} M.

3.7 Computer controlled potentiostat (for CV and DPV experiment)

In this study the current voltage system was a PC controlled potentiostat (μ-stat 8000, DropSens, Spain. A potentiostat system sets the control parameters of the experiments. Its purpose is to impose a cyclic linear potential sweep on the working electrode and to output the resulting current potential curve. This sweep is described in general by its initial (E_i), switching (E_s) and final (E_f) potentials and scan rate (V/s).

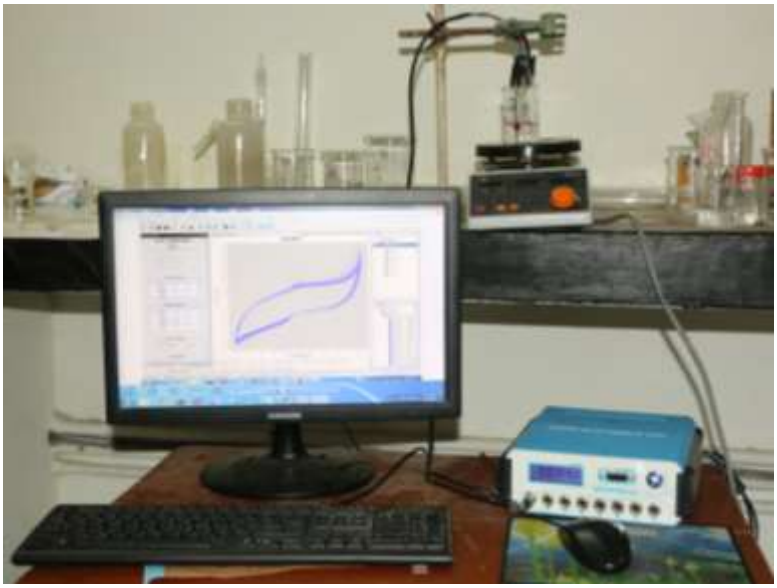

Figure 3.4: The computer controlled potentiostat (μ-stat 8000, DropSens).

3.8 Electrochemical cell

This research work was performed by a three electrodes electrochemical cell. The voltammetric cell also contains a Teflon cap. The electrochemical reaction of interest takes place at the working electrode and the electrical current at this electrode due to electron transfer is termed as faradic current. The counter electrode is driven by the potentiostatic circuit to balance the faradic process at the working electrode with an electron transfer of opposite direction.

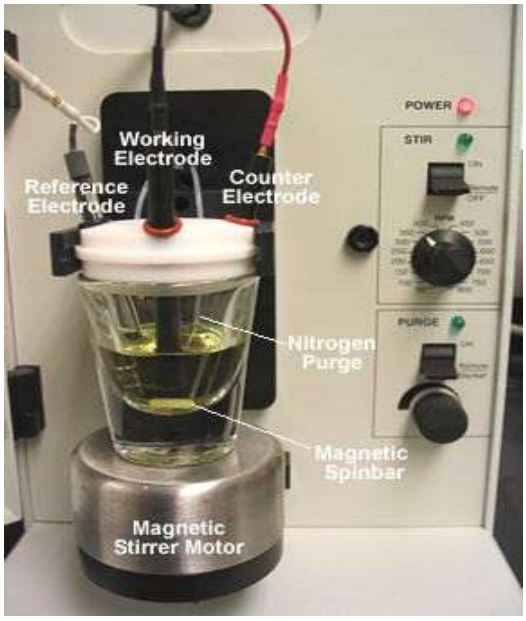

Figure 3.5: The three electrode system consisting of a working electrode, a reference electrode and a counter or auxiliary electrode.

An electrolytic cell consist three types of electrode. They are –

1. Working electrode
2. Counter electrode
3. Reference electrode

3.8.1 Working electrode

Working electrode is one on which electrochemical reaction occurs. Conventional working electrodes are Pt electrode, Au electrode, Glassy carbon electrode etc.

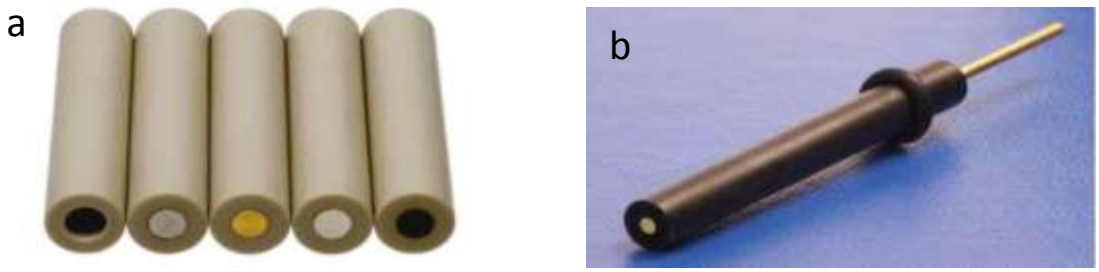

Figure 3.6: (a) Working electrodes, (b) 2D gold electrode.

The inner circles represent the working portion of the working electrode. The diameter varies generally from 0.5 mm to 3 mm. But in this experiment we have made and used the following PG working electrode.

Figure 3.7: PG working electrode.

3.8.2 Counter electrode

It is also called auxiliary electrode, is used to balance the electric current that is expected to flow through the working electrode. Generally spiral platinum wires are used. Sometimes mesh is also used. The surface area should be at least 3 times of the corresponding working electrode. For accurate electrochemical measurements generally we have used counter electrode made by platinum wire (spiral wire) that has surface area about 100 times of working electrode. The large surface area of counter electrode is efficient to pull up or take the excess current from the cell to the outside of the cell.

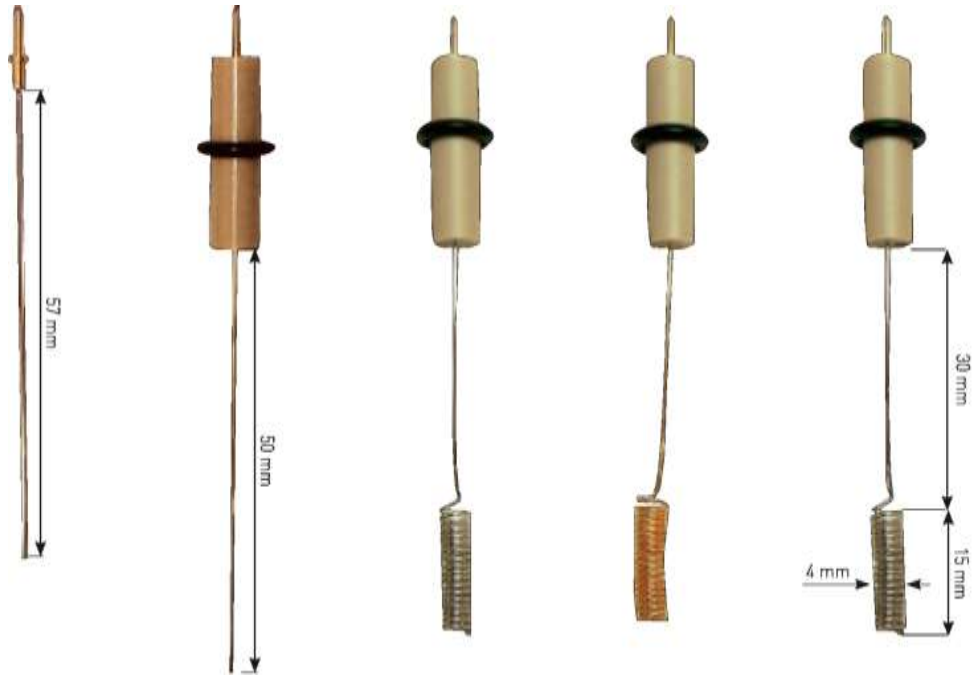

Figure 3.8: Some commercially available Counter electrodes (spiral wires).

Figure 3.9: (a) Counter electrodes (mesh) (b) Counter electrode used in our research.

3.8.3 Reference electrode

It is used to measure the potential of working electrode. For example, Standard calomel electrode, glass electrode, silver-silver chloride electrode etc. Every reference electrode has its own standard potential value. By comparing the potentials of working and reference electrodes, the exact value of potential of working electrode can be measured.

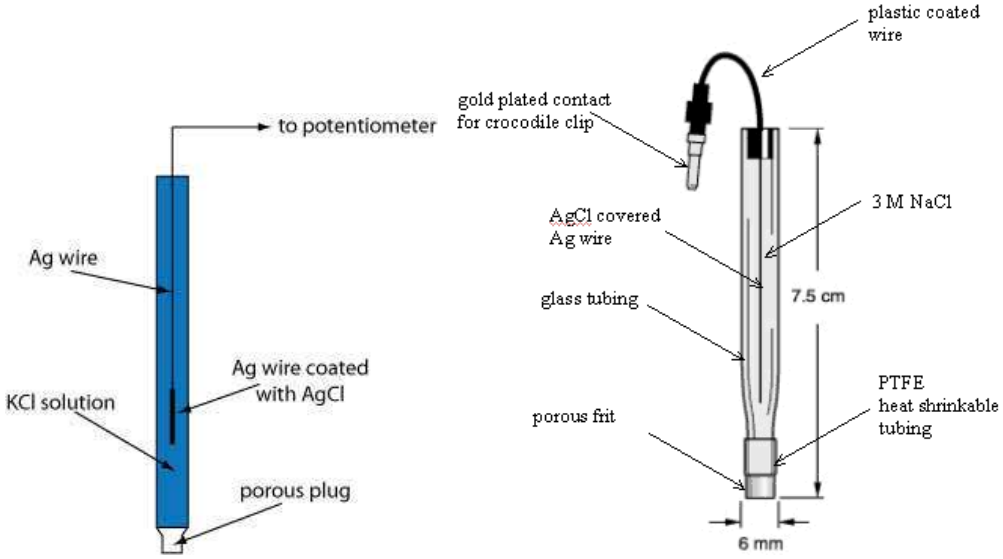

Figure 3.10: Silver | Silver Chloride (Ag | AgCl) reference electrode. The potential of a Ag/AgCl electrode is +0.222 V at 25^{o}C.

This electrode comprised of a silver chloride coated silver wire in a glass tube with a porous polymer tip. The glass tube formed an electrode compartment which was filled with 3M KCl.

Crocodile clips made by stainless steel are used to connect the electrolytic cell to the potentiometer as shown in the following picture.

Figure 3.11: Crocodile clips or connector used in electrolytic cell.

3.9 Electrodes used in experiment

(i) Working electrode is PGE with 2 mm diameter smooth graphite disc.

(ii) Ionic liquid modified PGEs are also used to increase the selectivity.

(iii) Ag/AgCl/Cl^- electrode used as reference electrode.

(iv) Counter electrode is a Pt-wire.

The working electrode is an electrode where the redox reactions of the substances take place. The reference electrode provides the current required to sustain in electrolysis at the working electrode so that is behavior remains essentially constant with the passage of small current. The counter electrode in the three-electrode system is made of an inert metal.

3.10 Preparation of Wooden Pencil Graphite Electrode

The working electrode used in this study is PGE. 2B pencil was brought from the local market and was cut into two pieces. Each piece is approximately 3 inches. To obtain graphite rod, wooden part of the two sides of the pencil was cut off by a sharp anti cutter. Then it was washed by distilled water and dried in air and the sun. One part of the graphite rod was painted by nail polish and the end tip of the rod was left free or unpainted for using as electrodes surface. Nail polish was used to cover the side portion of graphite rod, so that only uncovered portion can take part as surface of working electrode. It was used to make the surface area constant. Teflon tape or other covering substances, which do not take part in reaction or electric conduction, can be used. Then this end tip was polished by rubbing it on a smooth offset white paper. The resultant end tip of the rod surface would look like a shiny black mirror. Other part of the graphite rod

(unpainted part) was used to make the connection with the potentiostat. Steps of making of PGE has been shown in figure 3.15.

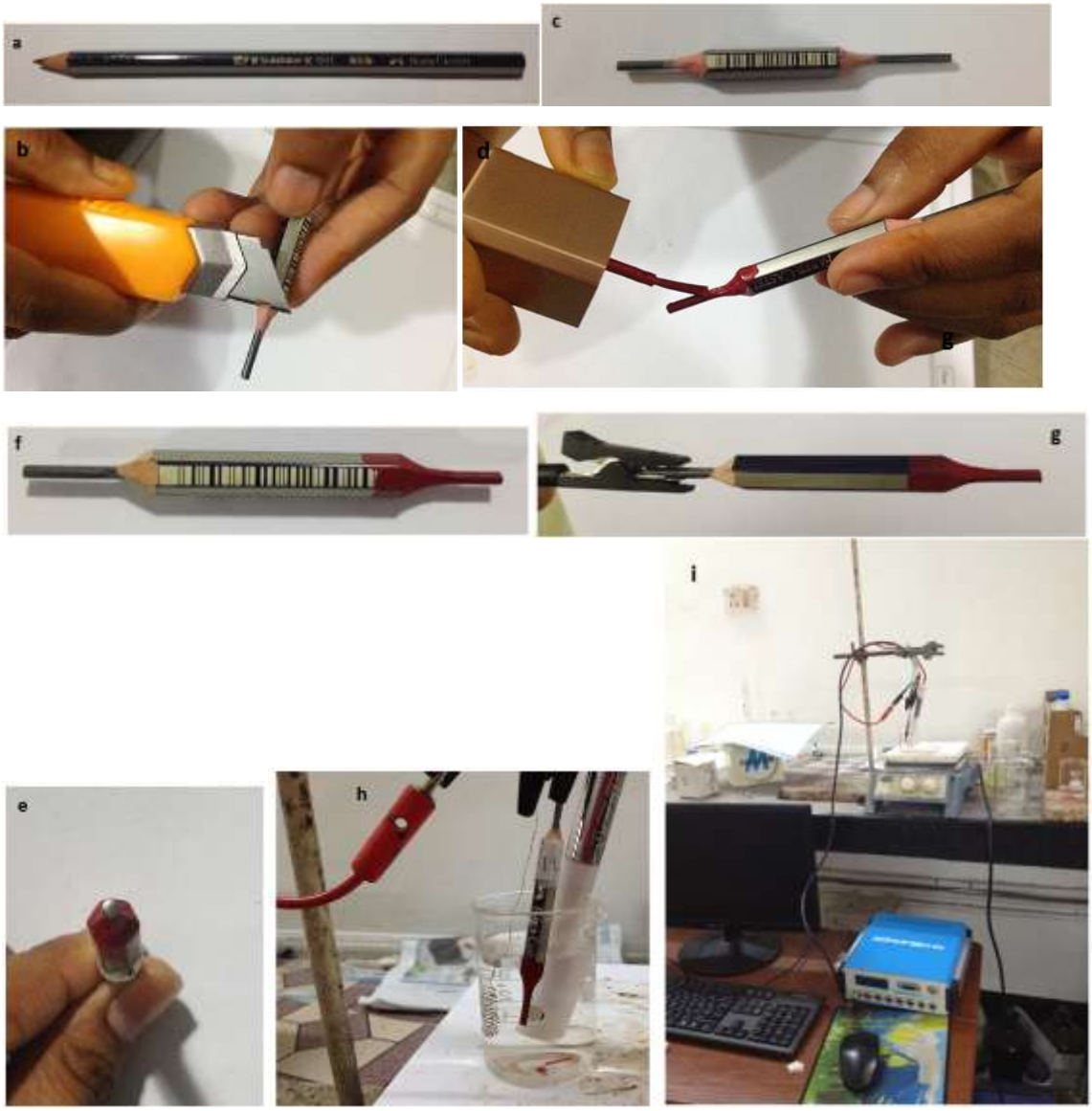

Figure 3.12: (a) A wooden graphite pencil of grade 2B, (b) Using anti cutter to cut off wooden part (c) Two sides of bare graphite rod, (d) Using nail polish to cover one part of graphite rod, (e) Active surface of PGE, (f) PGE used for experiment, (g) the uncovered graphite part was used to establish contact with potentiostat, (h) PGE in three electrode system, (i) A picture of working station with PGE in three electrode system and potentiostat.

3.11 Modification of PGE with 1-hexylpyridinium hexafluorophosphate

0.1 g of HIL was weighted and kept in 40 mL PBS (0.2 M, pH=7) in a beaker. The beaker was covered by parafilm and placed it in an ultrasonic bath for 1 hour. Then it was placed on a magnetic stirrer and stirred for 3 hours at 60°C. Prior to electrochemical

modification, the bare PGE with a diameter of 2 mm was polished on a paper. Then it was rinsed with distilled water. Then electrochemical cell was made ready by connecting electrodes (working: PGE, reference: Ag|AgCl|Cl^- and counter: Pt coil) to the computer controlled potentiostat as shown in figure 3.12(i). CV was run within the range of -0.5 to +1.5 V at 300 mV/s scan rate for 10 scans. These made the PGE modified by HIL. After modification, the modified electrode was electroactivated by CV from -0.5 to +1.0 V at 100 mV/s scan rate in PBS of pH 7.0. Then the electrode was ready for further use after the final washing with water. Hereafter the modified electrode will be referred as the HIL-PGE.

3.12 Modification of PGE with 1-butyl-3-methylimidazolium hexafluorophosphate

0.5 mL of BIL was weighted and kept in 40 mL PBS (0.2 M, PH=7) in a beaker. The beaker was covered by parafilm and placed it in an ultrasonic bath for 30 minutes. Then it was placed on a magnetic stirrer and stirred for 30 minutes at room temperature. Prior to electrochemical modification, the bare PGE with a diameter of 2 mm was polished on a paper. Then it was rinsed with distilled water. Then electrochemical cell was made ready by connecting electrodes (working: PGE, reference: Ag|AgCl|Cl^-(aq) and counter: Pt coil) to the computer controlled potentiostat as shown in figure 3.12(i). CV were run within the range of -0.5 to +1.5 V at 300 mV/s scan rate for 10 scans. These made the PGE modified by BIL. After modification, the modified electrode was electroactivated by CV from -0.5 to +1.0 V at 100 mV/s scan rate in PBS of pH 7.0. Then the electrode was ready for further use after the final washing with water. Hereafter the modified electrode will be referred as the BIL-PGE.

3.13 Removing Dissolved Oxygen from Solution

Sometimes removal of dissolved oxygen from electrochemical solution is needed because it may have interference in the cathodic signals. This was done by purging an inert gas, N_2 (99.99% pure and dry) through the solution for about 20 min.

3.14 Electrode polishing

The electrode was polished on a clean offset white paper before modification and after modification it was only ringed with distilled water.

3.15 Preparation of Various Stock Solutions

i) Catechol solution: Catechol solutions of different concentrations (1to10 mM) were prepared in phosphate buffer.
ii) Hydroquinone solution: Hydroquinone solutions of various concentrations (1to10 mM) were prepared in phosphate buffer solution.
iii) Resorcinol solution: Solutions of various concentration of Resorcinol (1to10 mM) were prepared in and phosphate buffer.
iv) 1-Hexylpyridinium hexafluorophosphate solution was made in PBS.
v) 1-Butyl-3-Methylimidazolium hexafluorophosphate solution was made in PBS.

3.16 Preparation of Buffer Solutions

Phosphate Buffer Solution: Phosphate buffer solution (pH 7.0) was prepared by mixing a solution of 0.2 M Sodium dihydrogen phosphate, NaH_2PO_4 with a solution of 0.2 M Disodium hydrogen phosphate, Na_2HPO_4. The pH of the prepared solution was measured with pH meter (Figure 3.13).

Figure 3.13: pH meter.

3.17 Standardization of the System

The whole electrochemical set-up was tested using a standard experiment. In the standard experiment we have studied the following redox couple at a PGE.

$$[Fe(III)(CN)_6]^{3-} + e^- \rightleftharpoons [Fe(II)(CN)_6]^{4-}$$

The reaction above was studied electrochemically by pumping electrons into the system from a PGE and by measuring the change in the flow of current during the reaction. This is done most conveniently by scanning the potential of the electrode at a constant rate.

3.18 Experimental procedure for cyclic voltammetry

The cell was assembled and filled with 10.0 mL of supporting electrolyte (Phosphate buffer) solution. The surface of the electrodes is completely immersed. To determine the potential window of the scanning is initially carried out with the supporting electrolyte solution to obtain the background voltammogram. The voltammogram containing the analyte in supporting electrolyte is taken under two different modes, at i) various scan rates and ii) various concentrations.

3.19 UV-Vis Spectrophotometry

In spectrometric analysis a source of radiation is used that extends into the ultraviolet region of the spectrum. The instrument employed for this purpose is a spectrophotometer.

An optical spectrometer is an instrument possessing an optical system which can produce dispersion of incident electromagnetic radiation, and with which measurements can be made of the quantity of transmitted radiation at selected wavelength of the spectral range. A photometer is a device for measuring the intensity of transmitted radiation. When combined in the spectrophotometer the spectrometer and photometer are employed conjointly to produce a signal corresponding to the difference between the transmitted radiation of a reference material and that of a sample of selected wavelengths. The essential parts of spectrophotometer are -

i) A source of radiant energy
ii) A monochromator
iii) Glass or silica cells for holding the solvent and for the solution under test
iv) A device to receive of measure the beam or beam of radiant energy passing through the solvent or solution.

Lambert law states that when monochromatic light passes through a transparent medium, the rate of decrease in intensity with the thickness of the medium is proportional to the intensity of light [136]. This is equivalent to stating that the intensity of the emitted light decrease exponentially as the thickness of the absorbing medium increase arithmetically, or that any layer of given thickness of the medium absorbs the same fraction of the light incident upon it.

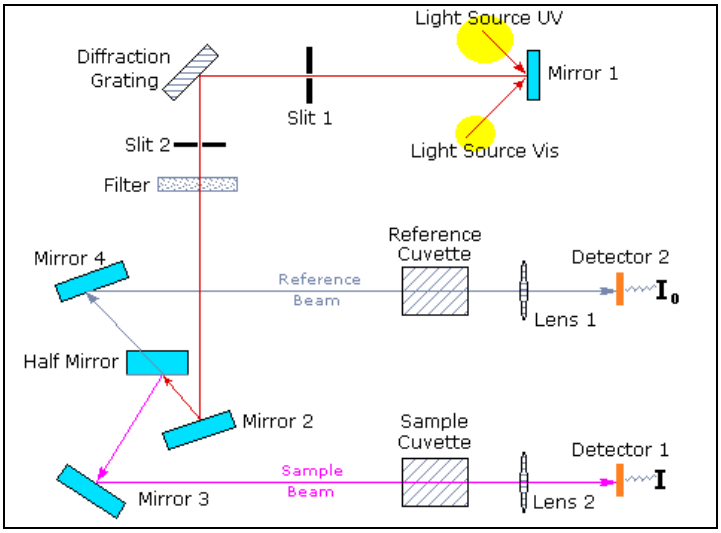

Figure 3.14: Schematic diagram of a UV-visible spectrophotometer.

Beer studied the effect of concentration of the colored constituent in solution upon the light transmission. He found the same relation between transmission and concentration as Lambert had discovered between transmission and thickness of the layer. By combining both of the theories the final expression can be written as,

$$A = \log \frac{I_0}{I_t} = acl$$

Here, I_o=intensity of the incident light; I_t=intensity of the transmitted light; A=Absorbance of the medium and l are dimensions of the cell.

Figure 3.15: UV-visible spectrophotometer.

A computer controlled spectrophotometer (Heλios γ, Thermo Scientific, USA) was used for UV-Vis experiment in a pair of quartz cells.

3.20 Scanning Electron Microscopy

The scanning electron microscope (SEM) is a powerful and frequently used instrument, in both academia and industry, to study, for example, surface topography, composition, crystallography and properties on a local scale. The spatial resolution is better than that of the optical microscope although not quite as good as for the transmission electron microscope (TEM). The SEM has an extremely large depth of focus and is therefore well suited for topographic imaging.

Besides surface topographic studies the SEM can also be used for determining the chemical composition of a material, its fluorescent properties and the formation of magnetic domains and so on. The specimen is bombarded by a convergent electron beam, which is scanned across the surface. This electron beam generates a number of different types of signals, which are emitted from the area of the specimen where the electron beam is impinging (Figure. 3.16).

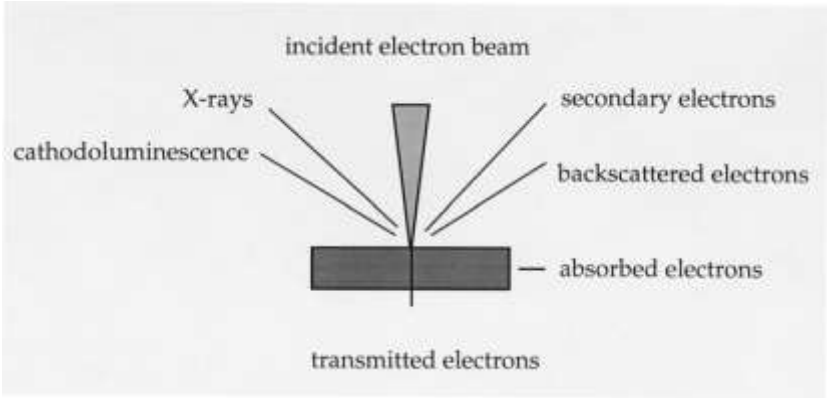

Figure 3.16: Example of some of the different types of signals produced when high-energy electron impinges on a material.

The induced signals are detected and the intensity of one of the signals (at a time) is amplified and used to as the intensity of a pixel on the image on the computer screen. The electron beam then moves to next position on the sample and the detected intensity gives the intensity in the second pixel and so on. The working principle of the SEM is shown in Figure 3.17. For improved signal-to-noise ratio in the image, one can use a

slower scan speed. This means that the electron beam stays a longer time at one position on the sample surface before moving to the next. This gives a higher detected signal and increased signal-to-noise ratio [137].

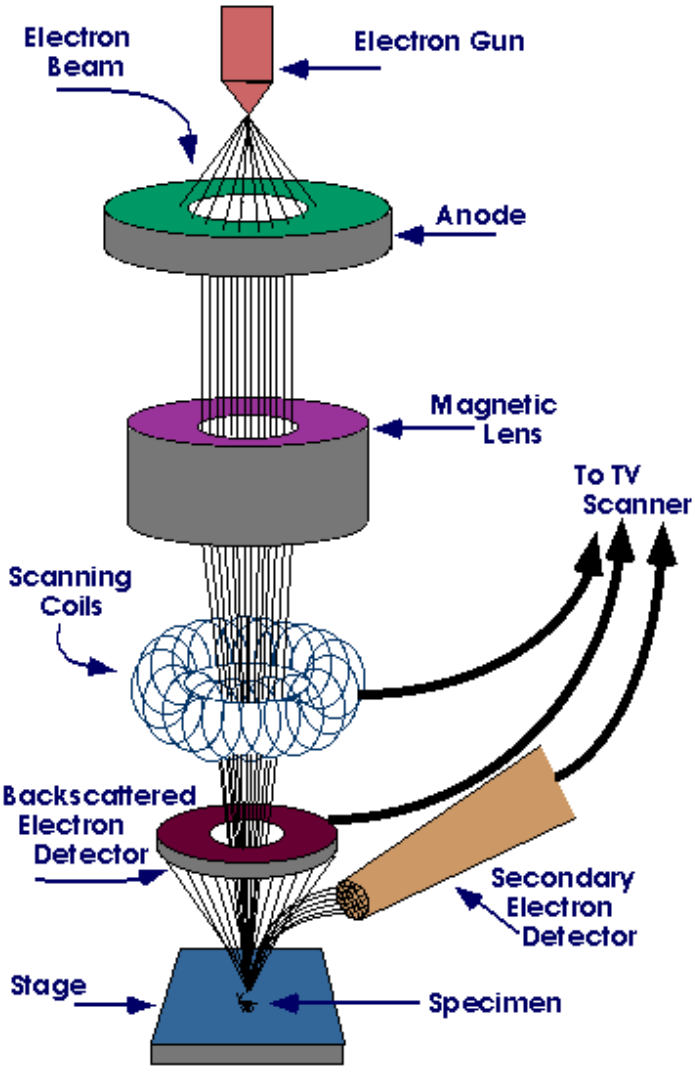

Figure 3.17: Schematic diagram of a SEM.

3.21 Energy Dispersive X-ray Microanalysis

EDX makes use of the X-ray spectrum emitted by a solid sample bombarded with a focused beam of electrons to obtain a localized chemical analysis. All elements from atomic number 4 (Be) to 92 (U) can be detected in principle, though not all instruments are equipped for 'light' elements ($Z < 10$). Qualitative analysis involves the identification of the lines in the spectrum and is fairly straightforward owing to the simplicity of X-ray spectra. Quantitative analysis (determination of the concentrations of the elements

present) entails measuring line intensities for each element in the sample and for the same elements in calibration Standards of known composition. EDX was used for element determination at the surface of bare PGE. By scanning the beam in a television-like raster and displaying the intensity of a selected X-ray line, element distribution images or 'maps' can be produced. Also, images produced by electrons collected from the sample reveal surface topography or mean atomic number differences according to the mode selected. The scanning electron microscope (SEM), which is closely related to the electron probe, is designed primarily for producing electron images, but can also be used for element mapping and even point analyses if an X-ray spectrometer is added. There is thus a considerable overlap in the functions of these instruments [138].

CHAPTER IV

Results and Discussion

General

New electrochemical sensors have been made to develop for the detection of DHBIs in the environment simultaneously. Electrode was made from locally available and cheap Pencil Graphite instead of conventional costly platinum, gold or GCE. Working electrode, PGE, was modified electrochemically by ILs. Modification of the electrode was confirmed by electrochemical as well as several optical techniques. CV and DPV were applied for detection technique. CV was taken to analyte HQ, CC and RS at various scan rates and concentrations. The changes of peak currents were observed with respect to scan rates and concentrations. The nature of the surface controlled reactions was evaluated. DPV was taken for the single, binary and ternary solutions of DHBIs. It can also separate the three isomers simultaneously with high sensitivity. The peak currents of the solutions were compared for HIL-PGE and BIL-PGE.

4.1 SEM images of working electrodes

It has been mentioned earlier in the experimental section 3.10 that PG electrode is used as working electrode and has been made from 2B wooden pencil collected from the local market. Figure 4.1(a) shows the surface morphologies of bare PG electrode. Greyish-black color corresponds to graphite on the surface. Surface is uneven as well. It is also seen from the picture that a lot of grooves present at surface morphology of the PGE. It indicates that the graphite rod of the pencil is not pure crystalline. A lot of defects and few foreign materials may be present there. Figure 4.1(b) and 4.1(c) are the SEM images of modified HIL-PGE and BIL-PGE respectively. It is noted here that modified HIL-PGE and BIL-PGE was obtained by the application of potential at PGE in presence of IL-PBS solution also discussed in section 3.11 and 3.12. The images of the surface of modified electrodes are different from the bare PGE. Both the surfaces of HIL-PGE and BIL-PGE are covered by many different sizes of white spots and fibrous lines. White spots and the fibrous lines may be thin films of IL spread over the surfaces of PGE. These modified PGE could be expected to be an attractive platform for the detection and separation of DHBIs and used to construct brilliant electrochemical sensors.

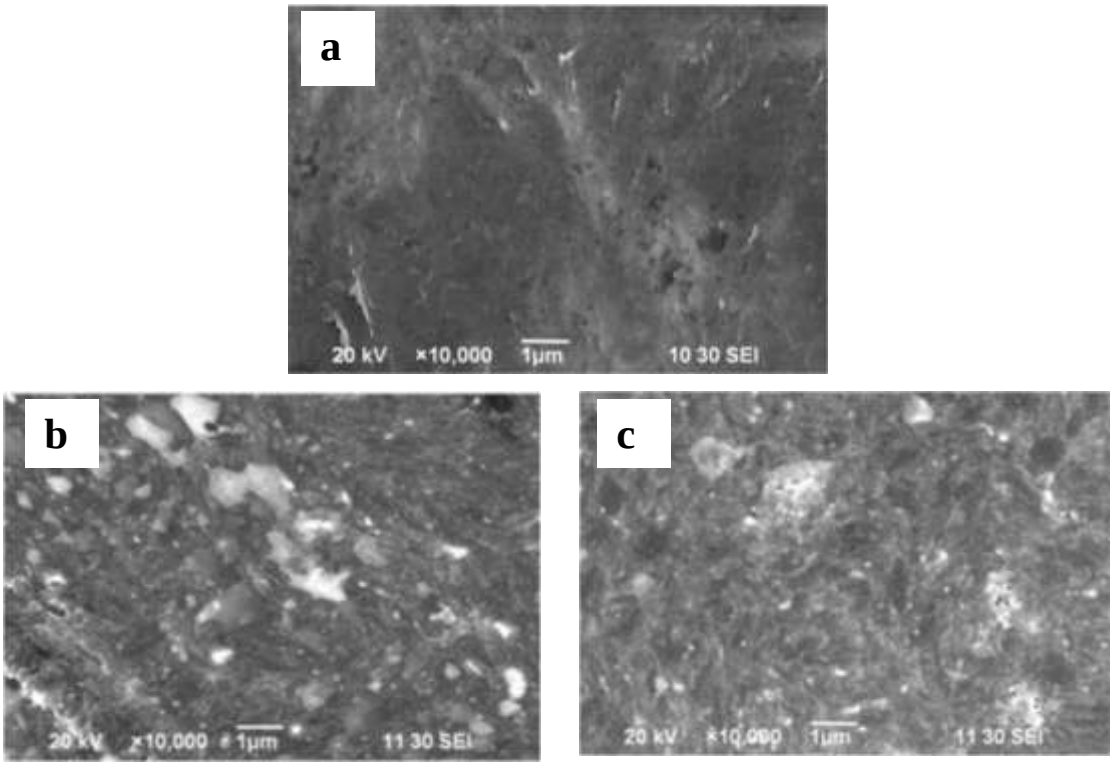

Figure 4.1: SEM image of (a) Bare PGE, (b) HIL-PGE, (c) BIL-PGE.

4.2 EDX of bare PGE

Figure 4.2 shows the EDX results of bare surface of PGE. It is seen from the graph that PGE surface are impure as guessed by SEM in the earlier section. Instead it is composed of 79.39% carbon, 10.03% Si, 3.06% O_2, 3.49% Al, 2.68% Fe and trace amount of Mg and Ca. In bare GCE, there is 100% carbon without impurities. So it may be concluded that PGE is mainly carbon composite material. In spite of impurities present in the graphite of PGE has been modified by IL successfully and exhibits noble response for the simultaneous detection of DHBIs.

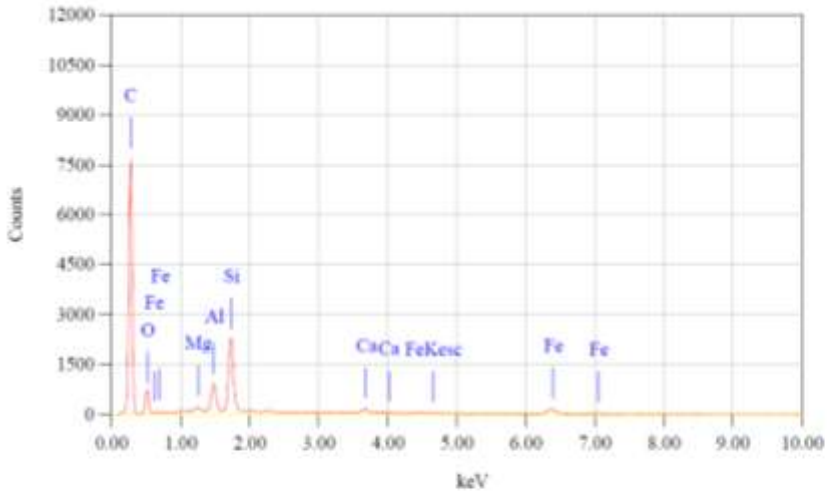

Acquisition Parameter
Instrument : 6490(LA)
Acc. Voltage : 20.0 kV
Probe Current: 1.00000 nA
PHA mode : T3
Real Time : 51.12 sec
Live Time : 50.00 sec
Dead Time : 2 %
Counting Rate: 2556 cps
Energy Range : 0 - 20 keV

Thin Film Standardless Standard Quantitative Analysis
Fitting Coefficient : 0.2641

Element	(keV)	Mass%	Counts	Error%	Atom%	Compound	Mass%	Cation	K
C K (Ref.)	0.277	79.39	42944.57	0.00	89.61				1.0000
O K	0.525	3.06	4350.90	0.03	2.59				0.3805
Mg K	1.253	0.40	786.01	0.39	0.22				0.2759
Al K	1.486	3.49	6562.16	0.05	1.75				0.2878
Si K	1.739	10.03	10574.91	0.02	4.84				0.2920
Ca K	3.690	0.96	1133.56	0.38	0.32				0.4559
Fe K	6.398	2.68	1617.48	0.27	0.65				0.8958
Total		100.00			100.00				

Figure 4.2: EDX of bare PGE.

4.3 Pictorial representation of whole experiment

In the experimental section, the whole research work was described but a pictorial diagram is represented here.

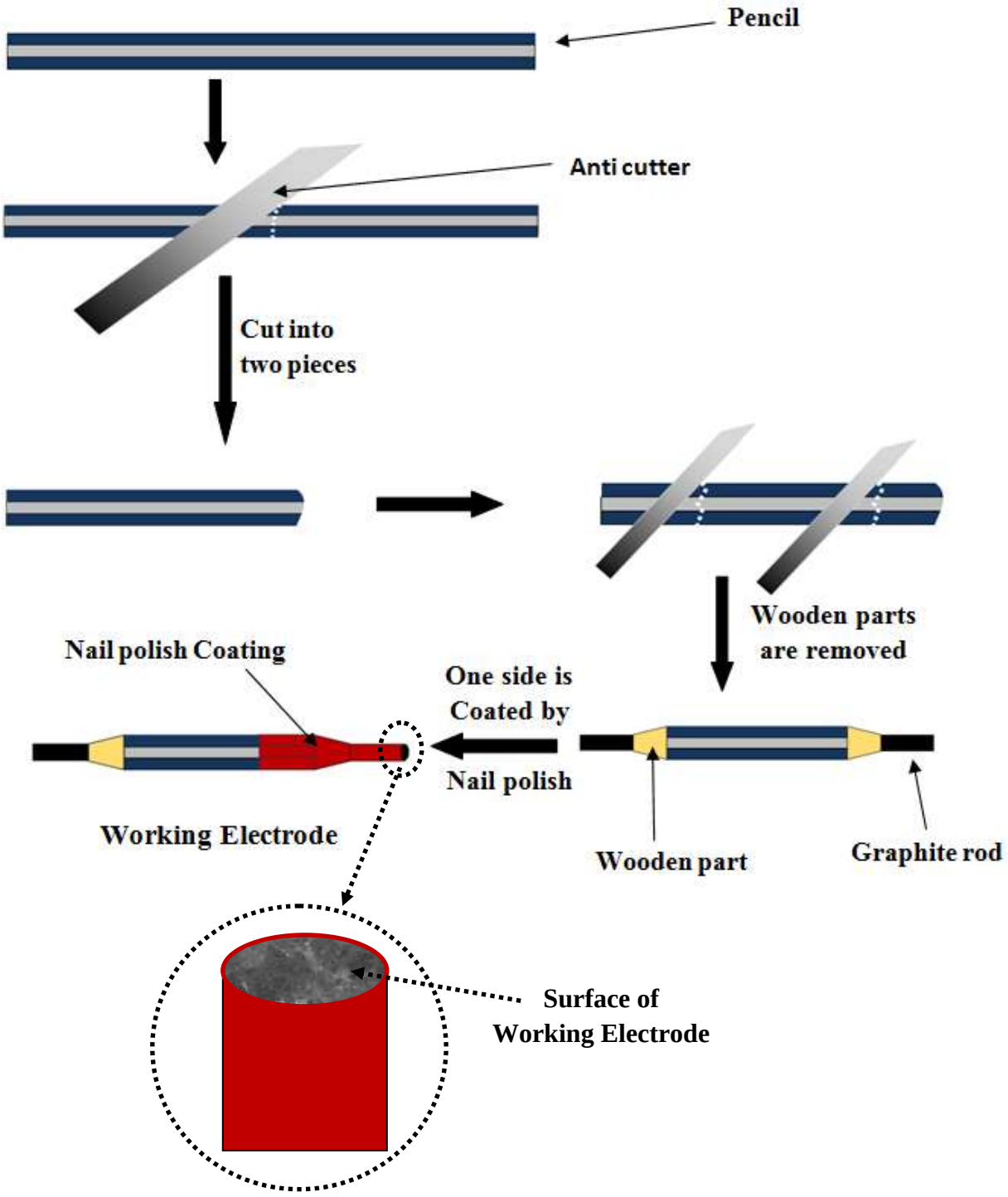

Figure 4.3: Fabrication of Working Electrode.

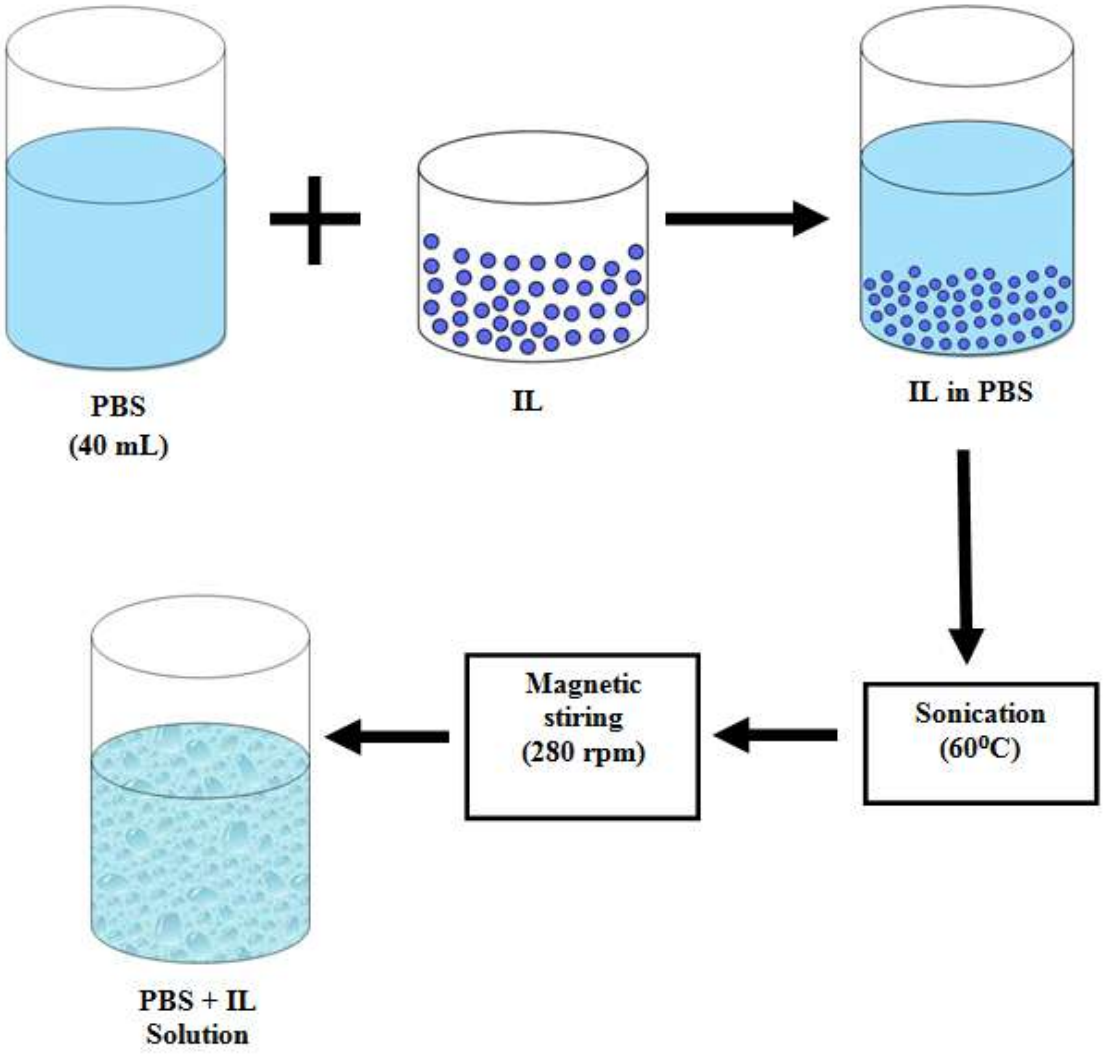

Figure 4.4: Preparation of IL-PBS solution for electrode modification.

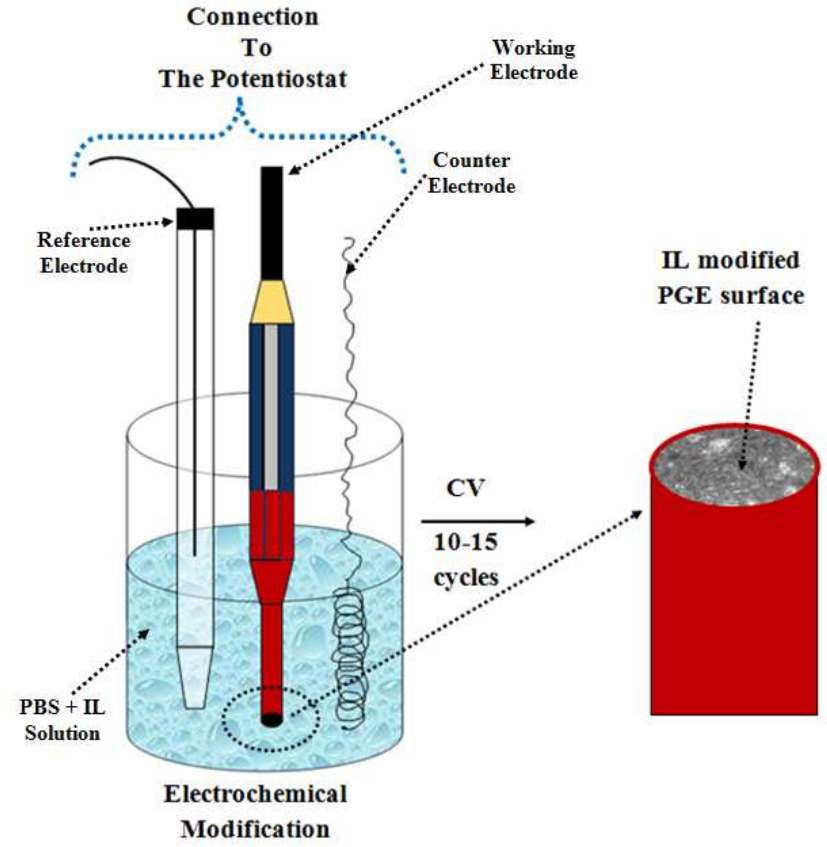

Figure 4.5: Electrochemical modification of PGE.

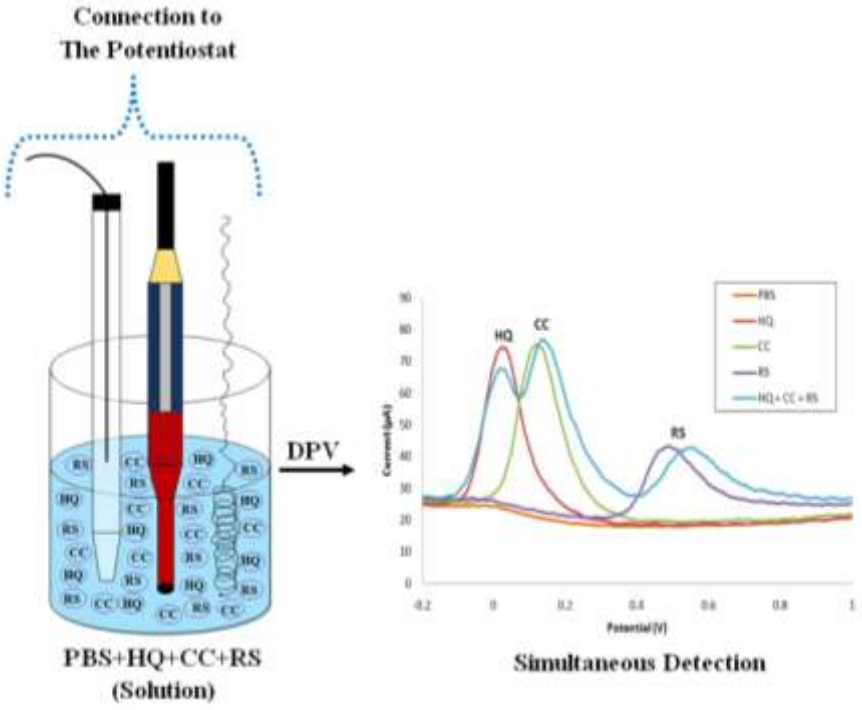

Figure 4.6: Simultaneous detection of HQ, CC and RS at IL modified PGE by DPV.

UV-Vis Spectroscopic Study

UV-Vis spectroscopy was employed for simultaneous detection of DHBIs by Hossain, M. E. [139] from the same research group under supervision of my supervisor as well by me. Almost similar results were obtained. Due to instrumental fault in the UV-Vis spectrophotometer (Heλios γ, Thermo Scientific, USA) the absorbance maxima were obtained at wavelengths for DHBIs with some irregularities in peak lines and also close to the previous one. But the results were compatible to my previous researcher. Here I used the results of UV-Vis spectroscopy of Hossain M. E. with prior permission of the respective researcher's and my data also been cited in appendix I.

4.4 Individual and simultaneous UV-Vis spectrum of CC and HQ

UV-Vis spectrum of CC and HQ was taken in which CC has an absorbance maxima at 275.4 nm and HQ has an absorbance maxima at 288.6 nm (Figure 4.7). When UV spectrum was taken for a binary mixture of CC and HQ in PBS, a single peak was found at 278.2 nm. Thus we can conclude that simultaneous detection of CC and HQ in a binary mixture is impossible using UV-Vis spectrophotometry.

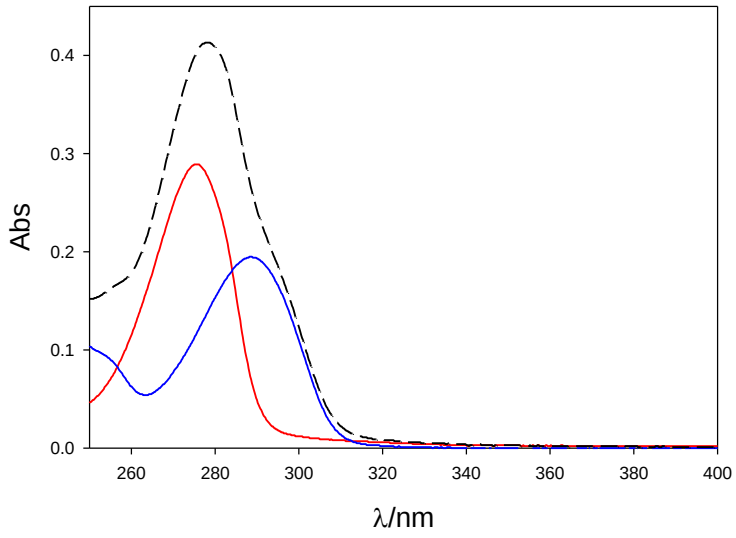

Figure 4.7: UV-Vis spectra of CC, HQ and binary mixture of CC+HQ in PBS.

4.5 Individual and simultaneous UV-Vis spectrum of CC and RS

UV-Vis spectrum of CC and RS was taken in which CC has an absorbance maxima at 275.4 nm and RS has an absorbance maxima at 273.2 nm. When UV spectrum was taken for a binary mixture of CC and RS in PBS, a single peak was found at 274.2 nm. Thus it

can be decided that simultaneous detection of CC and RS in a binary mixture is impossible using UV-Vis spectrophotometry.

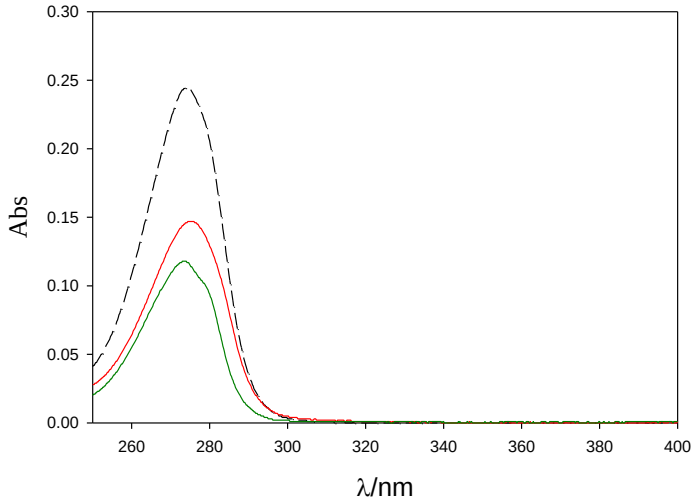

Figure 4.8: UV-Vis spectra of CC, RS and binary mixture of CC+RS in PBS.

4.6 Individual and simultaneous UV-Vis spectrum of HQ and RS

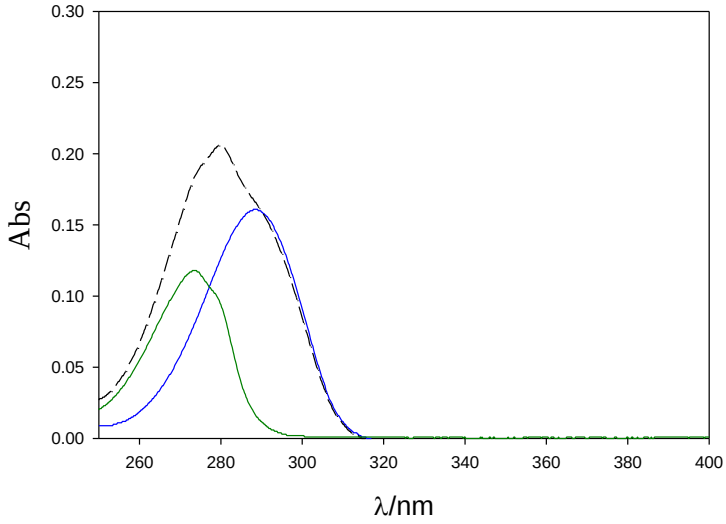

Figure 4.9: UV-Vis spectra of HQ, RS and binary mixture of HQ+RS in PBS.

UV-Vis spectrum of HQ and RS was taken in which HQ has a absorbance maxima at 288.6 nm and RS has an absorbance maxima at 273.2 nm. When UV spectrum was taken for a binary mixture of CC and RS in PBS, a single peak was found at 280.0 nm. Thus it can be told that the simultaneous detection of HQ and RS in a binary mixture is impossible using UV-Vis spectrophotometry.

4.7 Individual and simultaneous UV-Vis spectrum of HQ, CC and RS

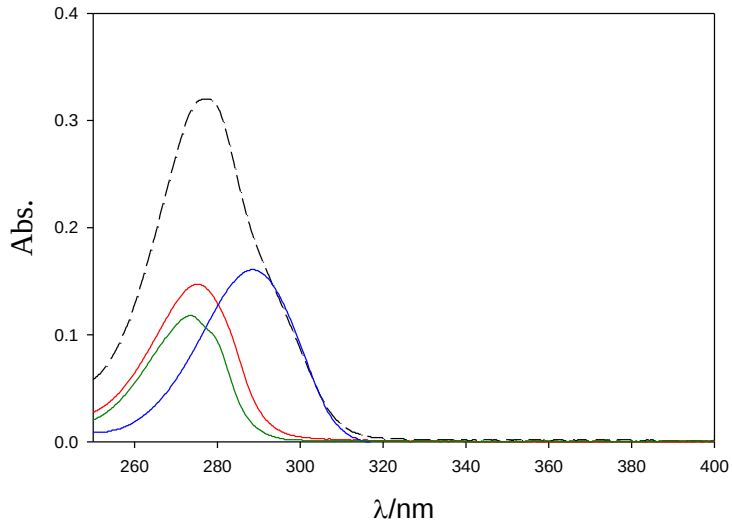

Figure 4.10: UV-Vis spectra of CC, HQ, RS and mixture of CC+HQ+RS in PBS.

UV-Vis spectrum of CC, HQ and RS was taken in which CC has an absorbance maxima at 275.4 nm, HQ has an absorbance maxima at 288.6 nm and RS has an absorbance maxima at 273.2 nm. When UV spectrum was taken for a mixture of CC, HQ and RS in PBS, a single peak was found at 277.4 nm. Thus it can be decided that simultaneous detection of CC, HQ and RS in a mixture is impossible using UV-Vis spectrophotometry.

Electrochemical Study

4.8 Cyclic voltammetric behavior of catechol at bare PGE

The reaction of CC, terms of electron transfer mechanism, corresponding to the following anodic and cathodic reaction [128]:

For the oxidation process, anodic peak corresponds to the following reaction:

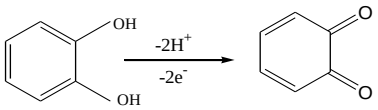

For the reduction process, cathodic peak corresponds to the following reaction:

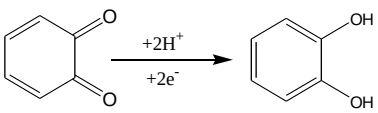

Figure 4.11 shows CV of CC of 5 mM at scan rate 50 mV/s with PBS (0.2 M, pH=7). There is no peak for PBS. Literature says that CC gives one anodic and one cathodic peak [128]. Because there is only CC in buffer solution, one anodic and one cathodic peak should be observed for CC.

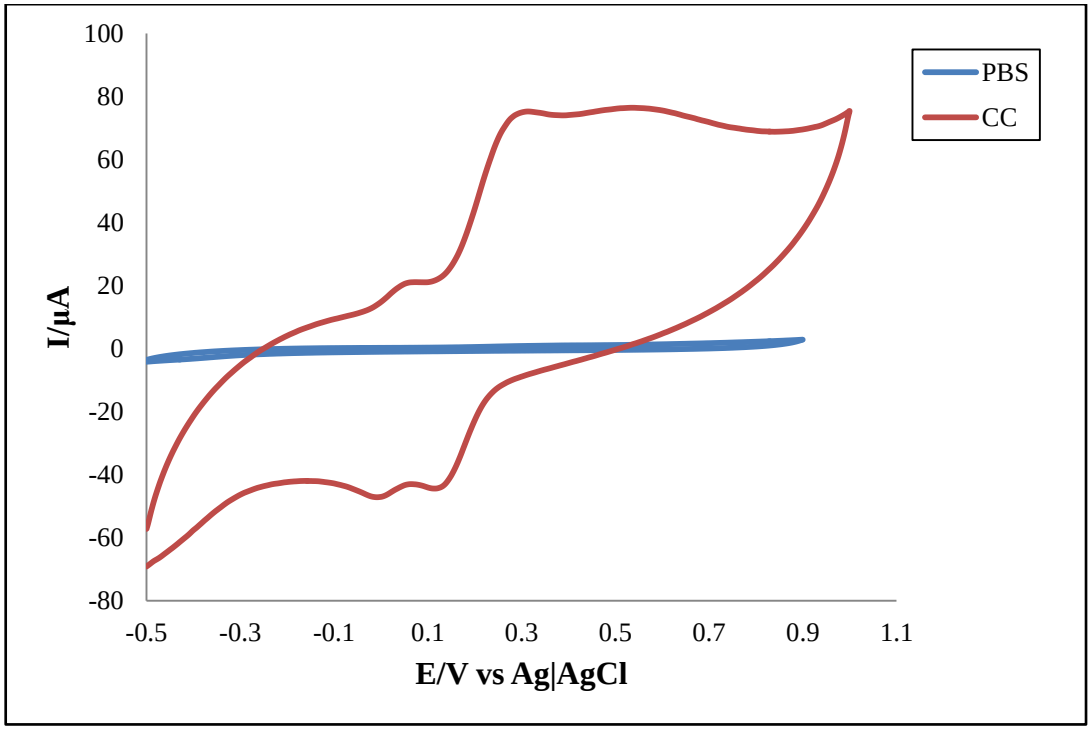

Figure 4.11: CV of 5 mM CC in PBS at 50 mV/s.

But the CV of CC is very confusing. There are two very small anodic peaks at +0.022 V and +0.266 V, a very small and broad anodic peak at +0.522 V and two small cathodic peaks at +0.154 V and +0.022V. This complex behavior of CV can be explained by the information of EDX of bare PGE. There are many other elements present in the working electrode surface. May be those elements are interfering with CV by giving some signals for CC.

4.8.1 Effect of concentration

CV of CC solutions with different concentrations at scan rate 0.05 V/s and at pH 7.0 were shown in Figure 4.12. It is seen that both of the anodic and cathodic current increases with the increase in concentration of CC. Anodic peak moves towards positive value and cathodic peak moves towards negative value with the increase of concentration.

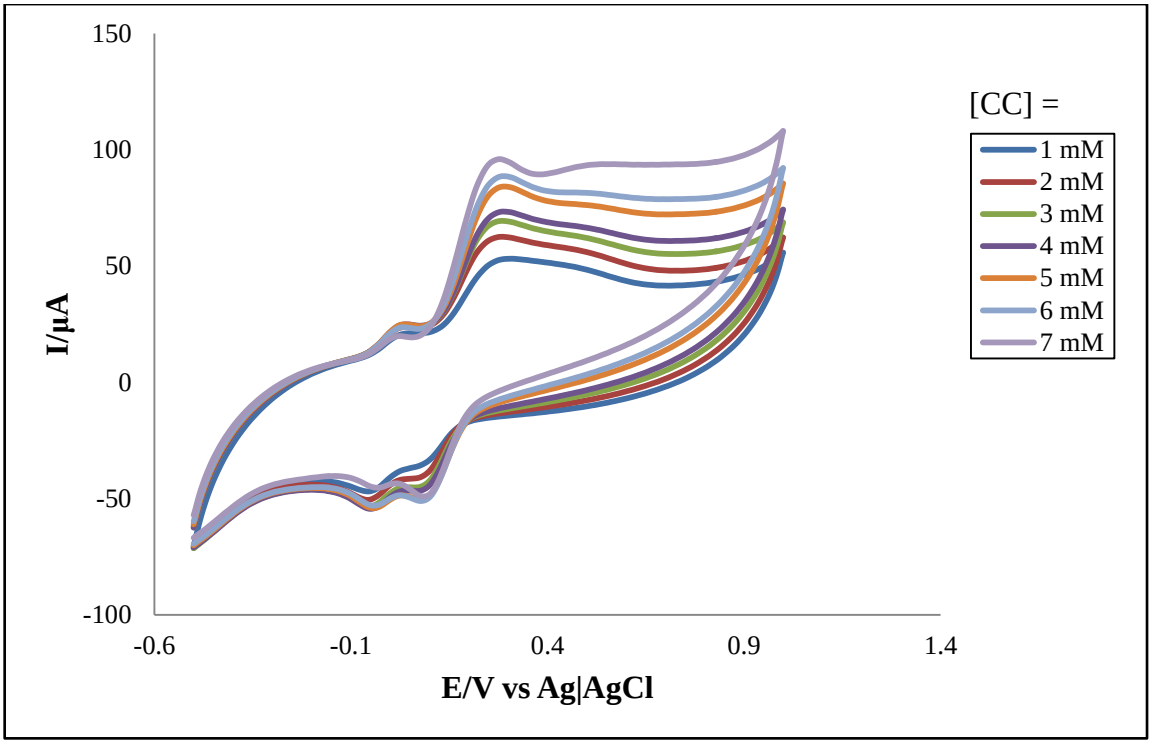

Figure 4.12: CV of CC at different concentration in PBS at 50mV/s.

From the voltammograms it is seen that, by increasing concentrations the anodic peak at +0.154 V increases and cathodic peak at +0.022 V increases linearly. So, may be those are the anodic and cathodic peaks for CC respectively.

4.9 Cyclic voltammetric behavior of hydroquinone at bare PGE

The reaction of HQ, terms of electron transfer mechanism, corresponding to the following anodic and cathodic reaction [128]:

For the oxidation process, the anodic peak may be corresponds to the following reaction mechanism:

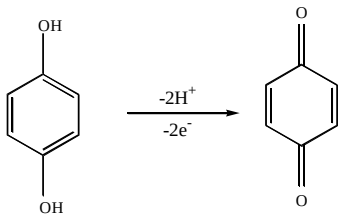

And for the reduction process, the cathodic peaks correspond to the following two-electron transfer reaction:

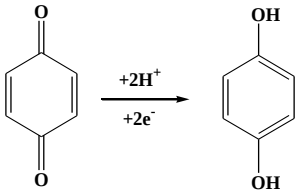

Figure 4.13 shows CV of 5 mM HQ at scan rate 50 mV/s with PBS (0.2 M, pH=7). There is no peak for PBS. Literature says that HQ gives one anodic and one cathodic peak [128]. Because there is only HQ in buffer solution, one anodic and one cathodic peak should be observed for CC. There is one sharp anodic peaks at +0.092 V and a cathodic peaks at +0.024 V.

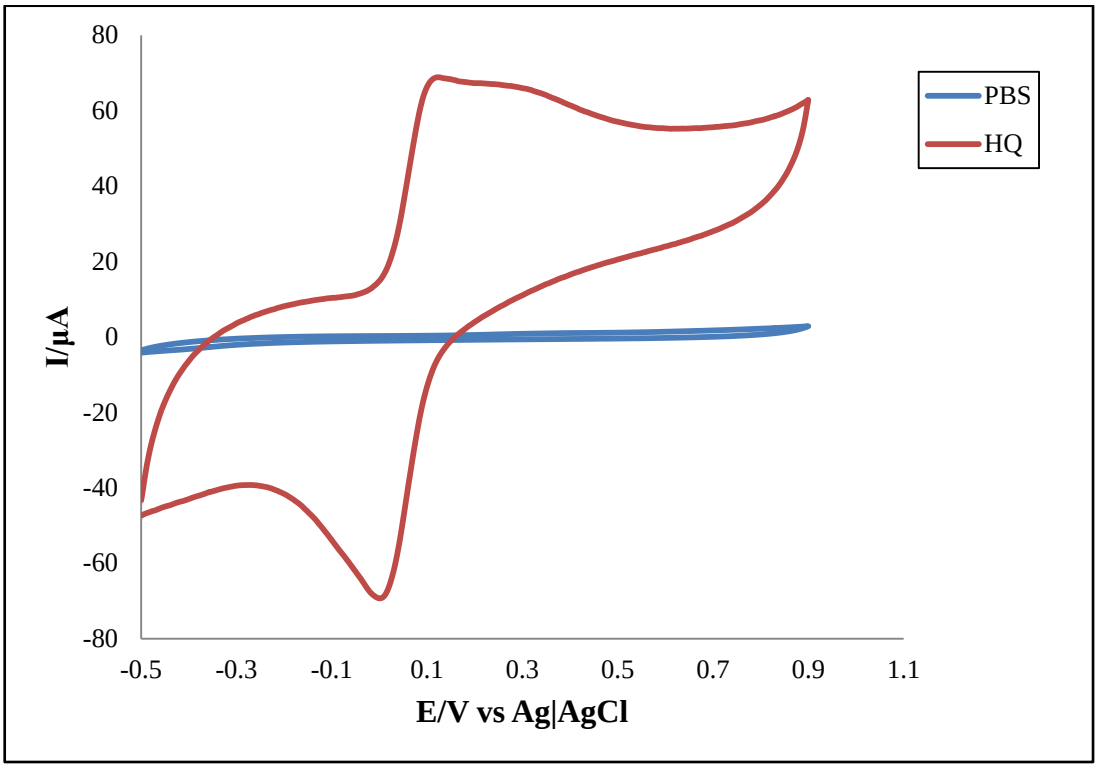

Figure 4.13: CV of 5 mM HQ in PBS at 50 mV/s.

4.9.1 Effect of concentration

CV of HQ solutions with different concentrations at scan rate 0.05 V/s and at pH 7.0 were shown in Figure 4.14. It is seen that both of the anodic and cathodic current increases with the increase in concentration of HQ. Anodic peak moves towards positive value and cathodic peak moves towards negative value with the increase of concentration.

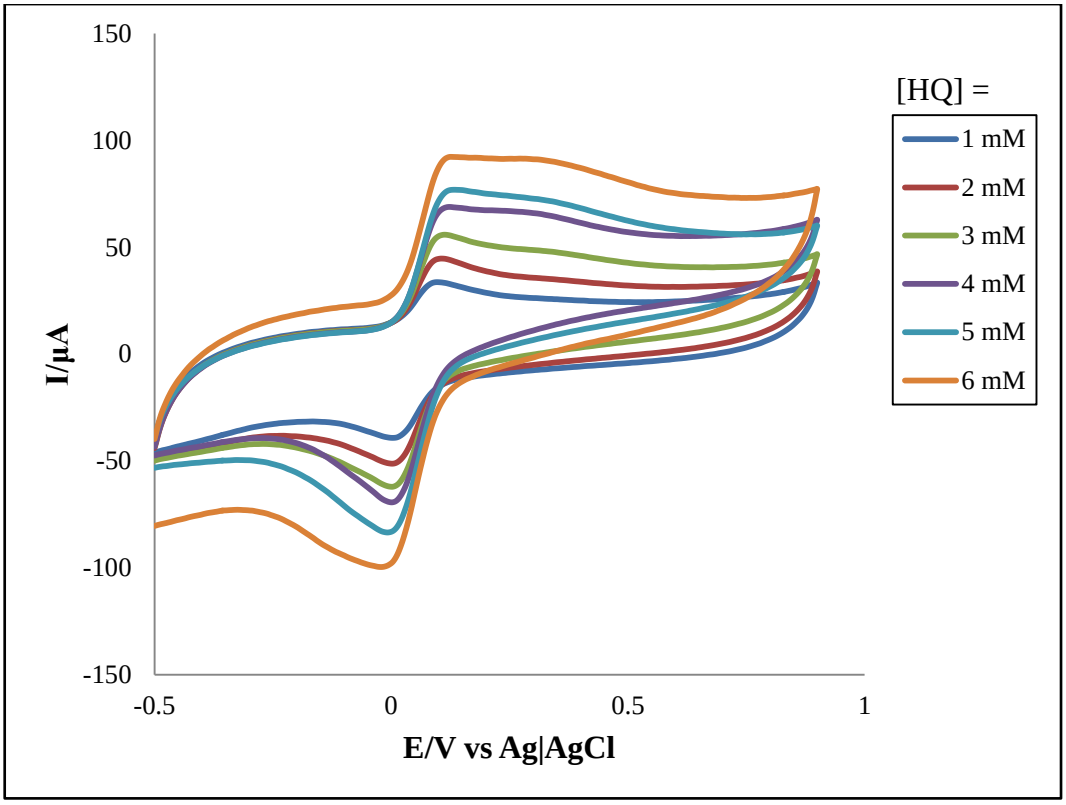

Figure 4.14: CV of HQ of different concentration in PBS at 50 mV/s.

But it does not mean that every time it shows same type of CV. Sometimes there more than one anodic and cathodic observed. CV of 1mM HQ in PBS is given bellow (Figure 4.15):

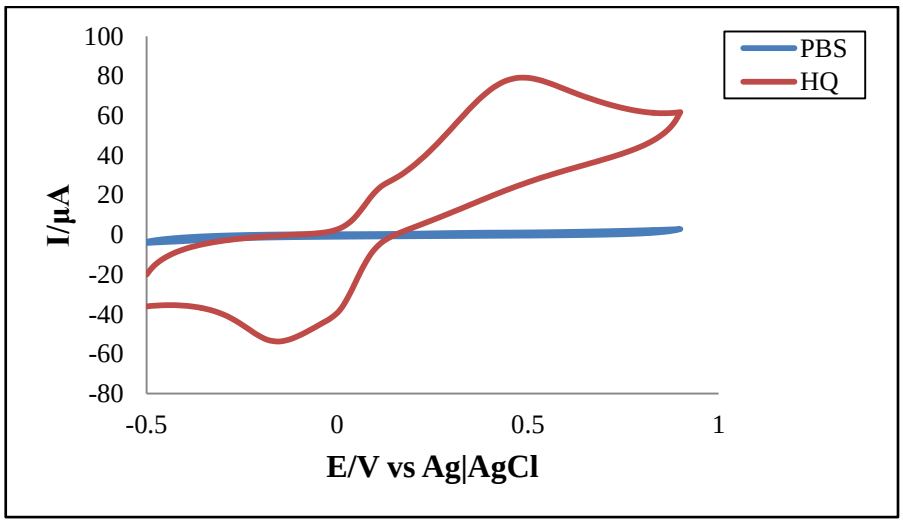

Figure 4.15: CV of 1 mM HQ in PBS at 50 mV/s.

There observed a small anodic peak at +0.09V, a broad anodic peak at +0.436V, a small cathodic peak at +0.02V and a broad peak at -0.034V. But according to the literature [128], the peaks at potential +0.436 V and -0.034 V are unreasonable for HQ. This complex behavior of CV can be explained by the information of EDX of bare PGE. There are many other elements present in the working electrode surface. May be those elements are interfering with CV by giving some signals for HQ.

4.10 Cyclic voltammetric behavior of resorcinol at bare PGE

The irreversible reaction of RS in PBS may be explained by the following electron transfer mechanism. For the oxidation process, the anodic peak may be corresponds to the following reaction mechanism.

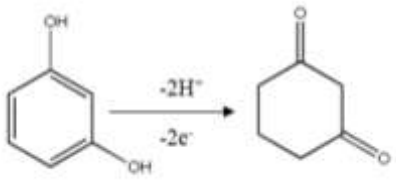

Figure 4.16 shows CV of RS of 5 mM at scan rate 50 mV/s with PBS (0.2 M, pH=7). There is no peak for PBS. Literature says that RS gives only one anodic [128]. Because there is only RS in buffer solution, one anodic should be observed for RS. There is one sharp anodic peaks at +0.61 V.

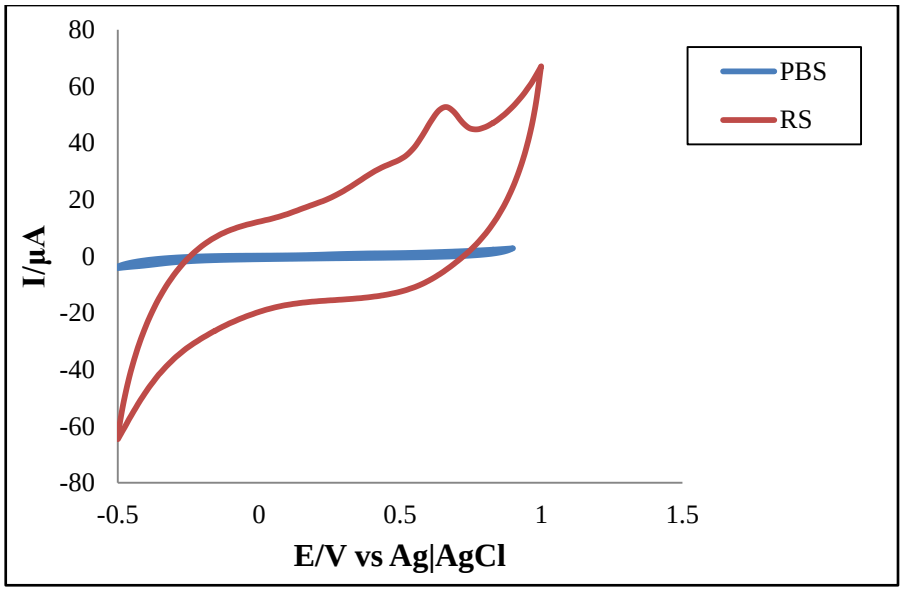

Figure 4.16: CV of 5 mM RS in PBS at 50 mV/s.

4.10.1 Effect of concentration

CV of RS solutions with different concentrations at scan rate 0.05 V/s and at pH 7.0 were shown in Figure 4.17. It is seen that the anodic current increases with the increase in concentration of RS. Anodic peak moves towards positive with the increase of concentration.

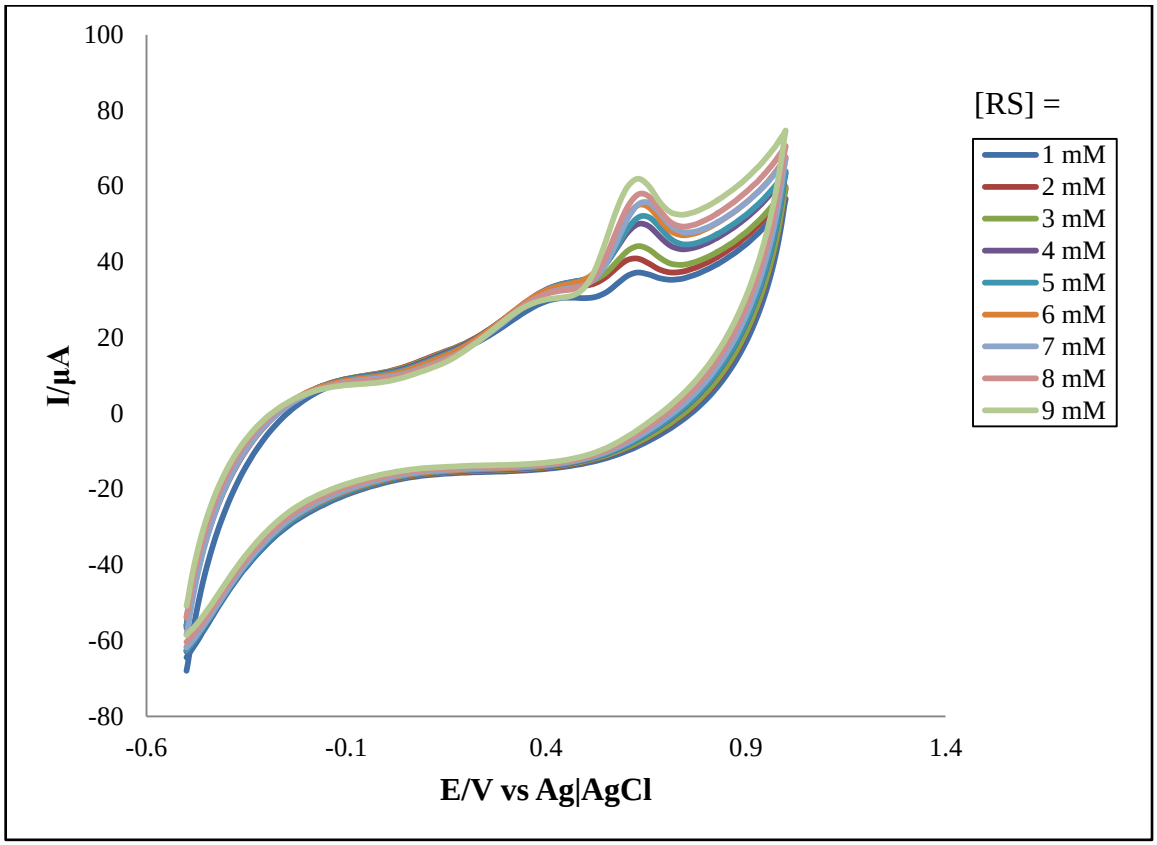

Figure 4.17: CV of RS of different concentration in PBS at 50 mV/s.

4.11 Simultaneous detection of CC and HQ in PBH at bare PGE by CV

CV of 5 mM CC and 5 mM HQ was taken simultaneously (1:1 solution mixture) at bare PGE in PBS of pH 7.0 at 50 mV/s. Individual voltammograms of 5mM CC and 5mM HQ was overlaid with the simultaneous voltammogram (Figure 4.18).

CC in PBS gave anodic and cathodic peaks at +0.17 V and -0.74 V respectively. On the other hand HQ gave anodic and cathodic peaks at +0.36 V and -0.82 V respectively. When investigated in a binary mixture of CC and HQ, a single anodic peak was found at +0.538 V which is at high potential than the peaks for individual CC and HQ. In addition two small cathodic peaks were found at +0.12 V and -0.044 V and a big cathodic peak

was also found at -0.262 V for the binary mixture which is at low potential than the peaks for individual CC and HQ. The anodic and cathodic peaks in the binary mixture are the combined peak of both of the species which is due to the fouling effect. As both isomers are similar compound their combined solution gives response as if a solution of double concentration. As they do not give individual response when both are present in the mixture, their simultaneous detection at bare PGE is impossible.

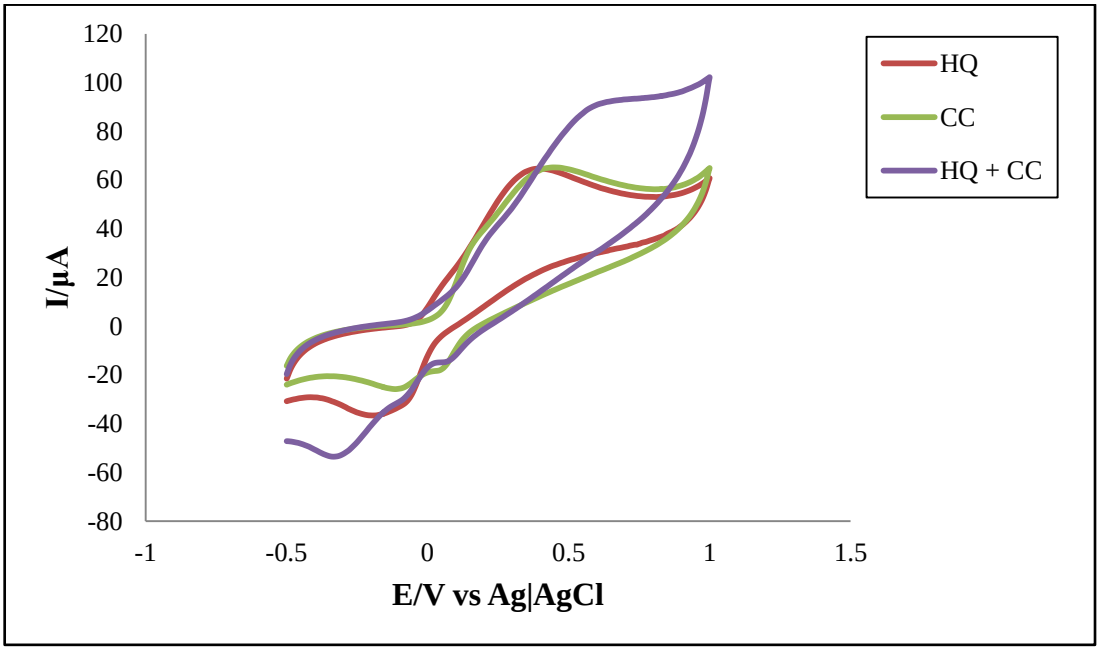

Figure 4.18: CV of 5 mM of CC, HQ and simultaneous CC+HQ in PBS at 50 mV/s.

4.12 Simultaneous detection of CC and RS in PBH at bare PGE by CV

CV of 5 mM CC and RS 5 mM was taken simultaneously at PGE in PBS of pH 7.0. Individual voltammogram of CC and RS was overlaid with the voltammogram of isomers simultaneously present in the solution (Figure 4.19).

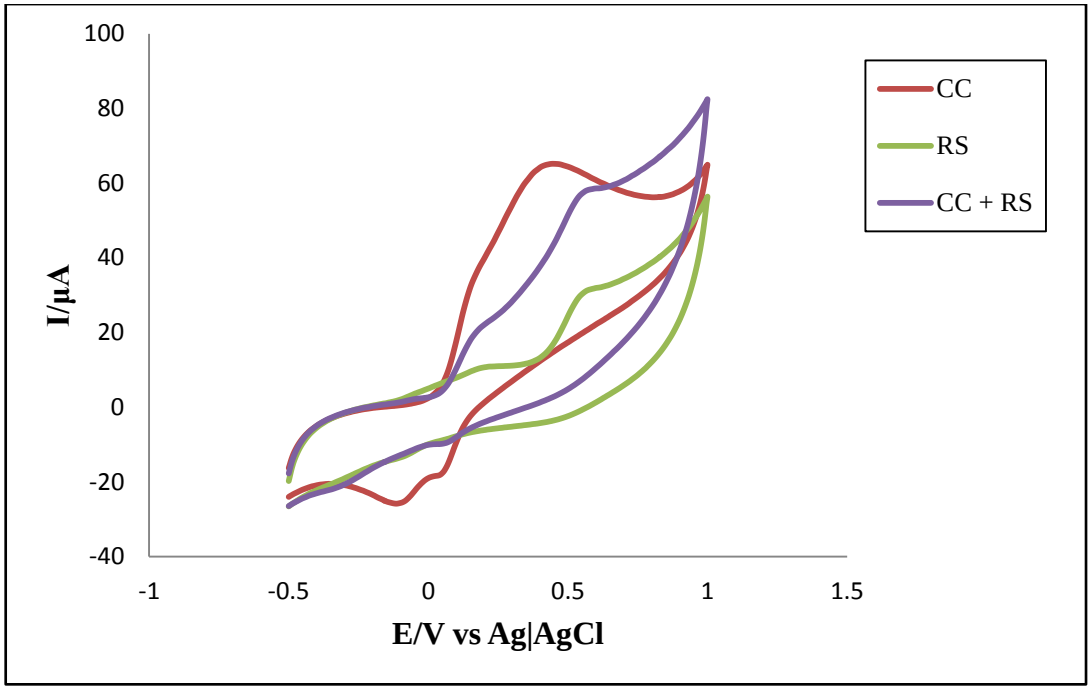

Figure 4.19: CV of 5 mM of CC, RS and simultaneous CC+RS in PBS at 50mV/s.

It is seen that (Figure 4.19), CC in PBS at bare PGE gave anodic and cathodic peaks at +0.17 V and -0.74 V respectively and. On the other hand RS gave two anodic peaks at +0.144 V and +0.526 V respectively. When investigated in a binary mixture of CC and RS two anodic peaks were found at +0.132 V and +0.516 V respectively and one small cathodic peak was observed at +0.128 V. But there should at least two cathodic peak for CC in comparison with the response for single CC at bare PGE. So, they did not give individual response when both are present in the mixture, their simultaneous detection at bare PGE is impossible.

4.13 Simultaneous detection of HQ and RS at bare PGE in PBS by CV

HQ (5mM) and RS (5mM) was investigated simultaneously at bare PGE in PBS of pH 7.0 using CV. Individual voltammograms of HQ and RS were overlaid with the simultaneous voltammogram and given in Figure 4.20.

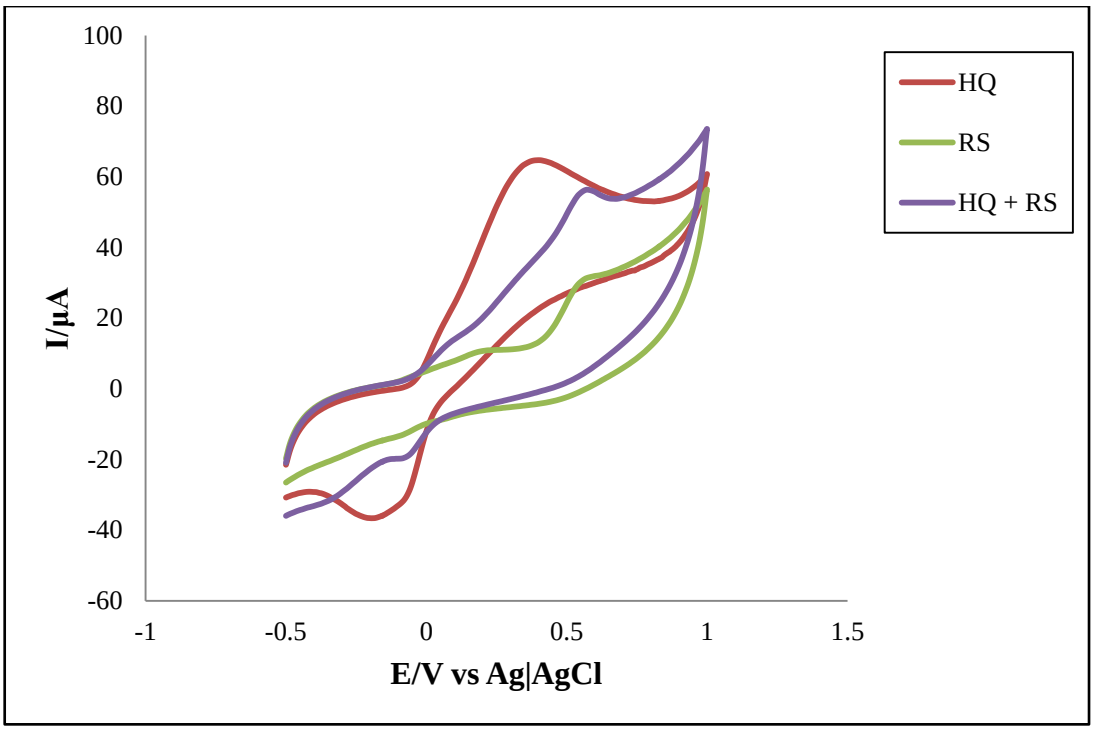

Figure 4.20: CV of 5 mM of HQ, RS and simultaneous HQ+RS in PBS at 50 mV/s.

HQ in PBS at bare PGE gave anodic and cathodic peaks at +0.36 V and -0.82 V respectively. On the other hand RS gave two anodic peaks at +0.144 V and +0.526 V respectively. When investigated in a binary mixture of HQ and RS, two anodic peaks were found at +0.036 V and +0.518 V and one very small cathodic peak was found at -0.02 V. But one big cathodic peak should be observed for HQ in comparison with the response for single HQ. As they did not give individual response when both were present in the mixture, their simultaneous detection at bare PGE is impossible.

4.14 Simultaneous detection of HQ, CC and RS at bare PGE in PBS by CV

CV of 5mM of CC, HQ and RS solution was studied simultaneously at bare PGE in PBS of pH 7.0 using. Individual voltammograms of CC, HQ and RS were overlaid with the simultaneous voltammogram and shown in Figure 4.21.

HQ in PBS at bare PGE gave anodic and cathodic peaks at +0.36 V and -0.82 V respectively, CC gave anodic and cathodic peaks at +0.17 V and -0.74 V respectively and RS gave two anodic peaks at +0.144 V and +0.526 V respectively. As both CC and HQ gave anodic and cathodic peaks very close, when investigated in a mixture of CC, HQ and RS one anodic peaks was found at +0.488 V and three cathodic peaks were found at +0.12 V, -0.026 V and -0.308 V respectively. As they did not give individual

response when all were present in the mixture, their simultaneous detection at bare PGE is impossible.

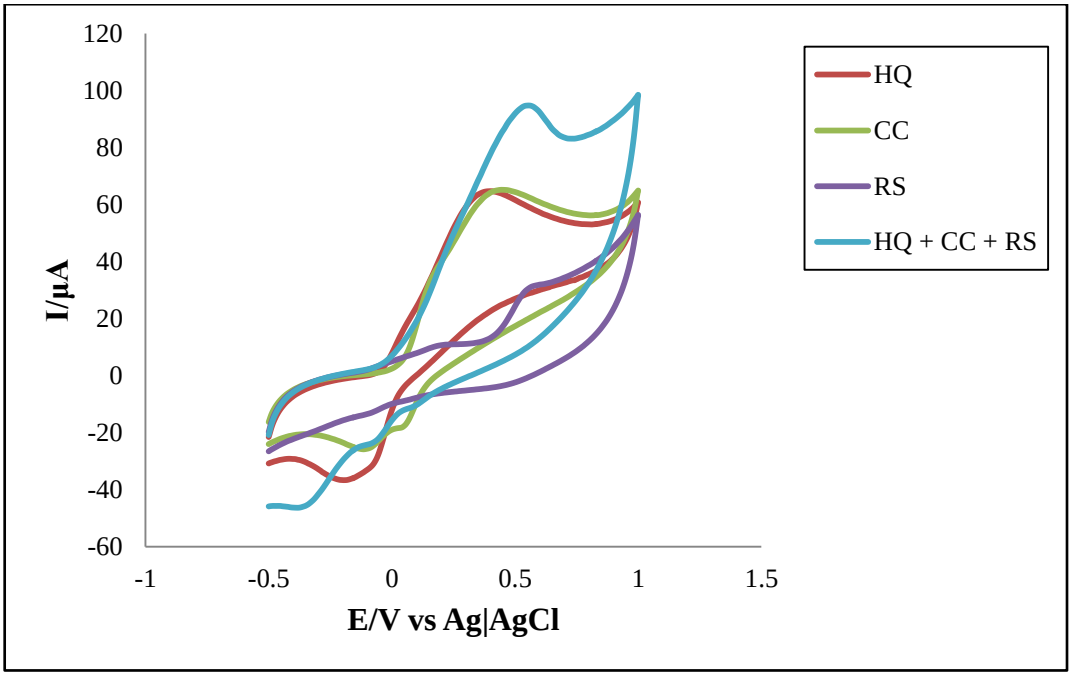

Figure 4.21: CV 5 mM of HQ, CC, RS and simultaneous HQ+CC+RS in PBS at 50 mV/s.

4.15 Modification of PGE with Ionic Liquid

In order to get response from CC, HQ and RS in a mixture and to improve the selectivity of PGE, it was modified with IL solution prepared in PBS of pH 7.0.

4.15.1 Modification of PGE with 1-hexylpyridinium hexafluorophosphate solution

Modification process: Prior to electrochemical modification, the bare PGE (grade 2B) with a diameter of 2 mm was chosen. Then it was cleaned by tissue paper, ringed with water and dried by air. After being cleaned, the electrode was then placed in HIL solution (prepared in 0.2M PBS of pH 7.0) which was previously dried with high purity nitrogen for 10 min. The electrode was treated with cyclic scanning between -0.5 V and +1.5 V at a scan rate of 300 mV/s, ten to fifteen times. Then the electrode was ready for use after the final washing with water.

Cyclic voltammogram of the modification process: Figure 4.22 displays the continuous CVs of HIL thin film formation onto a bare PGE in HIL-PBS solution over

the potential range of –0.5 V to +1.5 V for 10 cycles at a scan rate of 300 mVs^{-1}. As can be seen, the anodic peak currents decreased by 49 µA and cathodic peak currents decreased by 36 µA, indicating the formation and growth of an electro active layer on the PGE surface. After the ten cycles, the decrease of these peaks current tended to be stable. It is assumed that a uniform and thin film was present on the surface of PGE.

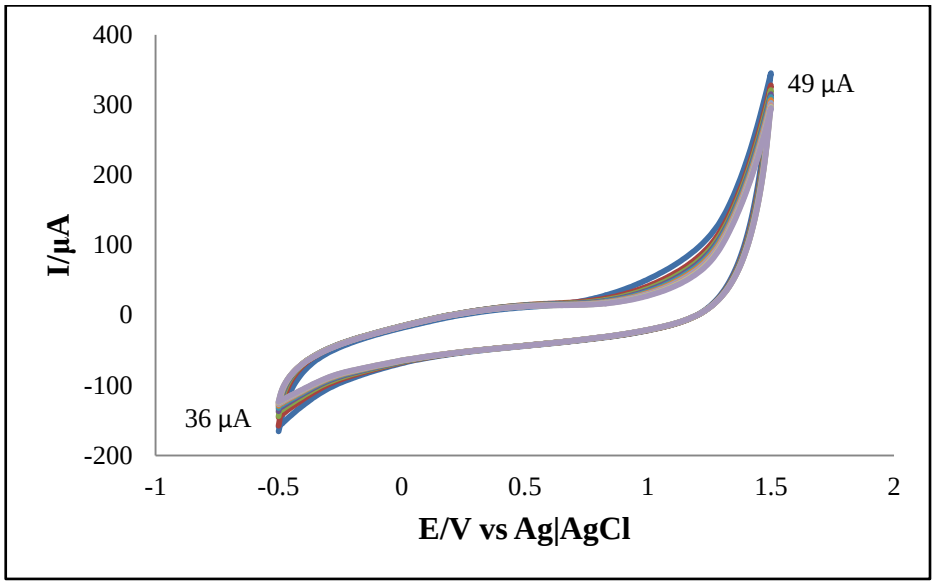

Figure 4.22: CV of HIL film growth on the surface of PGE at 300 mV/s.

4.15.2 Modification of PGE with 1-butyl-3-methylimidazolium hexafluorophosphate solution

Modification process: Prior to electrochemical modification, the bare PGE (grade 2B) with a diameter of 2 mm was chosen. Then it was cleaned by tissue paper, ringed with water and dried by air. After being cleaned, the electrode was then placed in BIL solution (prepared in 0.2M PBS of pH 7.0) which was previously dried with high purity nitrogen for 10 min. The electrode was treated with cyclic scanning between -0.5 V and +1.5 V at a scan rate of 300 mV/s, ten to fifteen times. Then the electrode was ready for use after the final washing with water.

Cyclic voltammogram of the modification process: Figure 4.23 displays the continuous CVs of BIL thin film formation onto a bare PGE in BIL solution over the potential range of –0.5 V to +1.5 V for 10 cycles at a scan rate of 300 mVs^{-1}. As can be seen, the anodic peak currents decreased by 146 µA and cathodic peak currents

decreased by 99 µA, indicating the formation and growth of an electro active layer on the PGE surface. After the ten cycles, the decrease of these peaks current tended to be stable. It is assumed that a uniform and thin film was present on the surface of PGE.

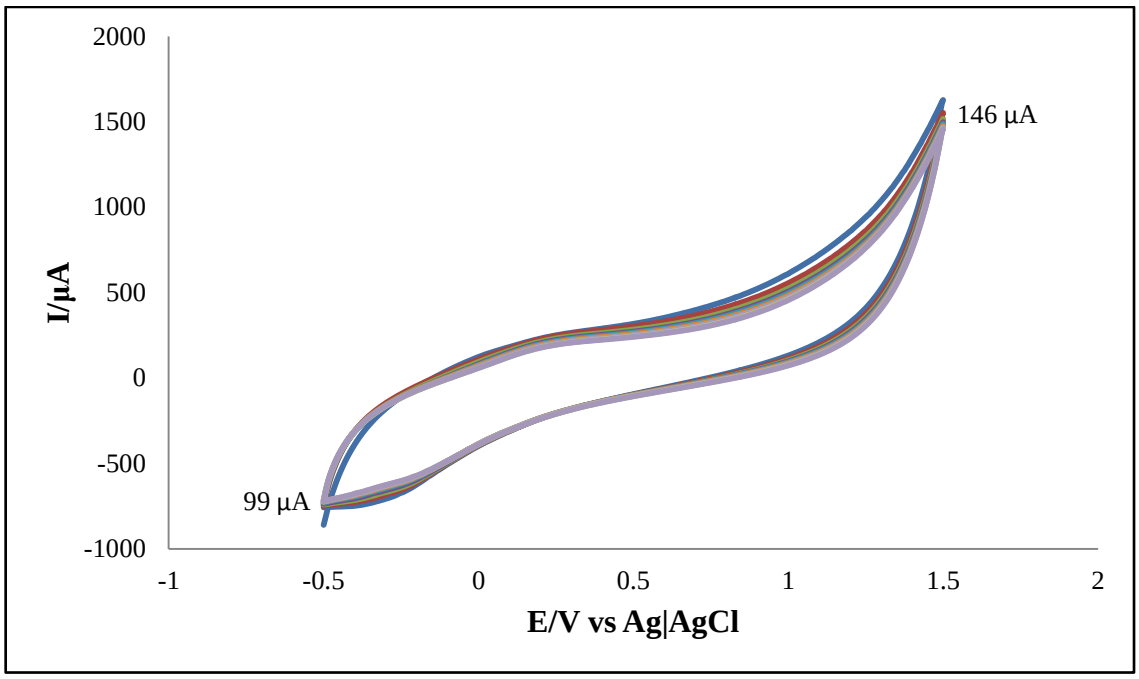

Figure 4.23: CV of BIL film growth on the surface of PGE at 300 mV/s.

4.16 Cyclic voltammetric behavior of catechol at HIL-PGE

Figure 4.24 shows CV of 5 mM CC in PBS at HIL-PGE. There is no peak for PBS but one sharp and well defined anodic peak and cathodic peak is observed for CC. The anodic and cathodic peaks are at +0.17 V and +0.11 V respectively.

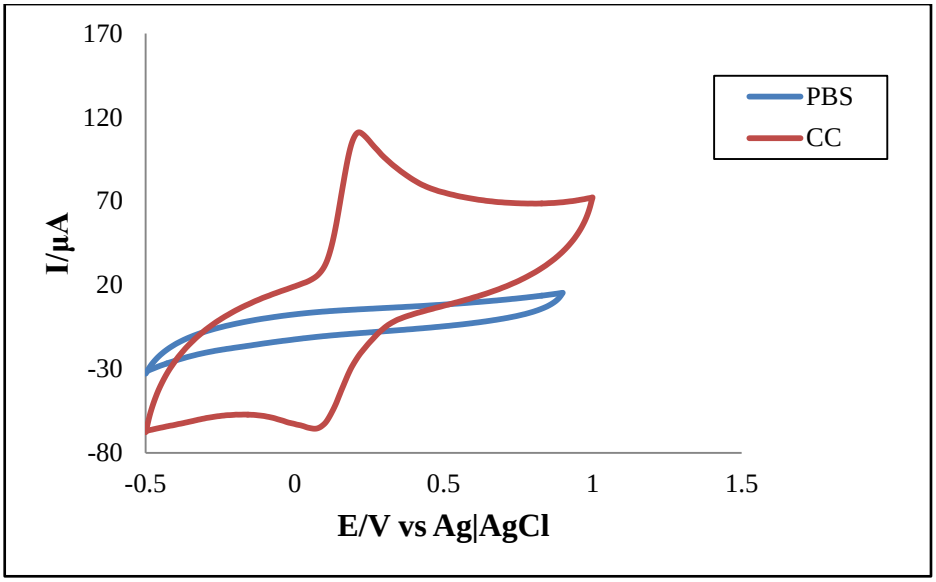

Figure 4.24: CV of 5 mM CC in PBS at 50 mV/s.

4.16.1 Comparison of CV of CC at Bare PGE and HIL-PGE

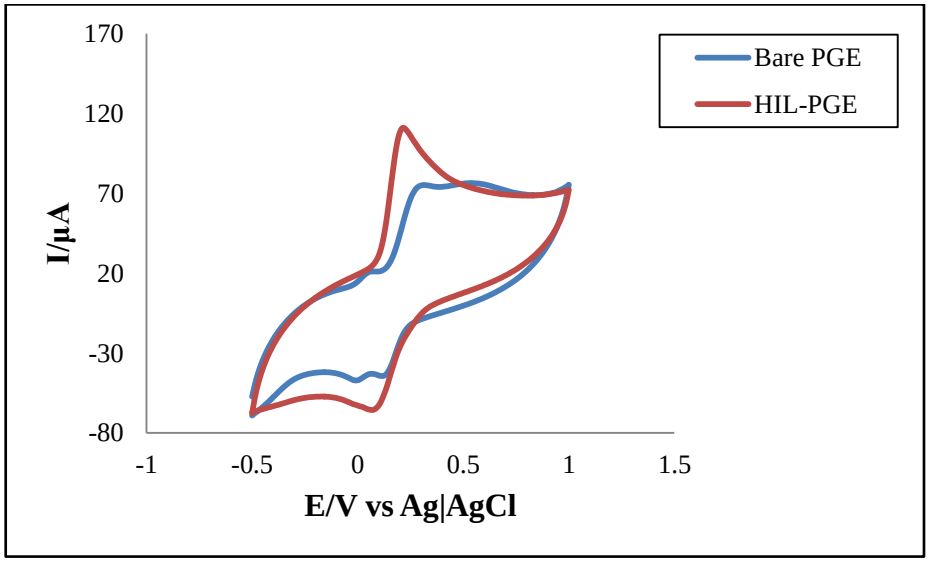

Figure 4.25: Comparison of CV of 5 mM CC at bare PGE and HIL-PGE in PBS at 50 mV/s.

At bare PGE CC gave one big anodic peak at +0.258V, a small peak at -0.1V and a broad peak at +0.52V. At bare PGE CC gave two cathodic peaks at +0.168V and +0.046V.

Both of the anodic and cathodic peaks of CC at HIL-PGE were sharper and well defined than that of bare PGE. The position of both of the anodic and cathodic peaks was shifted

significantly. In HIL-PGE CC have anodic and cathodic peaks at +0.17V and +0.11V respectively.

4.16.2 Effect of scan rate

The CVs of 5 mM CC in PBS of pH 7.0 were taken at different scan rates (Figure 4.26) at HIL-PGE. The current potential data, peak potential separation, peak current ratio are represented in Table 4.1.

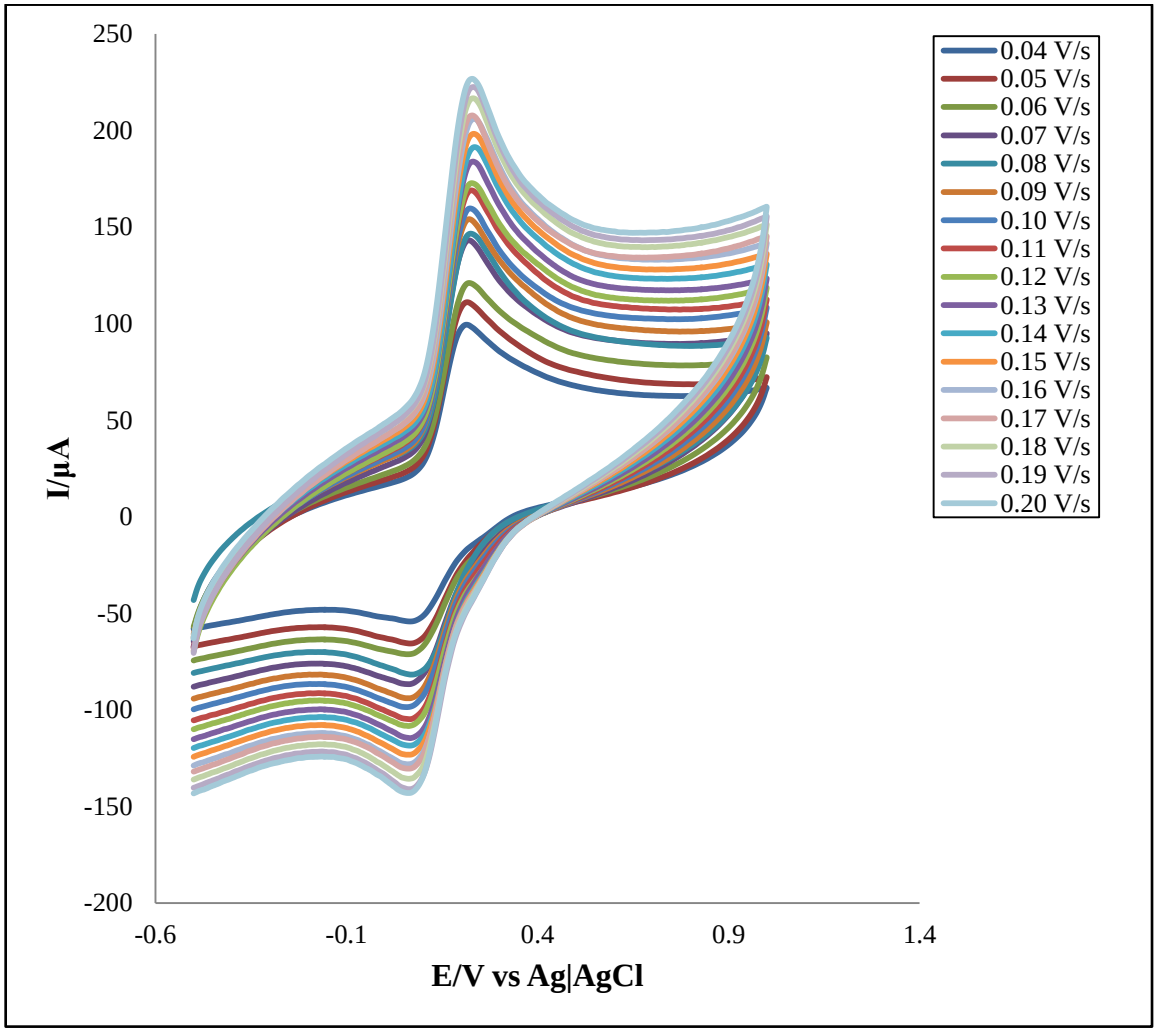

Figure 4.26: CV of 5mM CC in PBS at different scan rates.

Table 4.1: Current-potential data, peak potential separation, peak current ratio of the voltammograms of 5 mM CC in PBS at different scan rates

ν (V/s)	√ν ($V^{1/2}s^{-1/2}$)	E_{pa} (V) (+)	E_{pc} (V) (-)	i_{pa} (μA)	i_{pc} (μA)	ΔE= E_{pa} -E_{pc} (V)	i_{pa}/i_{pc}
0.04	0.200	0.196	0.092	67.883	35.743	0.104	1.899
0.05	0.223	0.198	0.092	76.037	42.281	0.106	1.798
0.06	0.244	0.200	0.092	80.495	46.111	0.108	1.745
0.07	0.264	0.196	0.088	95.704	54.493	0.108	1.756
0.08	0.282	0.200	0.092	98.380	54.367	0.108	1.809
0.09	0.300	0.200	0.088	104.144	55.859	0.112	1.864
0.10	0.316	0.200	0.088	106.327	57.862	0.112	1.837
0.11	0.331	0.206	0.092	112.485	58.550	0.114	1.921
0.12	0.346	0.206	0.088	114.834	61.460	0.118	1.868
0.13	0.360	0.210	0.090	121.468	68.432	0.120	1.775
0.14	0.374	0.214	0.094	125.773	71.192	0.120	1.766
0.15	0.387	0.210	0.088	129.781	72.579	0.122	1.788
0.16	0.400	0.210	0.088	133.443	79.172	0.122	1.685
0.17	0.412	0.210	0.084	136.034	79.029	0.126	1.721
0.18	0.424	0.210	0.086	141.247	81.385	0.124	1.735
0.19	0.435	0.210	0.086	147.964	85.268	0.124	1.735
0.20	0.447	0.216	0.090	149.326	85.245	0.126	1.751

ν= scan rate; $\nu^{1/2}$= square root of scan rate; E_{pa}= anodic peak potential; E_{pc}= cathodic peak potential; i_{pa}= anodic peak current; i_{pc}= cathodic peak current; ΔE= peak potential separation

From Table 4.1, it is seen that for the cathodic peaks, the peak potentials are gradually increased with the increase of scan rate whereas for the anodic peaks the peak potentials are gradually increased with the scan rate. But in both cases the rate of change of potential is very small. This behavior can be described by slower charge propagation, enhancement of diffusion layer and permeability.

From Table 4.1 it is apparent that the peak current increases with scan rate. This can be rationalized by considering the size of the diffusion layer and the time taken to record

the scan. The voltammograms takes longer to record as the scan rate is decreased. Therefore, the size of the diffusion layer above the electrode surface becomes different depending upon the voltage scan rate used. In a low voltage scan the diffusion layer grows much further from the electrode in comparison to a fast scan. Consequently, the flux to the electrode surface is considerably smaller at slow scan rates than it is at faster rates. As the current is proportional to the flux towards the electrode the magnitude of the current becomes lower at slow scan rates and higher at high scan rates. The general conclusion is that the redox system is diffusion controlled [136].

From Figure 4.27 it is seen that, the peak potential separation increases with the increase in scan rate. It indicates that there is a limitation due to charge transfer kinetics or ohmic potential (IR) drop [136]. The peak current of both anodic and cathodic peaks are increased with increasing $v^{1/2}$ (Figure 4.28), the corresponding trend line is a straight line which passed through the origin indicating that the process is diffusion controlled [136]. Again the peak current ratio is found to be greater than unity which implies that the process is quasi-reversible and gradually approaches unity with the increase of scan rate.

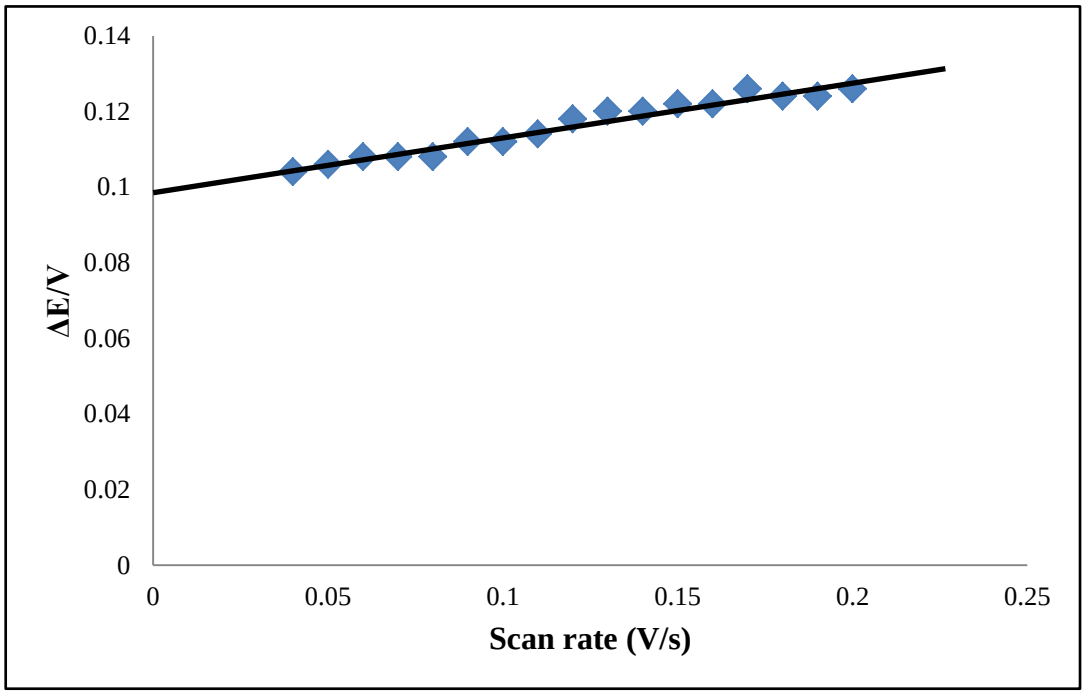

Figure 4.27: Variation of peak potential separation with scan rate.

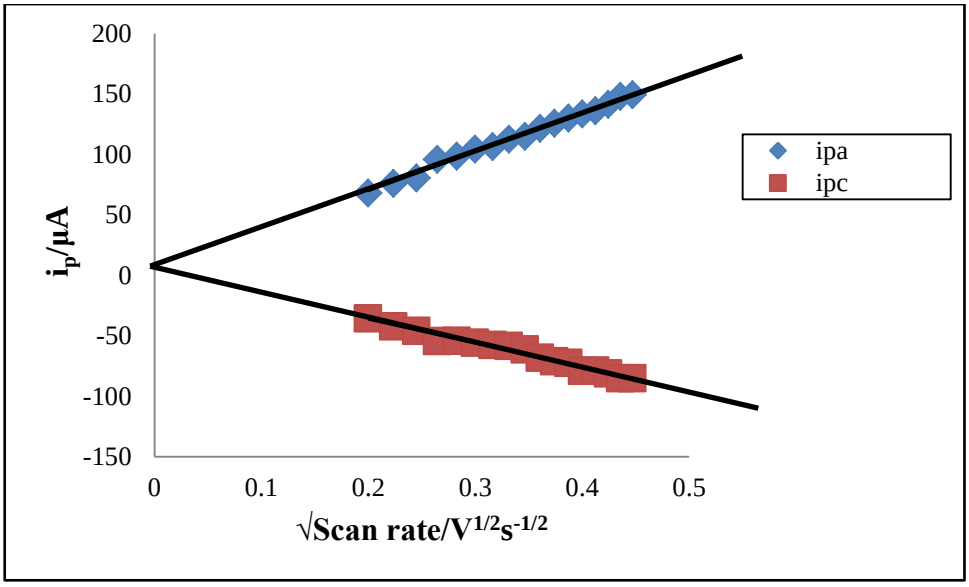

Figure 4.28: Variation of peak current with square root of scan rate.

4.16.3 Effect of concentration

CV of CC solutions with different concentrations (1 mM to 10 mM) at scan rate 50 mV/s and at pH 7.0 were shown in Figure 4.29.

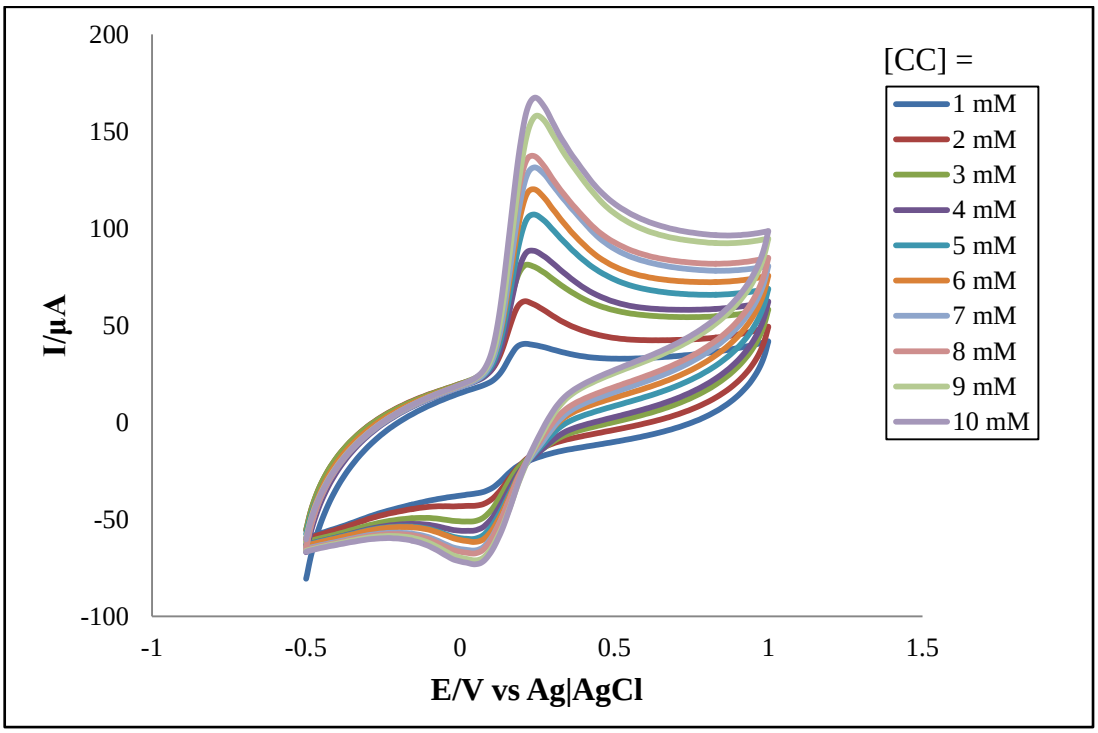

Figure 4.29: CV of CC at different concentration in PBS at 50 mV/s.

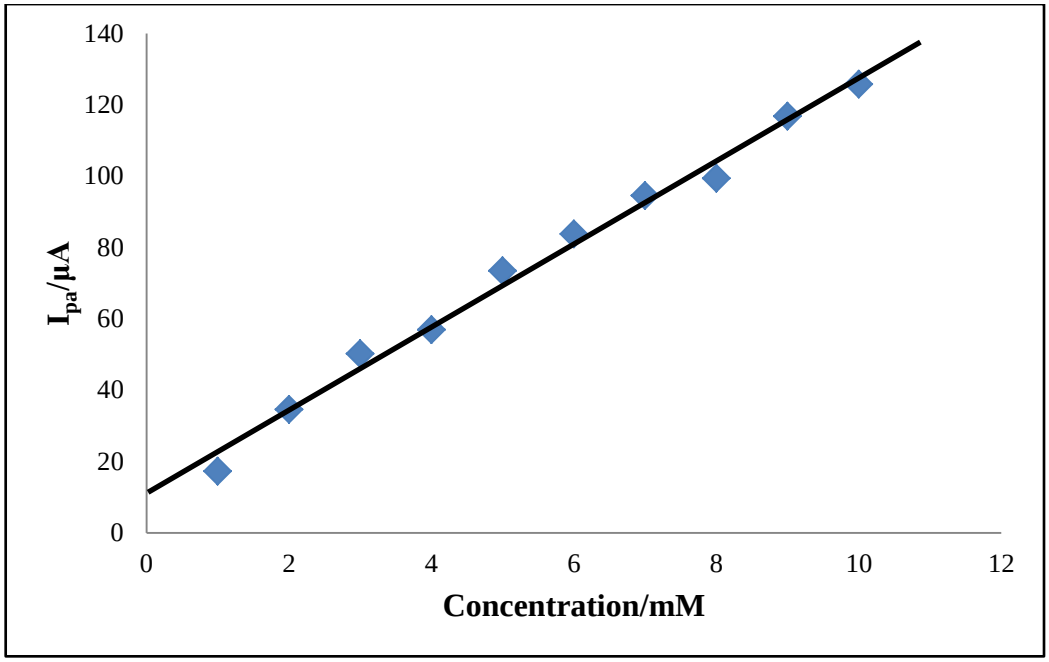

Figure 4.30: Variation of anodic peak current with the concentration.

It is seen that both of the anodic and cathodic current increases with the increase in concentration of CC. Anodic peak moves towards positive value and cathodic peak moves towards negative value with the increase of concentration. The anodic peak current increases linearly when plotted against concentration (Figure 4.30).

4.17 Cyclic voltammetric behavior of hydroquinone at HIL-PGE

Figure 4.31 shows CV of 5 mM HQ in PBS at HIL-PGE. There is no peak for PBS but one sharp and well defined anodic peak and cathodic peak is observed for HQ. The anodic and cathodic peaks are at +0.088 V and +0.014 V respectively.

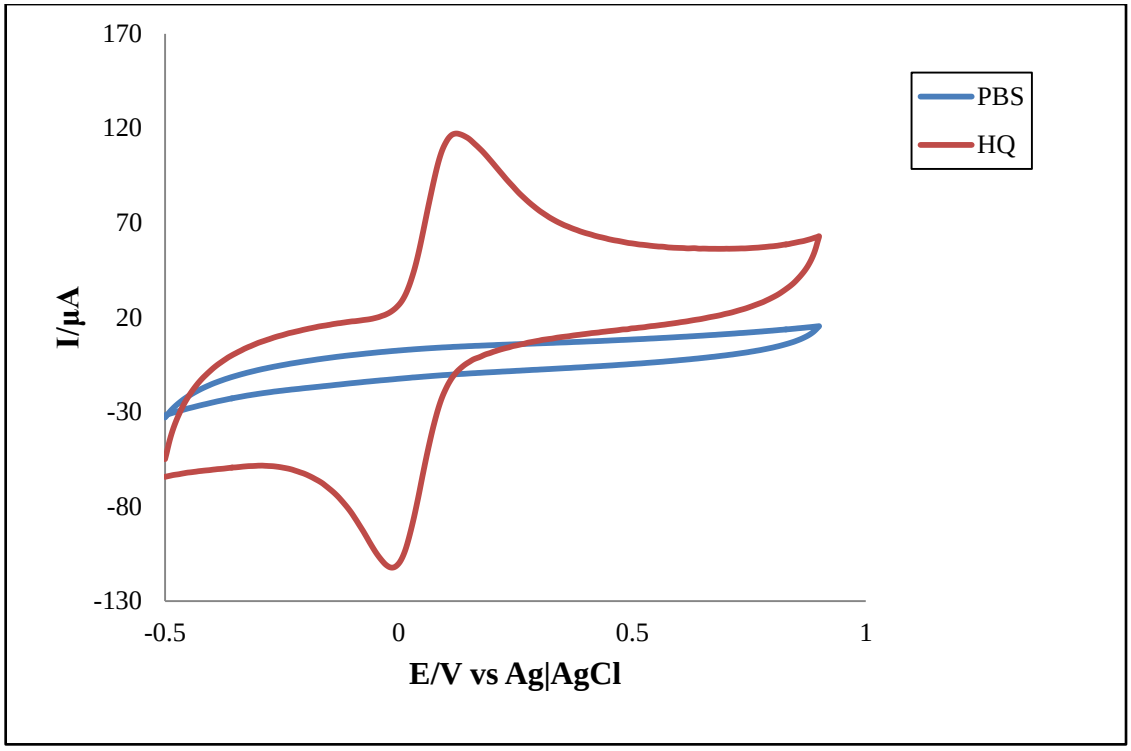

Figure 4.31: CV of 5 mM HQ in PBS at 50 mV/s.

4.17.1 Comparison of CV of HQ at Bare PGE and HIL-PGE

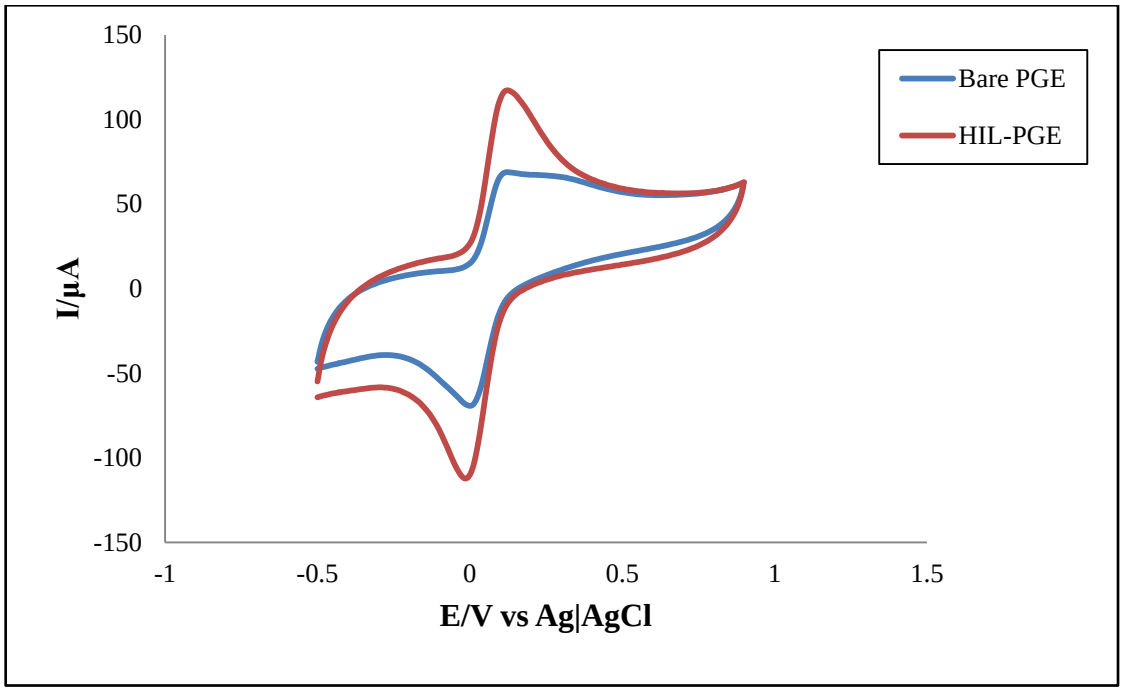

Figure 4.32: Comparison of CV for 5 mM HQ at bare PGE and HIL-PGE in PBS at 50 mV/s.

At bare PGE HQ gave one anodic peak at +0.88V and one cathodic peak +0.052V and it gave a broad peak at the right side of the anodic peak at +0.302V.

Both of the anodic and cathodic peaks of HQ at HIL-PGE were sharper and well defined than that of at bare PGE. The position of both of the anodic and cathodic peaks was shifted significantly. In HIL-PGE, HQ has anodic and cathodic peaks at +0.088 V and +0.014 V respectively.

4.17.2 Effect of scan rate

CVs of 5 mM HQ in PBS at different scan rates are displayed in Figure 4.33. The current potential data, peak potential separation, peak current ratio of the voltammograms at different scan rates are organized in Table 4.2.

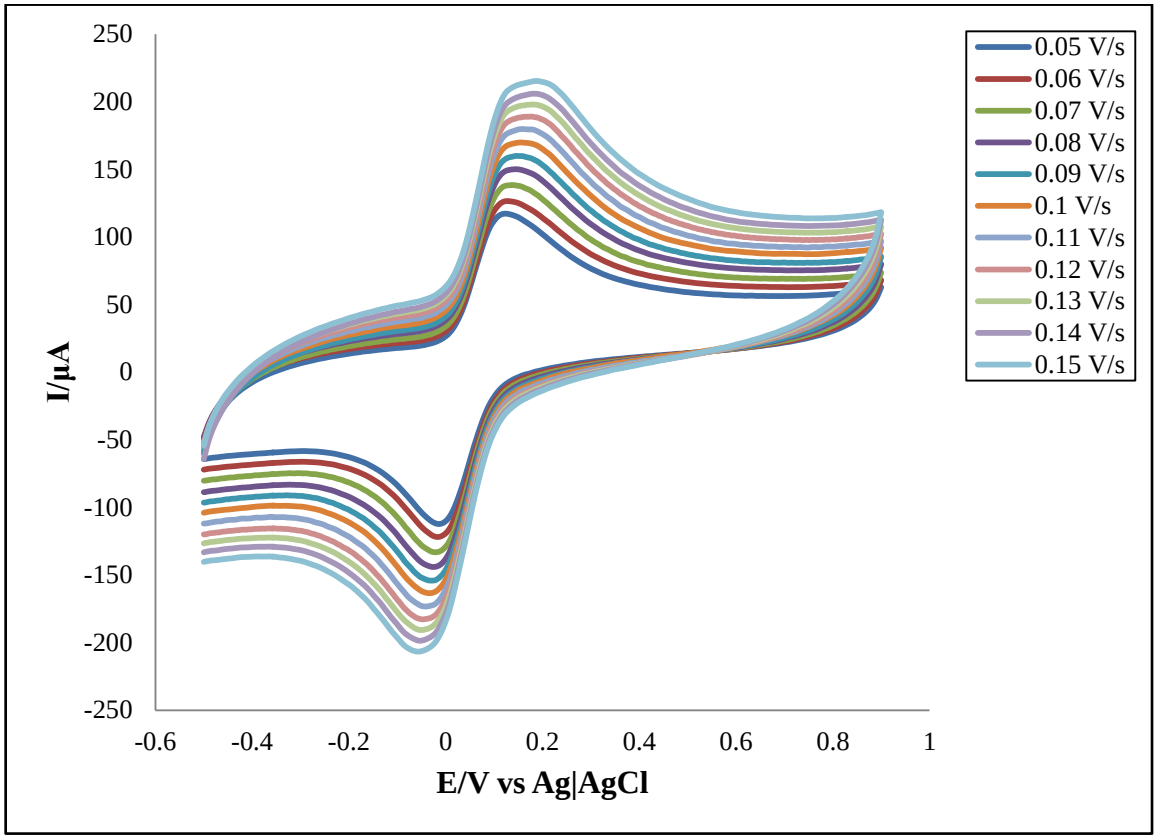

Figure 4.33: CV of 5 mM HQ in PBS at different scan rate.

Table 4.2: Current-potential data, peak potential separation, peak current ratio of the voltammograms of 5 mM HQ in PBS at different scan rates

ν(V/s)	$\sqrt{\nu}$ ($V^{1/2}s^{-1/2}$)	E_{pa} (V)	E_{pc} (V)	i_{pa} (μA)	i_{pc} (μA)	$\Delta E = E_{pa} \sim E_{pc}$ (V)	i_{pa}/i_{pc}
0.05	0.223	0.168	0.024	80.965	90.808	0.144	0.891
0.06	0.244	0.180	0.026	90.543	96.370	0.154	0.939
0.07	0.264	0.200	0.030	98.031	104.221	0.170	0.940
0.08	0.282	0.212	0.034	105.570	110.160	0.178	0.958
0.09	0.300	0.228	0.038	113.575	116.190	0.190	0.977
0.10	0.316	0.244	0.042	117.378	121.635	0.202	0.965
0.11	0.331	0.264	0.050	122.925	126.607	0.214	0.970
0.12	0.346	0.286	0.056	128.943	131.675	0.230	0.979
0.13	0.360	0.306	0.062	134.276	135.246	0.244	0.992
0.14	0.374	0.314	0.062	139.153	139.940	0.252	0.994
0.15	0.387	0.330	0.066	143.683	143.714	0.264	0.999

ν= scan rate; $\nu^{1/2}$= Square root of scan rate; E_{pa}= anodic peak potential; E_{pc}= cathodic peak potential; i_{pa}= anodic peak current; i_{pc}= cathodic peak current; ΔE= peak potential separation

From Table 4.2, it is understood that for the cathodic peaks, the peak potentials are gradually decreased as the scan rate increased and for the anodic peaks the peak potentials are gradually increased as the scan rate increased. But in both cases the rate of change of potential is very small. This behavior can be described by slower charge propagation, enhancement of diffusion layer and permeability.

Table 4.2 also reveals that the peak current increases with scan rates. This can be rationalized by considering the size of the diffusion layer and the time taken to record the scan. The voltammograms take longer to record as the scan rate is decreased. Therefore, the size of the diffusion layer above the electrode surface becomes different depending upon the voltage scan rate used. In a slow voltage scan the diffusion layer grows much further from the electrode in comparison to a fast scan. Consequently, the flux to the electrode surface is considerably smaller at slow scan rates than it is at faster rates. As the current is proportional to the flux towards the electrode the magnitude of the current becomes lower at slow scan rates and higher at high scan rates. The general conclusion is that the redox system is diffusion controlled [136].

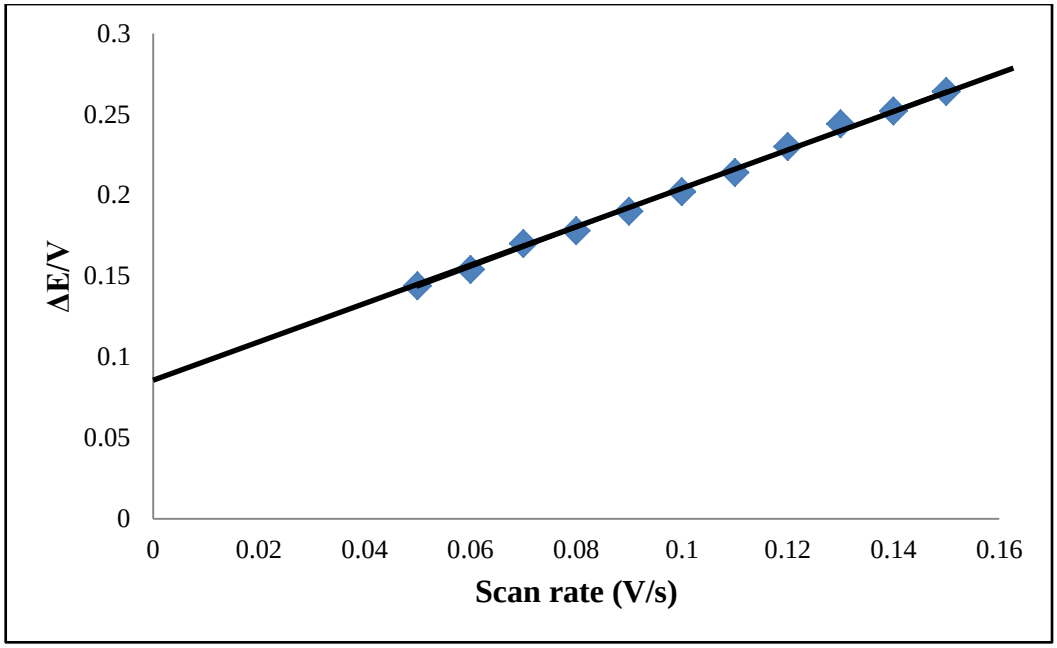

Figure 4.34: Variation of peak potential separation with scan rate.

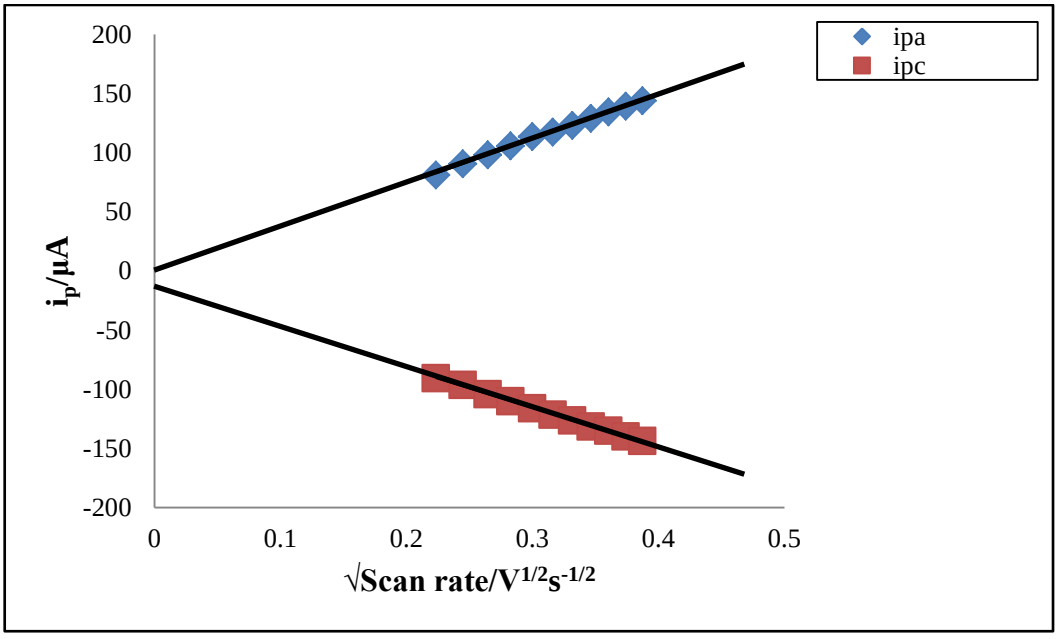

Figure 4.35: Variation of peak current with square root of scan rate.

With increasing scan rate (Figure 4.34), the peak potential separation increases because the cathodic peak shifts towards negative and that of anodic towards positive. It indicates that there is a limitation due to charge transfer kinetics or ohmic potential (IR) drop [136]. Current passage through either a Galvanic or an electrolytic cell requires a driving force or a potential to overcome the resistance of the ions to move towards the anode or the cathode. Just as in metallic conduction, this force follows ohm's law and is

equal to the product of current in amperes and the resistance of the cell in ohms. The force is generally referred to as the ohmic potential or the IR drop.

The peak current of both anodic and cathodic peaks are increased with increasing $v^{1/2}$ (Figure 4.35), the corresponding trend line is a straight line which passed through the origin indicating that the process is diffusion controlled [136].The peak current ratio is found to be nearly one. So the system is fairly reversible.

4.17.3 Effect of concentration

The CV of HQ solutions of various concentrations (1 mM to 10 mM) in PBS at 50 mV/s is shown in Figure 4.36. The variation of anodic current against concentration is given in Figure 4.36.

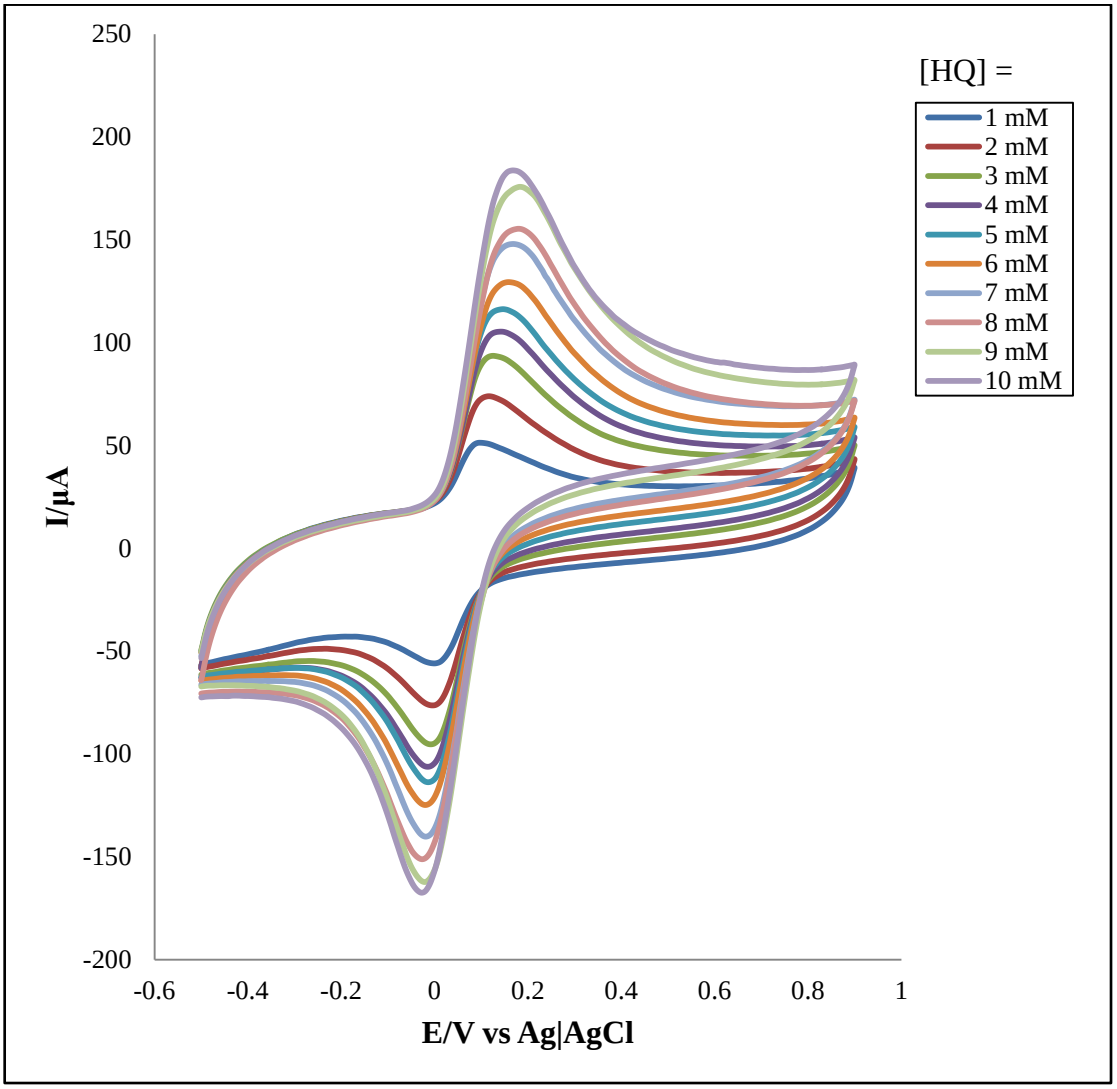

Figure 4.36: CV of HQ of different concentration in PBS at 50 mV/s.

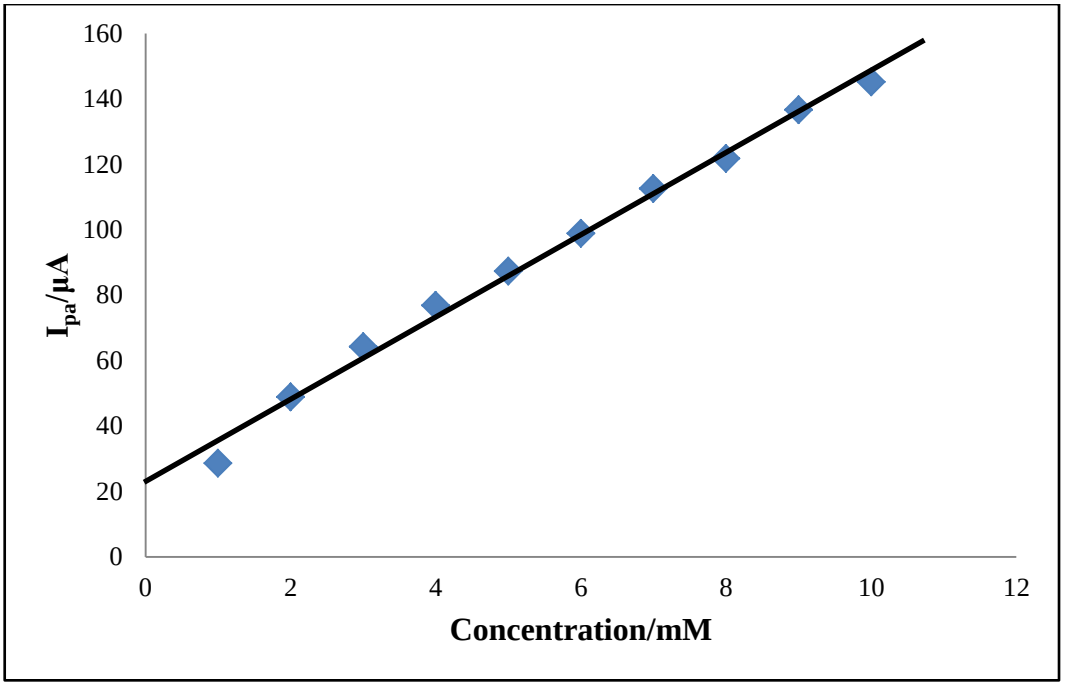

Figure 4.37: Variation of Anodic peak current with the Concentration of HQ in PBS.

Both anodic and cathodic currents increase gradually with the increase of concentration of the analyte solution. Anodic peaks tend to move towards positive value and cathodic peak tend to move toward negative peaks. The current change with the change of concentration changes regularly. Figure 4.37 described that the anodic current increases with the increase of concentration of HQ.

4.18 Cyclic voltammetric behavior of resorcinol at HIL-PGE

Figure 4.38 shows CV of 5 mM RS in PBS at HIL-PGE. There is no peak for PBS but one sharp and well defined anodic peak is observed for RS. The anodic peak is at +0.636 V.

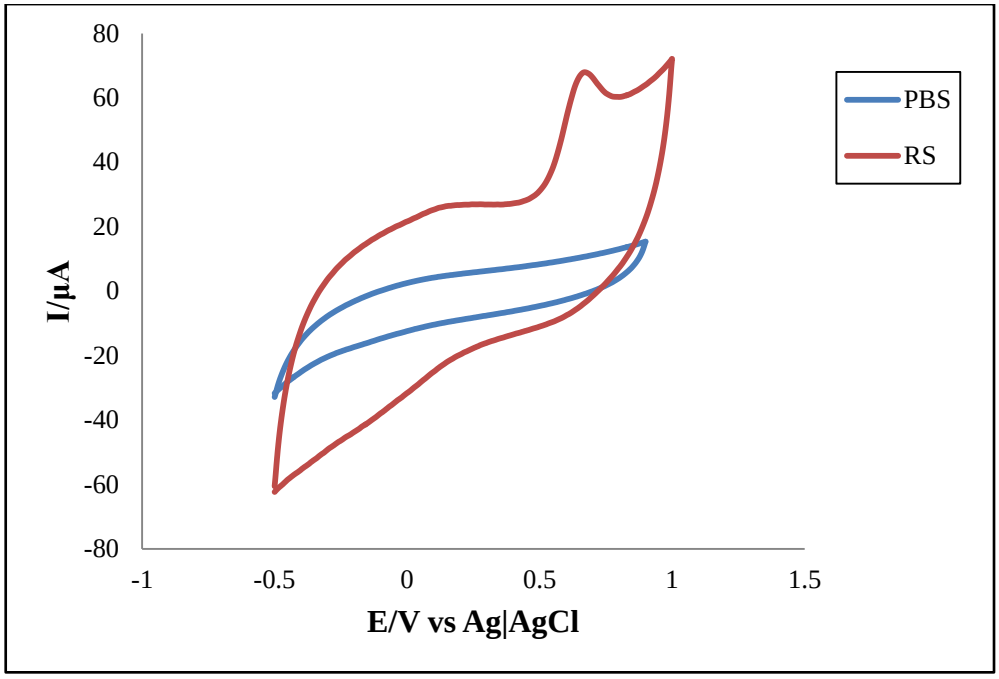

Figure 4.38: CV of 5 mM RS in PBS at 50 mV/s.

4.18.1 Comparison of CV of RS at Bare PGE and HIL-PGE

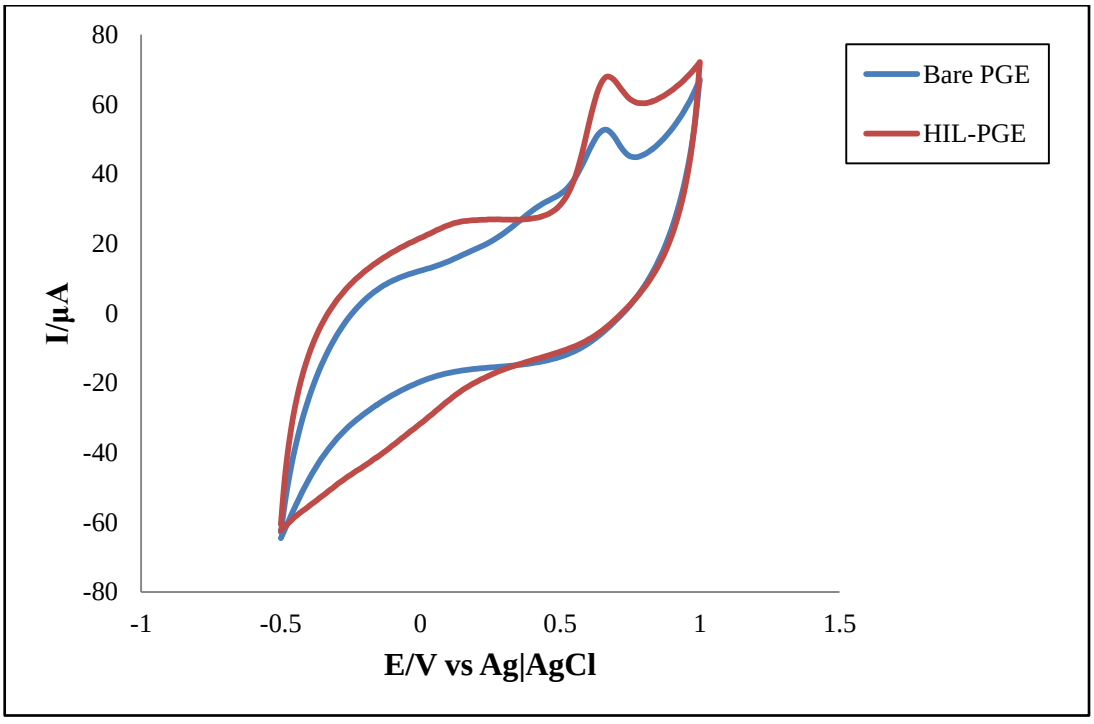

Figure 4.39: Comparison of CV of 5 mM RS at bare PGE and HIL-PGE in PBS at 50 mV/s.

At bare PGE RS gave a sharp anodic peak at +0.624 V with a very small anodic peak at +0.38 V.

RS gave irreversible peaks at HIL-PGE. The anodic peak was sharper and well defined than that of at the bare PGE. The position of the anodic peak was shifted right. In HIL-PGE RS gave sharp anodic peak at +0.636 V.

4.18.2 Effect of scan rate

CV of 5 mM RS in PBS at different scan rates is shown in Figure 4.40. The current potential data, peak potential separation, peak current ratio of the voltammograms at different scan rates are tabulated in Table 4.3.

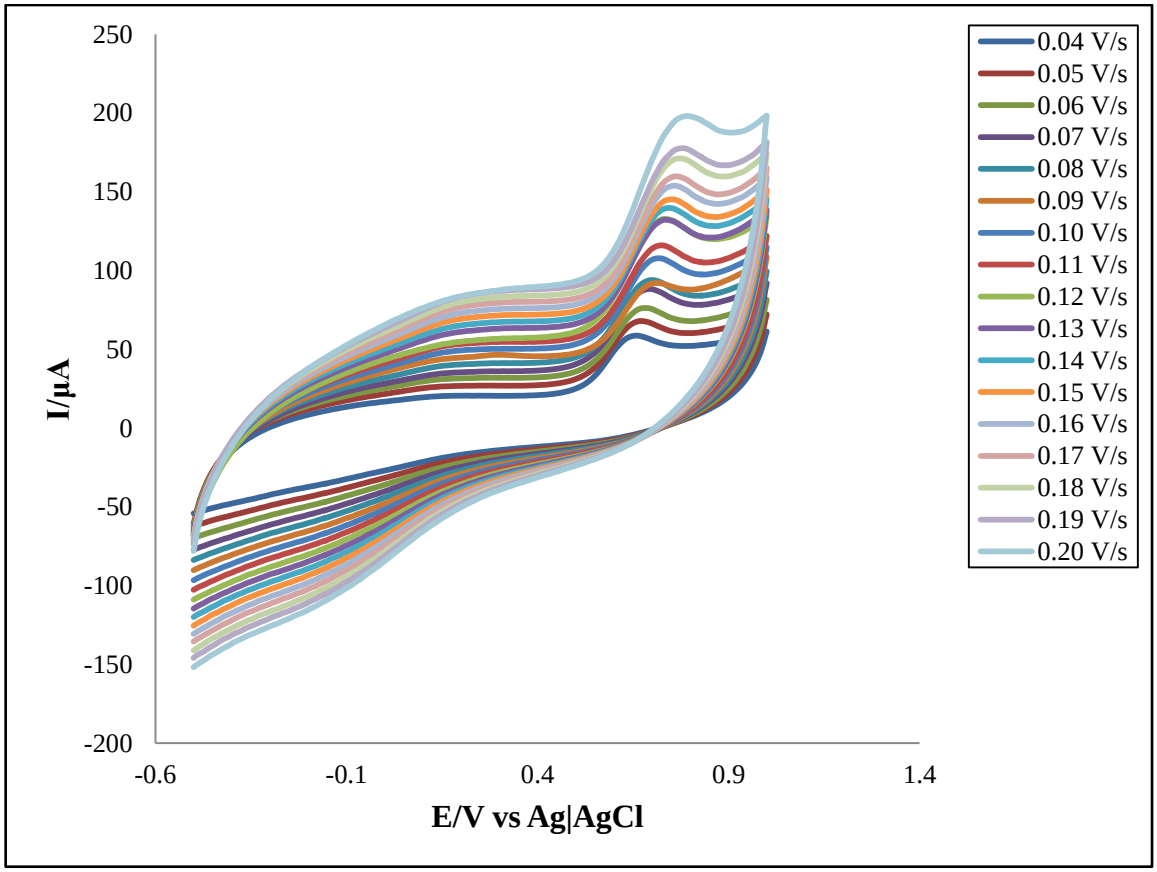

Figure 4.40: CV of 5 mM RS in PBS at different scan rate.

Table 4.3: Current-potential data, peak potential separation, peak current ratio of the voltammograms of 5 mM RS in PBS at different scan rates

ν(V/s)	√ν ($V^{1/2}s^{-1/2}$)	E_{pa} (V) (+)	E_{pc} (V)	i_{pa} (μA)	i_{pc} (μA)
0.04	0.200	0.672	0	20.695	0
0.05	0.223	0.678	0	22.584	0
0.06	0.244	0.686	0	23.875	0
0.07	0.264	0.696	0	25.586	0
0.08	0.282	0.702	0	27.532	0
0.09	0.300	0.710	0	29.144	0
0.10	0.316	0.720	0	30.215	0
0.11	0.331	0.728	0	31.004	0
0.12	0.346	0.736	0	31.799	0
0.13	0.360	0.740	0	32.536	0
0.14	0.374	0.748	0	34.530	0
0.15	0.387	0.758	0	34.751	0
0.16	0.400	0.760	0	36.204	0
0.17	0.412	0.770	0	37.581	0
0.18	0.424	0.774	0	40.390	0
0.19	0.435	0.784	0	40.810	0
0.20	0.447	0.792	0	42.925	0

ν= scan rate; $\nu^{1/2}$= Square root of scan rate; E_{pa}= anodic peak potential; E_{pc}= cathodic peak potential; i_{pa}= anodic peak current; i_{pc}= cathodic peak current; ΔE= peak potential separation

From Table 4.3, we can see that for the anodic peaks the peak potentials are gradually increased with the scan rate. But in the cases the increasing and decreasing rate of potential is very small. This behavior can be described by slower charge propagation, enhancement of diffusion layer and permeability.

Table 4.3 also demonstrates that the peak current increases with scan rate. This can be rationalized by considering the size of the diffusion layer and the time taken to record the scan. The voltammogram takes longer to record as the scan rate is decreased.

Therefore, the size of the diffusion layer above the electrode surface becomes different depending upon the voltage scan rate used. In a slow voltage scan the diffusion layer grows much further from the electrode in comparison to a fast scan. Consequently, the flux to the electrode surface is considerably smaller at slow scan rates than it is at faster rates. As the current is proportional to the flux towards the electrode the magnitude of the current becomes lower at slow scan rates and higher at high scan rates. The general conclusion is that the redox system is diffusion controlled [136].

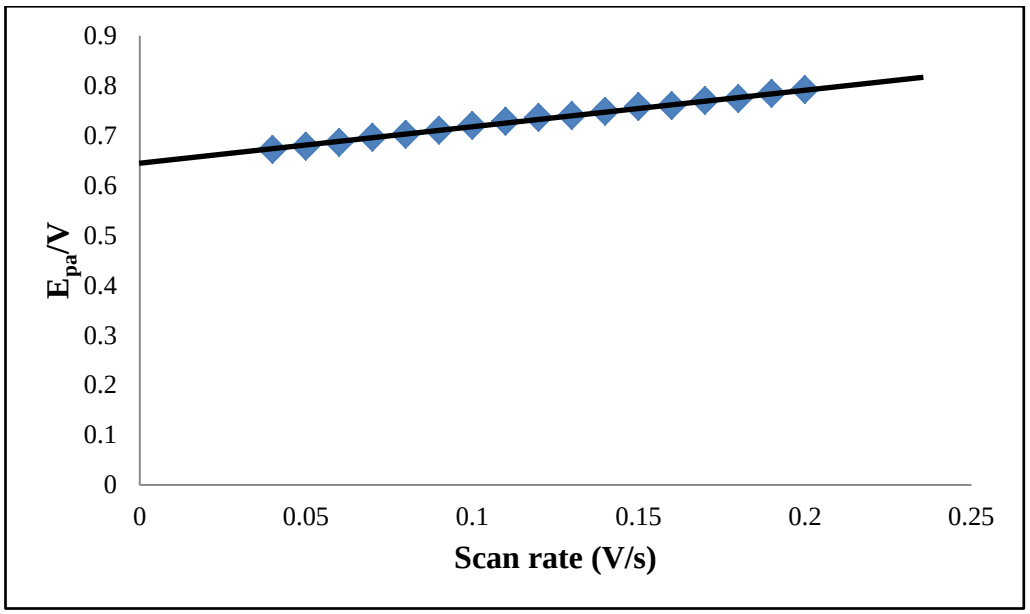

Figure 4.41: Variation of peak potential separation with scan rate.

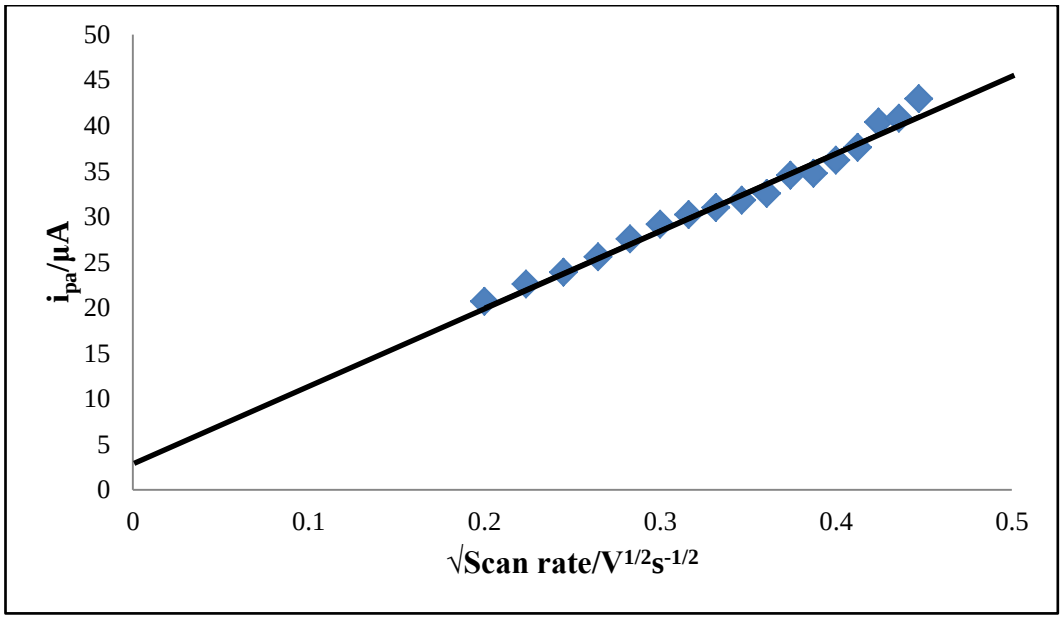

Figure 4.42: Variation of peak current with square root of scan rate.

With increasing scan rate, the peak potential separation increases (Figure 4.41) because the anodic peak shifts positive. Here the cause is the effect of IR drop [136]. Current passage through either a Galvanic or an electrolytic cell requires a driving force or a potential to overcome the resistance of the ions to move towards the anode or the cathode. Just as in metallic conduction, this force follows ohm's law and is equal to the product of current in amperes and the resistance of the cell in ohms. The force is generally referred to as the ohmic potential or the IR drop.

From Figure 4.42 it is seen that with increasing $v^{1/2}$, the anodic peak currents increases, but the corresponding trend is a straight line which passed near the origin indicating that the process is impure diffusion controlled [136]. Again the peak current ratio is found to be greater than unity which implies that the process is irreversible.

4.18.3 Effect of concentration

CV of RS solutions with different concentrations (1 mM to 9 mM) at scan rate 0.05 V/s and at pH 7.0 were shown in Figure 4.43. It is seen that the anodic current increases with the increase in concentration of RS. Anodic peak moves towards positive with the increase of concentration. The anodic peak current increases linearly when plotted against concentration (Figure 4.44).

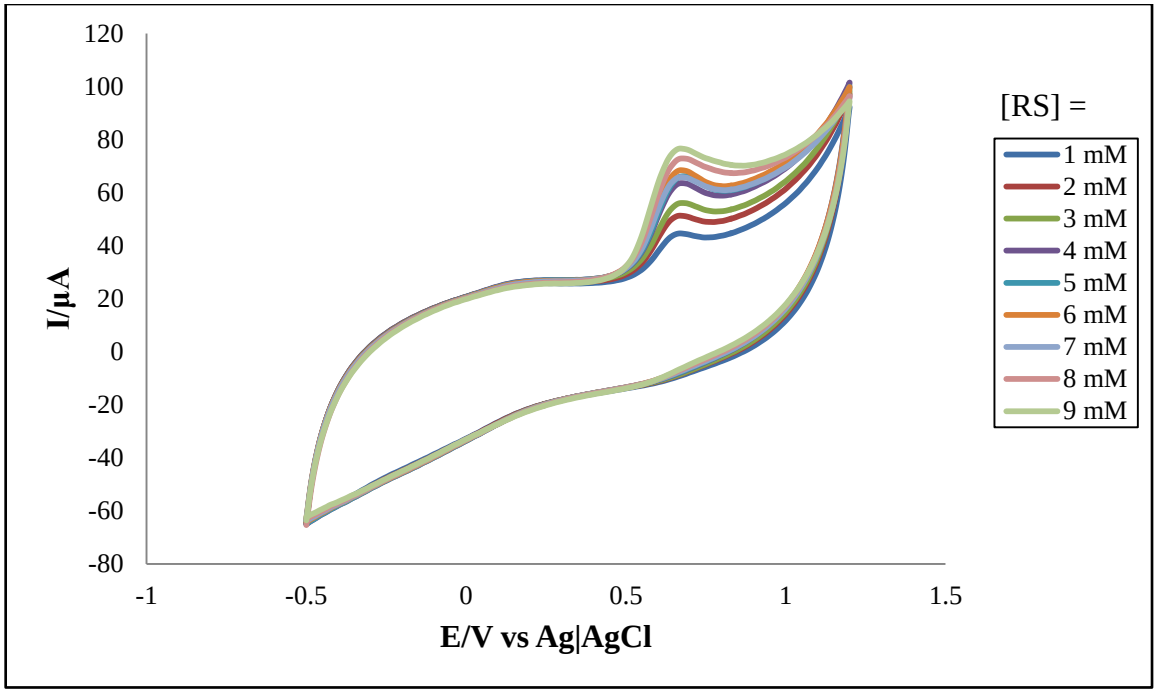

Figure 4.43: CV of RS of different concentration in PBS at 50 mV/s.

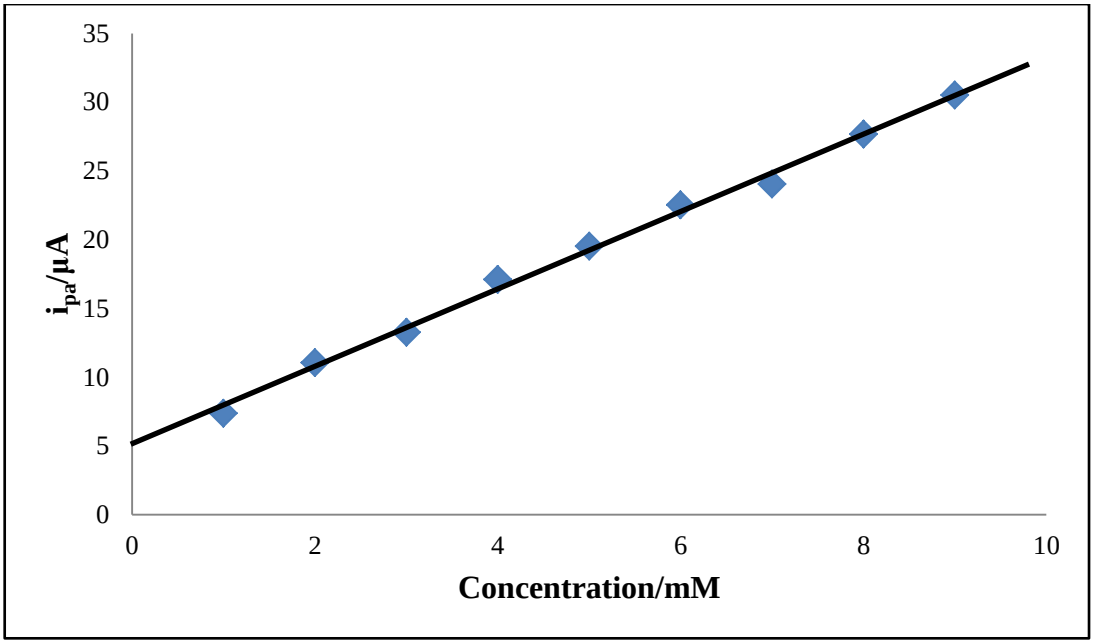

Figure 4.44: Variation of anodic peak current with the concentration of RS.

4.19 Simultaneous detection of CC and HQ at HIL-PGE in PBS by CV

CV of a binary mixture (5mM) of CC and HQ in PBS both at bare PGE and HIL-PGE is compared in Figure 4.45. The CV of HQ, CC and the binary mixture (5mM) of CC and HQ in PBS at HIL-PGE is shown in Figure 4.46. In HIL-PGE, HQ and CC gave two anodic peaks +0.182 V and +0.17V respectively, and two cathodic peaks at +0.16 V and +0.11V respectively. For the mixture of HQ and CC, there only one peak was seen that is the overlap peak of both CC and HQ, the anodic and cathodic peaks were at +0.352V and -0.17V respectively with. From the positions of the anodic and cathodic peaks it can be inferred that the peaks of both CC and HQ was overlapped. The HIL-PGE could not separate the anodic and cathodic peaks of CC and HQ when they are present in a mixture.

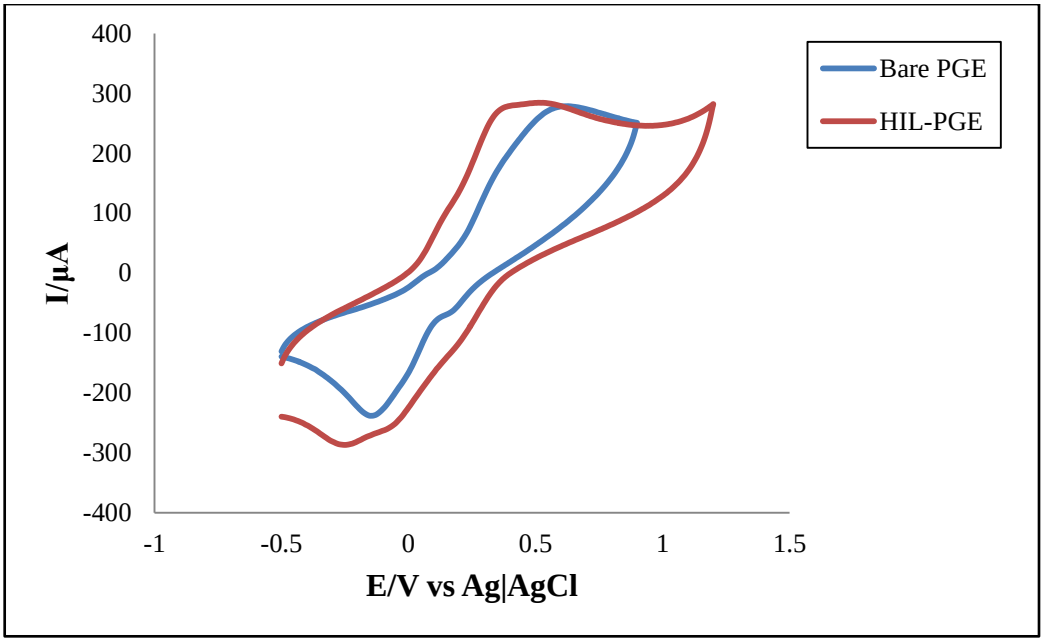

Figure 4.45: Comparison CV of binary mixture (1:1) of CC and HQ at bare PGE and HIL-PGE in PBS at 50 mV/s.

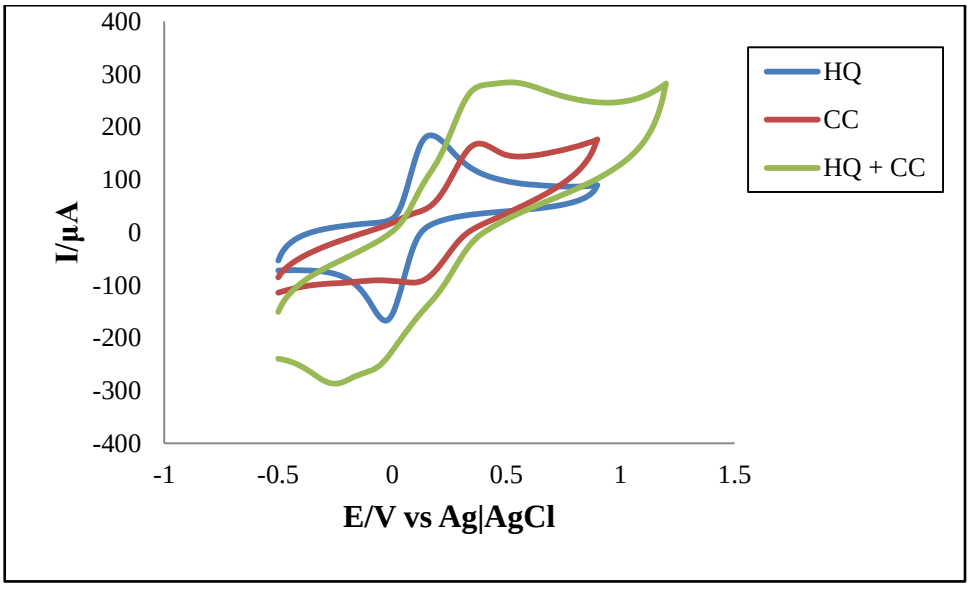

Figure 4.46: CV of CC, HQ and simultaneous CC+HQ in PBS at HIL-PGE 50 mV/s.

4.20 Simultaneous detection of CC and RS at HIL-PGE in PBS by CV

CV of a binary mixture (5mM) of CC and RS in PBS both at bare PGE and HIL-PGE is shown in Figure 4.47. The CV of CC, RS and the binary mixture (5mM) of CC and RS in PBS at HIL-PGE is shown in Figure 4.48. At HIL-PGE, CC and RS gave two anodic peaks at +0.17 V and +0.636 V respectively and one cathodic peak at +0.11 V. At HIL-

PGE, for binary mixture of CC and RS, two anodic peaks were found at +0.324 V and +0.738 V respectively and two very small cathodic peaks were found at +0.31 V and +0.116 V. The peaks are sharp and well defined for HIL-PGE while at Bare PGE the peaks are confusing. From the positions of the anodic peaks it can be said that the peaks of both CC and RS was found. The HIL-PGE electrode could separate the anodic peaks of CC and RS though they are present in a binary mixture. This separating ability of the HIL-PGE can be used to detect both CC and RS in presence of other qualitatively.

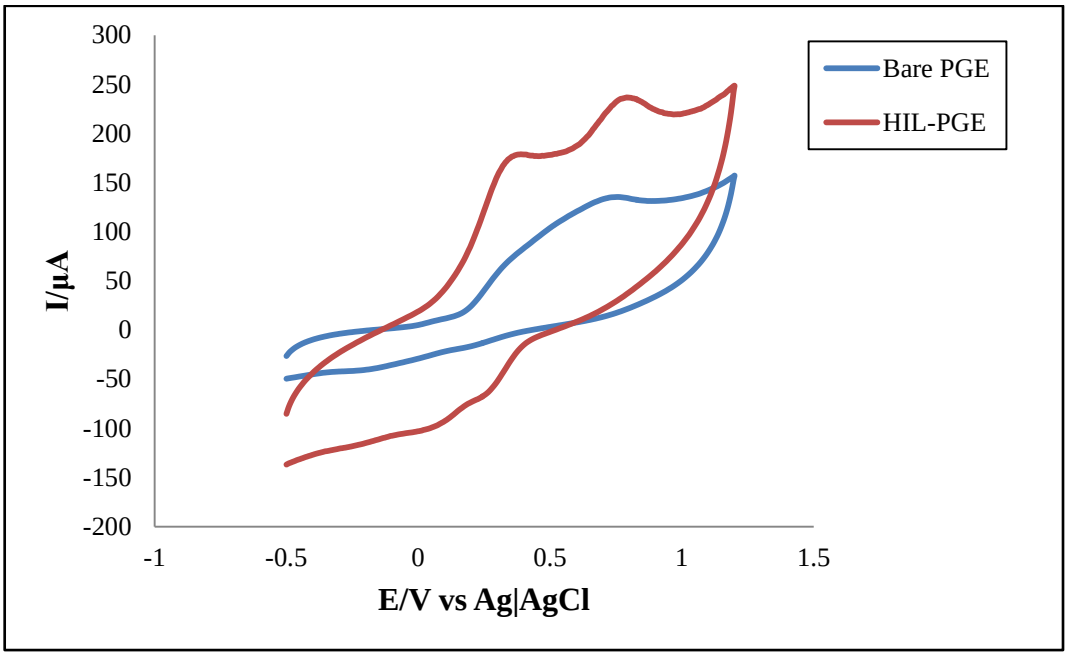

Figure 4.47: Comparison CV of binary mixture (1:1) of CC and RS at bare PGE and HIL-PGE in PBS at 50 mV/s.

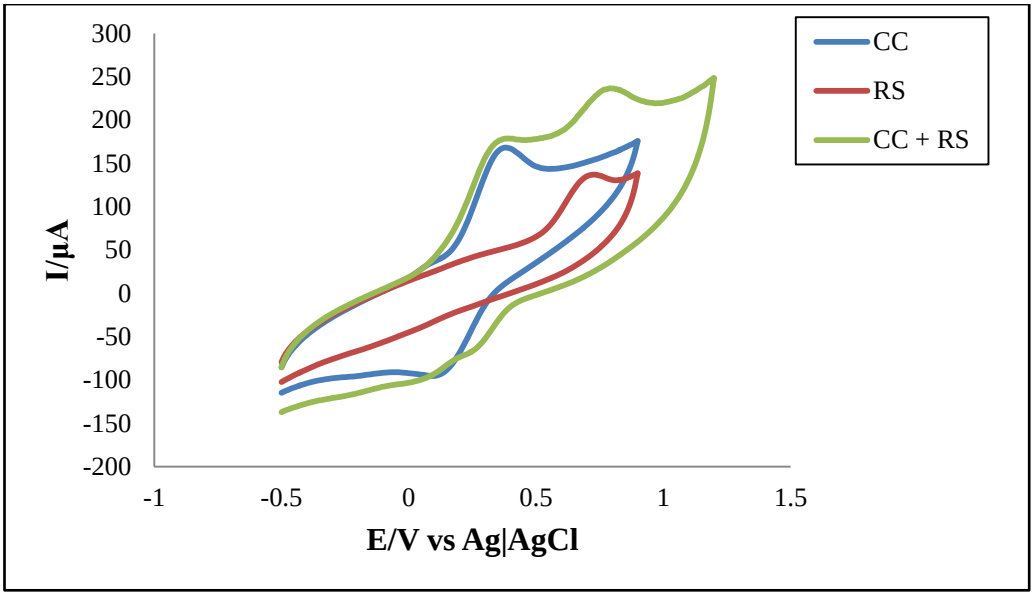

Figure 4.48: CV of CC, RS and simultaneous CC+RS in PBS at HIL-PGE 50 mV/s.

4.21 Simultaneous detection of HQ and RS at HIL-PGE in PBS by CV

CV of a binary mixture (5mM) of HQ and RS in PBS both at bare PGE and HIL-PGE is shown in Figure 4.49. The CV of HQ, RS and the binary mixture (5mM) of HQ and RS in PBS at HIL-PGE is shown in Figure 4.50.

At HIL-PGE, HQ and RS gave two anodic peaks at +0.182 V and +0.636 V respectively and one cathodic peak at +0.014 V. At HIL-PGE, for binary mixture of HQ and RS, two anodic peaks were found at +0.14 V and +0.676 V respectively and two cathodic peaks were found at +0.094 V and -0.212 Vrepectively. The peaks are sharp and well defined for HIL-PGE while at Bare PGE the peaks are confusing. From the positions of the anodic and cathodic peaks it can be said that the peaks of both HQ and RS was found. The HIL-PGE electrode could separate the anodic peaks of HQ and RS though they are present in a binary mixture. This separating ability of the HIL-PGE can be used to detect both CC and RS in presence of other qualitatively.

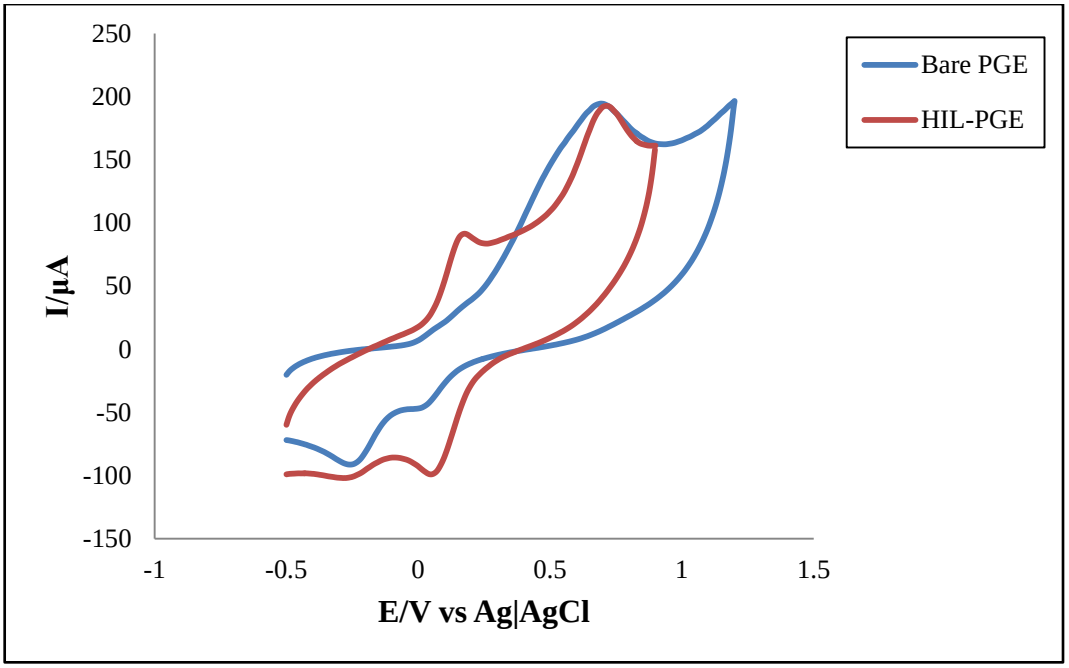

Figure 4.49: Comparison CV of binary mixture (1:1) of HQ and RS at bare PGE and HIL-PGE in PBS at 50 mV/s.

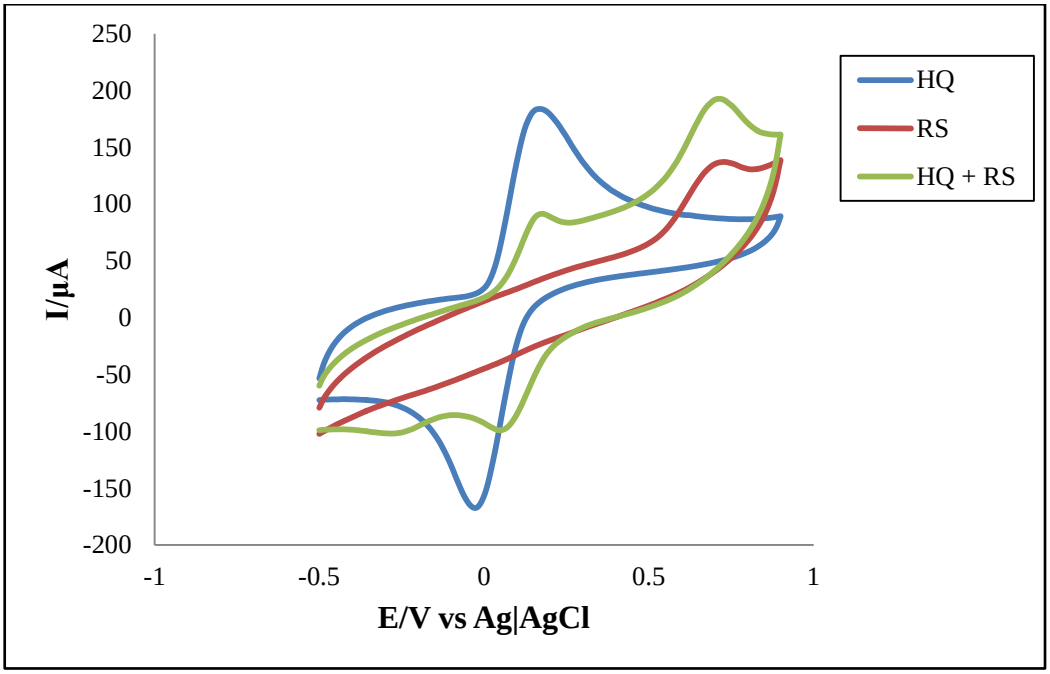

Figure 4.50: CV of HQ, RS and simultaneous HQ+RS in PBS at HIL-PGE 50 mV/s.

4.22 Simultaneous detection of CC, HQ and RS at HIL-PGE in PBS by CV

CV of a mixture (1:1:1) (5mM) of CC, HQ and RS in PBS both at bare PGE and HIL-PGE is compared in Figure 4.51. The CV of the mixture (5mM) of CC, HQ and RS in PBS at HIL-PGE is shown in Figure 4.52.

The HIL-PGE showed two sharp anodic peaks while Bare PGE showed one broad peak. At HIL-PGE, the CV of the mixture of three isomers shows two well defined anodic peaks at +0.31 V and +0.712 V respectively and a very small peak at 0.153 V, one big cathodic peak at 0.108 V and two very small peak at 0.326 V and -0.206 V. From the positions of the anodic and cathodic peaks it can be inferred that the peak of RS was found but the peaks of HQ and CC were overlap in such a way that they are far away from detection. The HIL-PGE could not separate the anodic and cathodic peaks of CC, HQ and RS when they are present in a mixture. This separating ability of the HIL-PGE cannot be used to detect CC, HQ and RS in presence of other qualitatively.

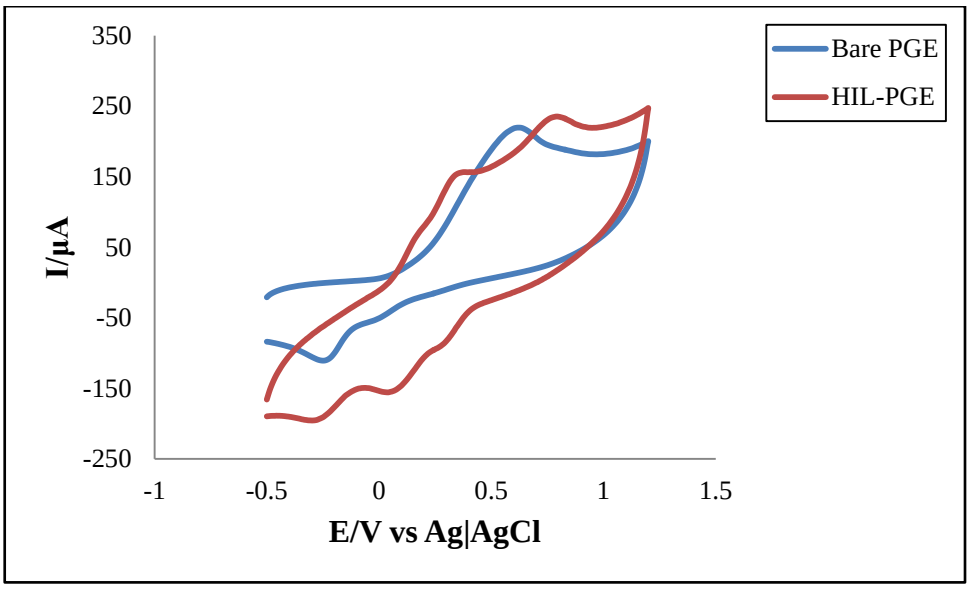

Figure 4.51: Comparison CV of CC, HQ and RS mixture (1:1:1) at bare PGE and HIL-PGE in PBS at 50 mV/s.

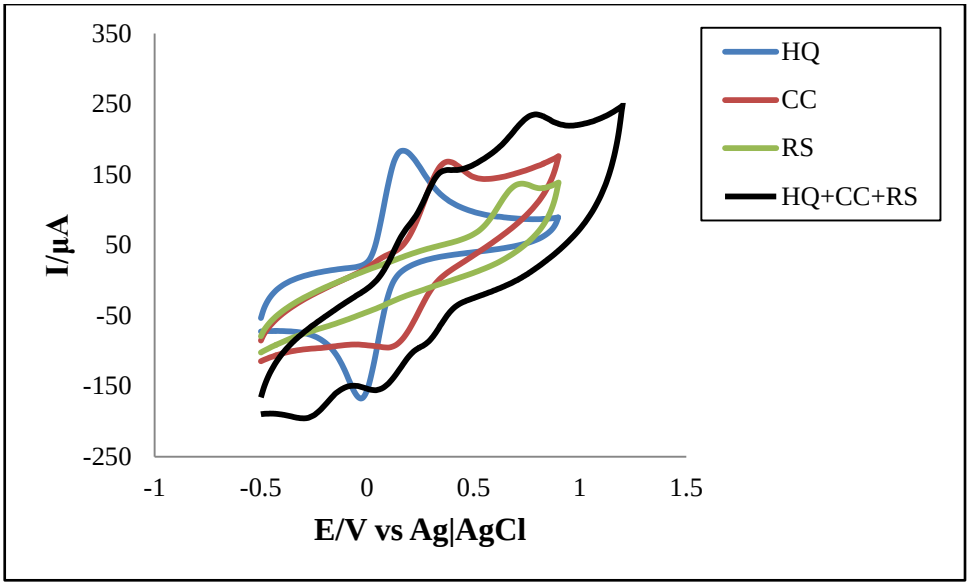

Figure 4.52: CV of CC, HQ, RS and simultaneous CC+HQ+RS in PBS at HIL-PGE 50 **mV/s.**

By using CV simultaneous detection of DHBIs was impossible. So DPV was employed. All the DPV experiments were taken at Epulse = 0.02 V and tpulse = 20 ms.

4.23 Simultaneous detection of CC and HQ at HIL-PGE in PBS by DPV

DPV of a binary mixture (5mM) of CC and HQ in PBS both at bare PGE and HIL-PGE is compared in Figure 4.53. The DPV of HQ, CC and the binary mixture (5mM) of CC and HQ in PBS at HIL-PGE is shown in Figure 4.54. In HIL-PGE, HQ and CC gives two peaks at +0.01 V and +0.105 V with peak currents 31 µA and 34 µA but at bare PGE the response is very low and there is no well-defined peak. For the mixture of HQ and CC, there two peaks were seen at +0.005 V and +0.13 V with peak currents 15 µA and 24 µA. The HIL-PGE could separate the peaks of CC and HQ when they are present in a mixture.

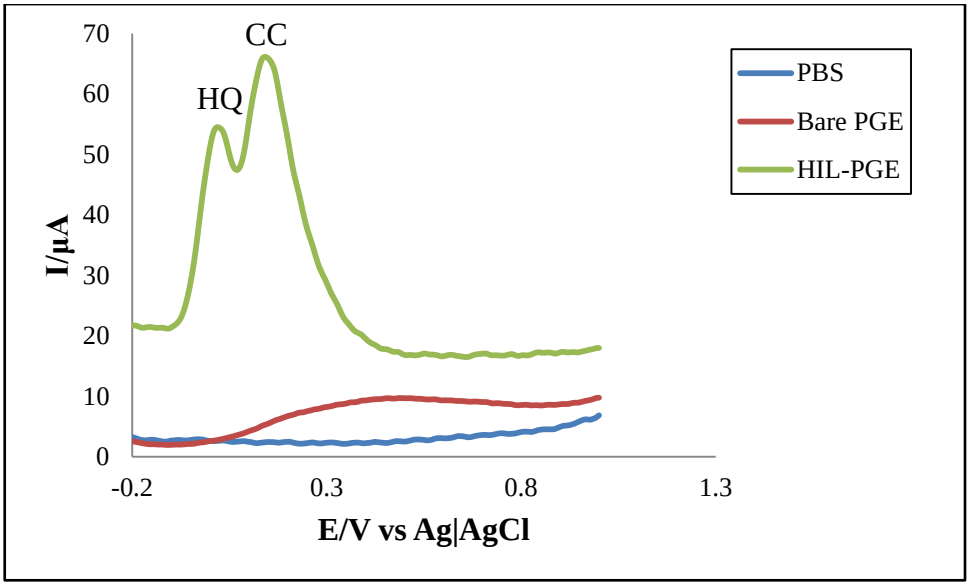

Figure 4.53: Comparison DPV of binary mixture (1:1) of CC and HQ at bare PGE and HIL-PGE in PBS at 50 mV/s.

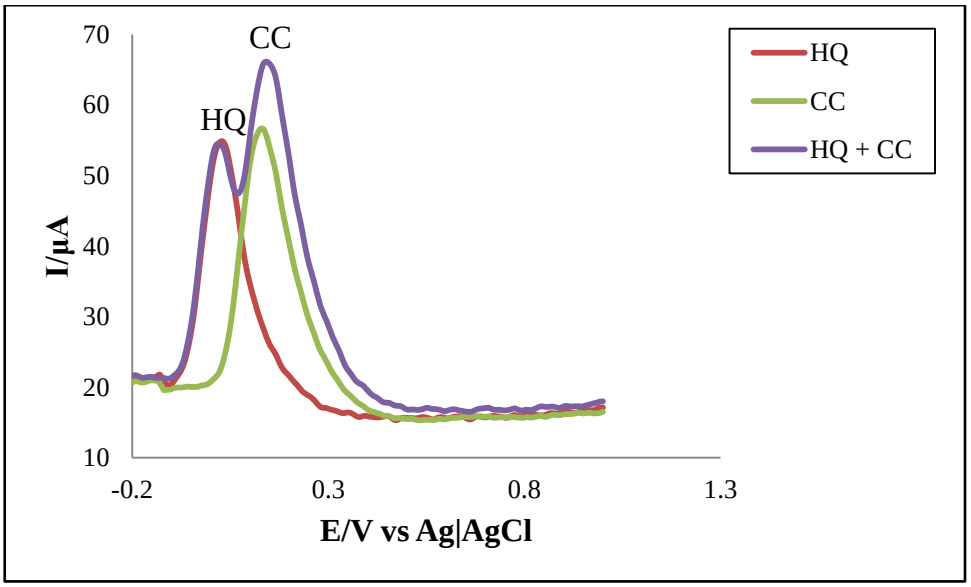

Figure 4.54: DPV of CC, HQ and simultaneous CC+HQ in PBS at HIL-PGE at 50mV/s.

4.24 Simultaneous detection of CC and RS at HIL-PGE in PBS by DPV

DPV of a binary mixture (5mM) of CC and RS in PBS both at bare PGE and HIL-PGE is compared in Figure 4.55. The DPV of CC, RS and the binary mixture (5mM) of CC and RS in PBS at HIL-PGE is shown in Figure 4.56. In HIL-PGE, CC and RS gives two peaks at +0.105 V and +0.505 V with peak currents 34 µA and 15 µA respectively but at bare PGE the response is very low and only the peak of RS can be detected. For the

mixture of CC and RS, there two peaks were seen at +0.125 V and +0.535 V with peak currents 30 µA and 9 µA. The HIL-PGE could separate the peaks of CC and RS when they are present in a mixture.

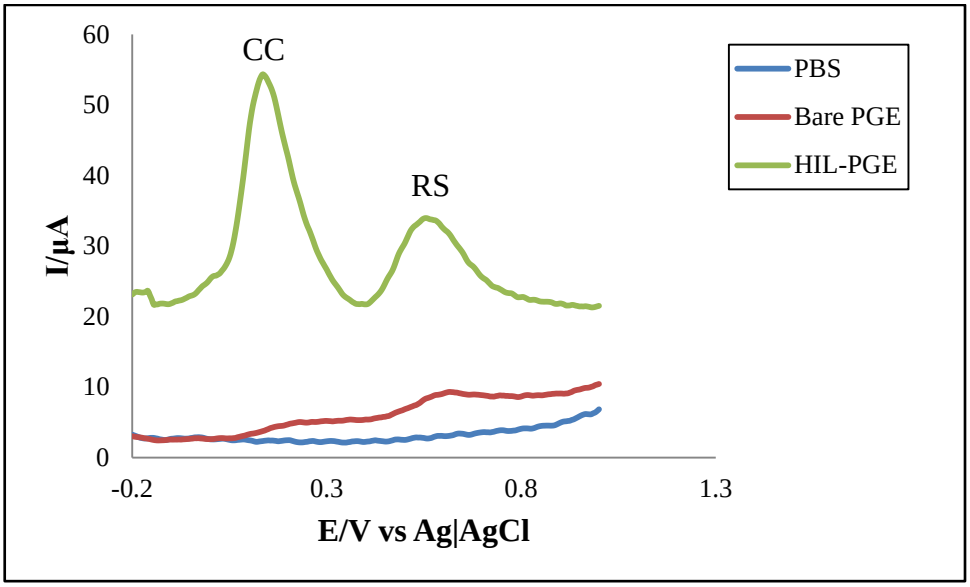

Figure 4.55: Comparison DPV of binary mixture (1:1) of CC and RS at bare PGE and HIL-PGE in PBS at 50 mV/s.

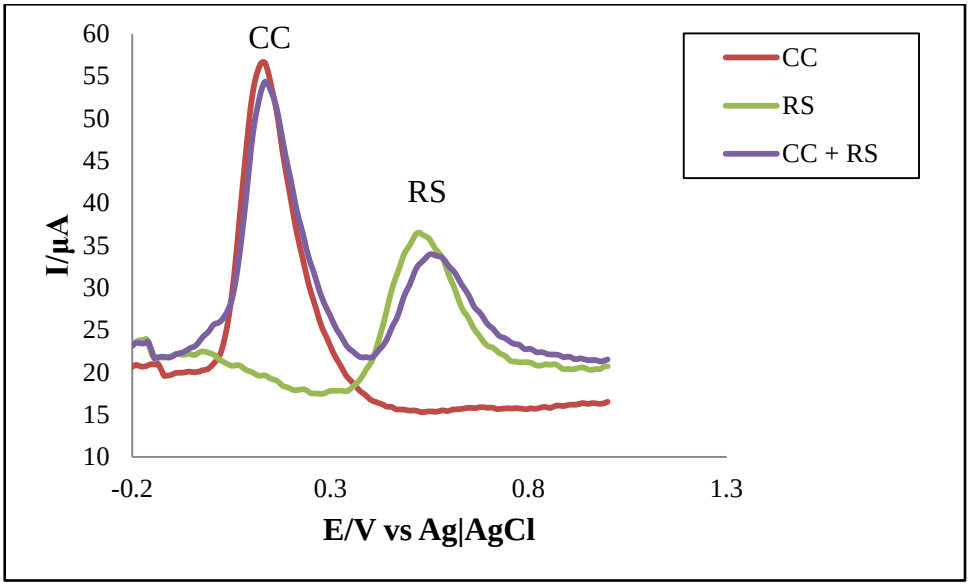

Figure 4.56: DPV of CC, RS and simultaneous CC+RS in PBS at HIL-PGE at 50 mV/s.

4.25 Simultaneous detection of HQ and RS at HIL-PGE in PBS by DPV

DPV of a binary mixture (5mM) of HQ and RS in PBS both at bare PGE and HIL-PGE is compared in Figure 4.57. The DPV of HQ, RS and the binary mixture (5mM) of HQ and RS in PBS at HIL-PGE is shown in Figure 4.58. In HIL-PGE, HQ and RS gives two peaks at +0.01 V and +0.505 V with peak currents 31 µA and 15 µA respectively but at bare PGE the response is very low and only the peak of RS can be detected. For the mixture of HQ and RS, there two peaks were seen at +0.015 V and +0.525V with peak currents 29 µA and 16 µA. The HIL-PGE could separate the peaks of HQ and RS when they are present in a mixture.

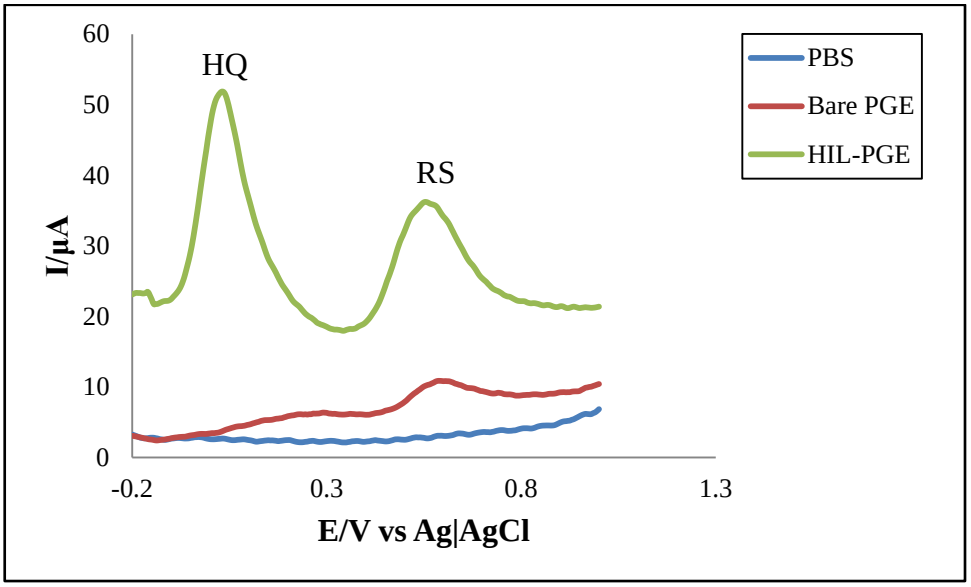

Figure 4.57: Comparison DPV of binary mixture (1:1) of HQ and RS at bare PGE and HIL-PGE in PBS at 50 mV/s.

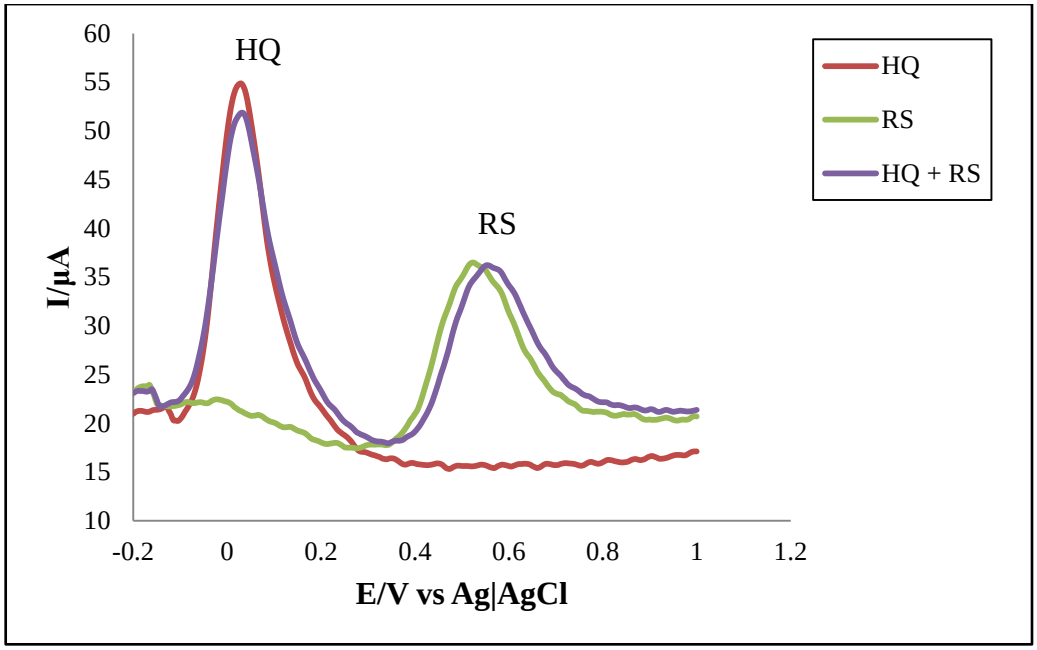

Figure 4.58: DPV of HQ, RS and simultaneous HQ+RS in PBS at HIL-PGE at 50 mV/s.

4.26 Simultaneous detection of CC, HQ and RS at HIL-PGE in PBS by DPV

DPV of a ternary mixture (5mM) of HQ, CC and RS in PBS both at bare PGE and HIL-PGE is shown in Figure 4.59. The DPV of HQ, RS and the binary mixture (5mM) of HQ and RS in PBS at HIL-PGE is shown in Figure 4.60. At HIL-PGE HQ, CC and RS gave three peaks at +0.01 V, +0.105 V and +0.505 V with peak currents 31 µA, 34 µA and 15 µA respectively but at bare PGE the response is very low and there is no well-defined peak. For ternary mixture of HQ, CC and RS, there three peaks were seen at +0.015 V, +0.13 V and +0.53 V with peak currents 12 µA, 17 µA and 8 µA respectively. The HIL-PGE could separate the peaks of HQ and RS when they are present in a mixture.

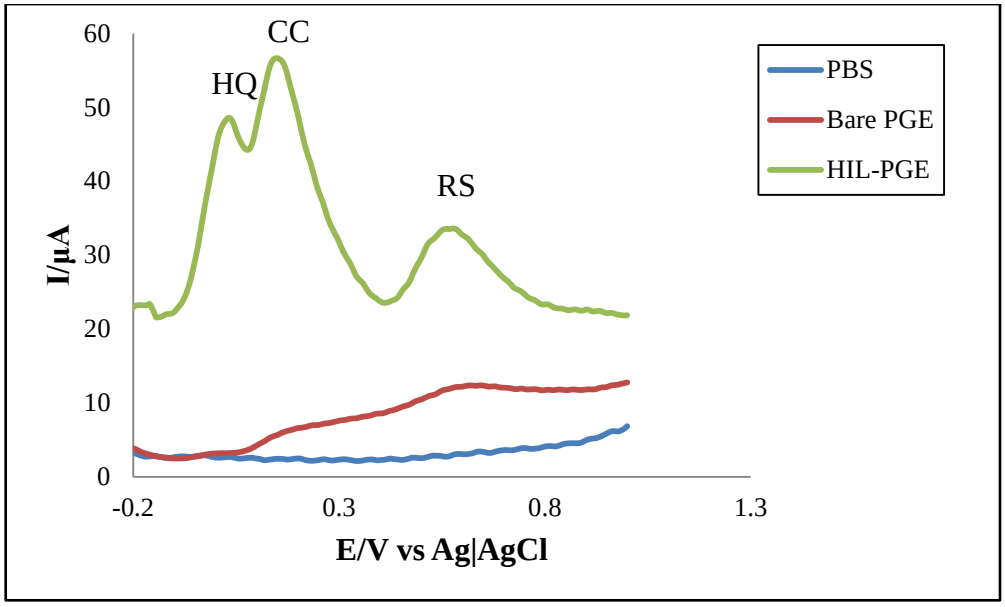

Figure 4.59: Comparison DPV of CC, HQ and RS mixture (1:1:1) at bare PGE and HIL-PGE in PBS at 50 mV/s.

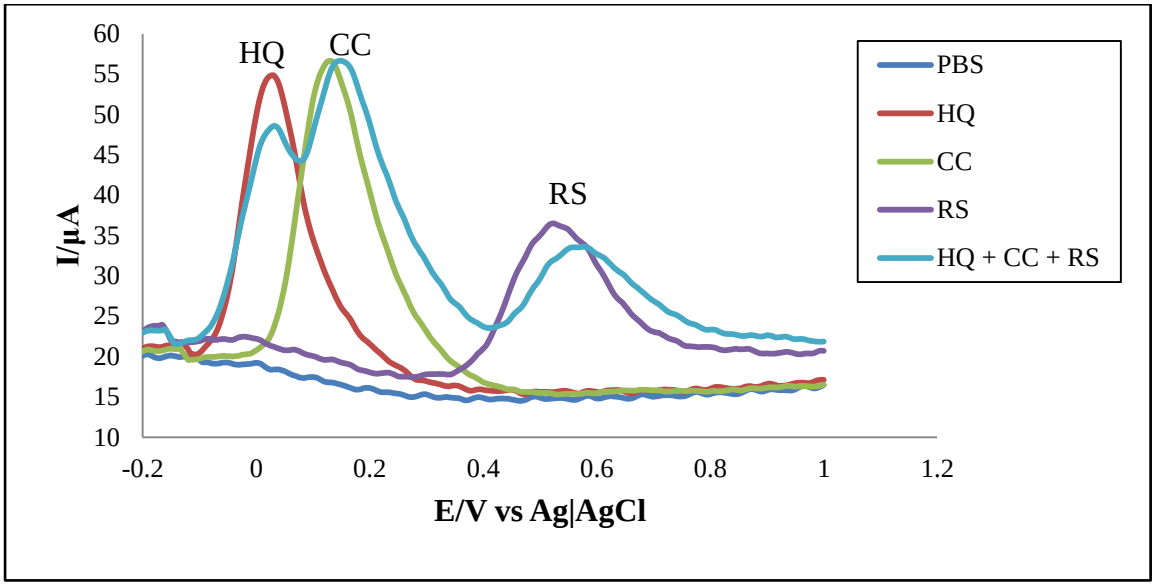

Figure 4.60: DPV of CC, HQ, RS and simultaneous CC+HQ+RS in PBS at HIL-PGE 50 mV/s.

4.27 Quantitative estimation of CC in presence of HQ in PBS at HIL-PGE

DPV of the binary mixture of CC, HQ at HIL-PGE in the potential range of -200 mV to +1000 mV in PBS was taken. Concentration of HQ was kept constant and the concentration of CC was varied successively by added definite amount of solution using a micro pipette. The DPV is shown in Figure 4.61. A calibration curve (Figure 4.62) was

drawn for different concentrations of CC. This calibration curve can be used to determine CC in presence of HQ quantitatively in a binary mixture. In case of CC the peak current increases approximately 5 µA per mM.

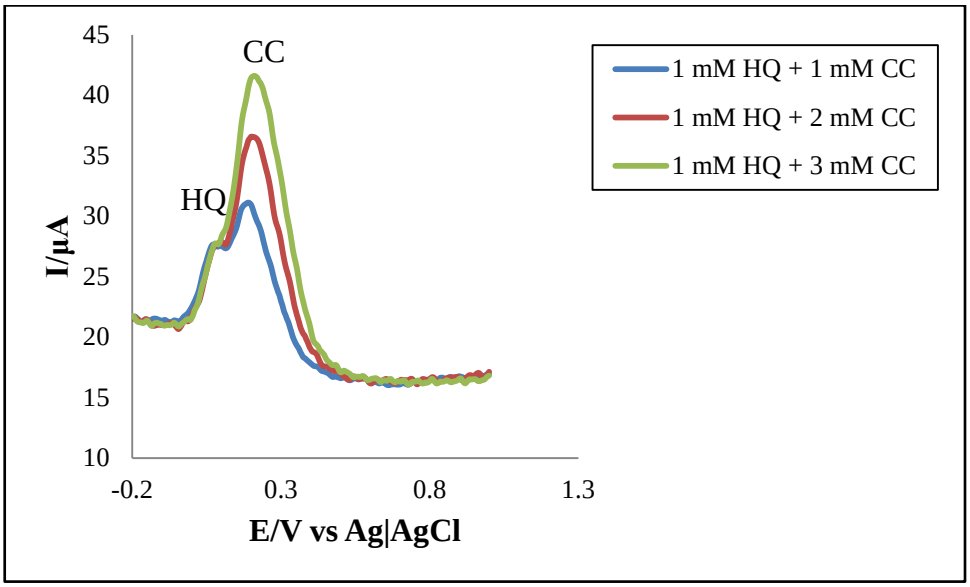

Figure 4.61: DPV for quantitative estimation of CC in presence of HQ at HIL-PGE in PBS.

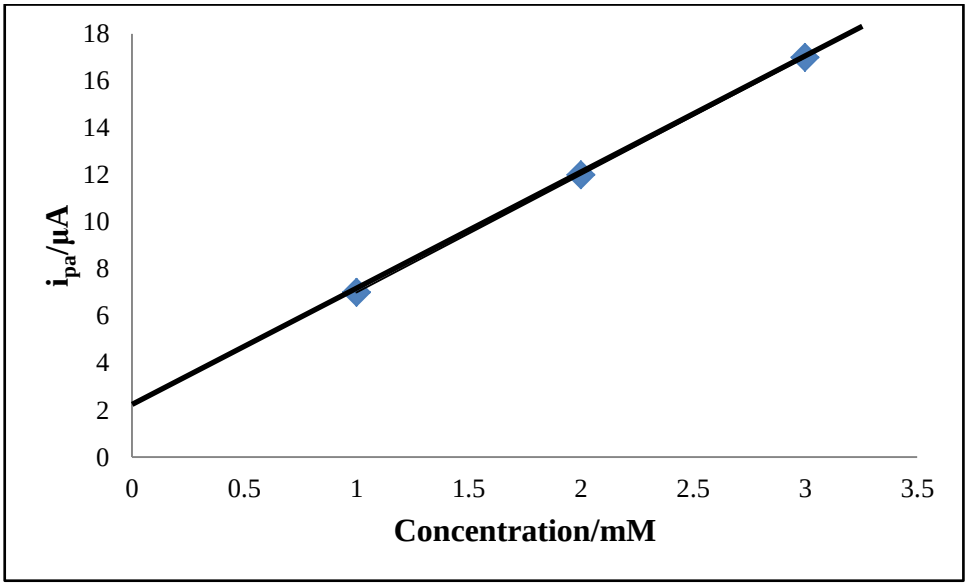

Figure 4.62: Calibration curve for estimation of CC in presence of HQ (current response with variation of concentration).

4.28 Quantitative estimation of CC in presence of RS in PBS at HIL-PGE

DPV of the binary mixture of CC, RS at HIL-PGE in the potential range of -200 mV to +1000 mV in PBS was taken. Concentration of RS was kept constant whereas the concentration of CC was varied successively by added definite amount of solution using a micro pipette. The DPV is shown in Figure 4.63.

A calibration curve (Figure 4.64) was drawn for different concentrations of CC. This calibration curve can be used to determine CC in presence of RS quantitatively in a binary mixture. In case of CC the peak current increases approximately 5 µA per mM.

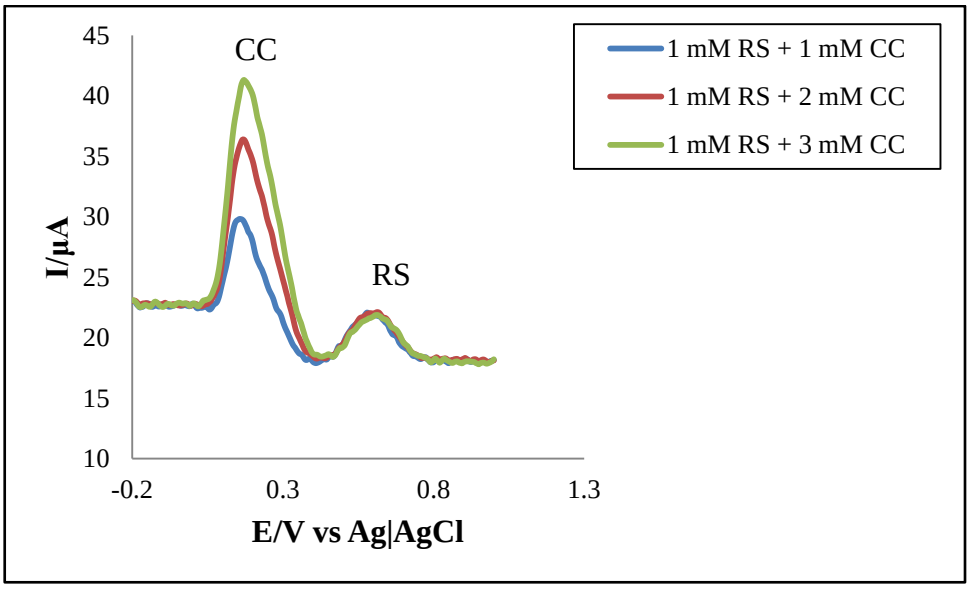

Figure 4.63: DPV for quantitative estimation of CC in presence of RS at HIL-PGE in PBS.

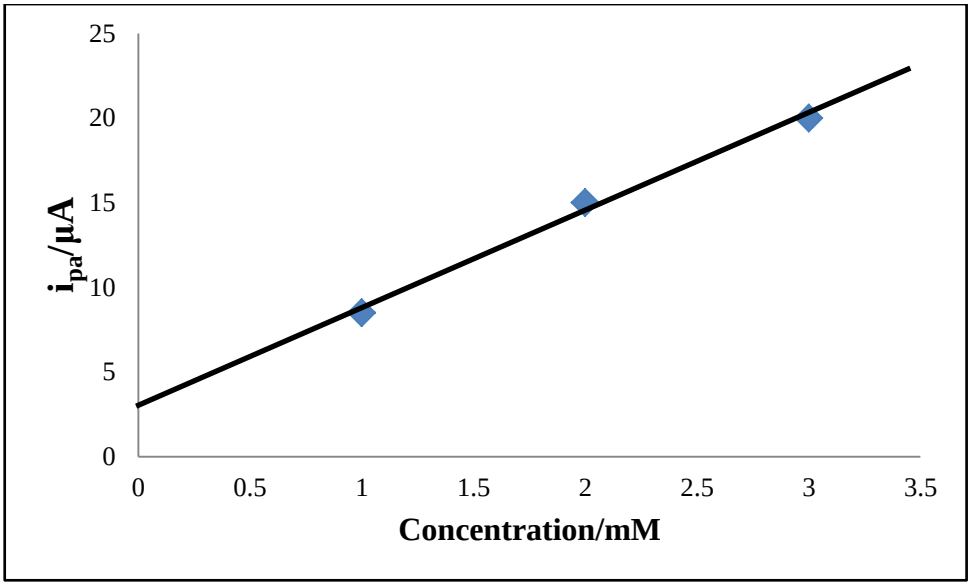

Figure 4.64: Calibration curve for estimation of CC in presence of RS (current response with variation of concentration).

4.29 Quantitative estimation of HQ in presence of RS in PBS at HIL-PGE

DPV of the binary mixture of HQ, RS at HIL-PGE in the potential range of -200 mV to +1000 mV in PBS was taken. Concentration of RS was kept constant whereas the concentration of HQ was varied successively by added definite amount of solution using a micro pipette. The DPV is shown in Figure 4.65.

A calibration curve (Figure 4.66) was drawn for different concentrations of HQ. This calibration curve can be used to determine HQ in presence of RS quantitatively in a binary mixture. In case of HQ the peak current increases approximately 6 µA per mM.

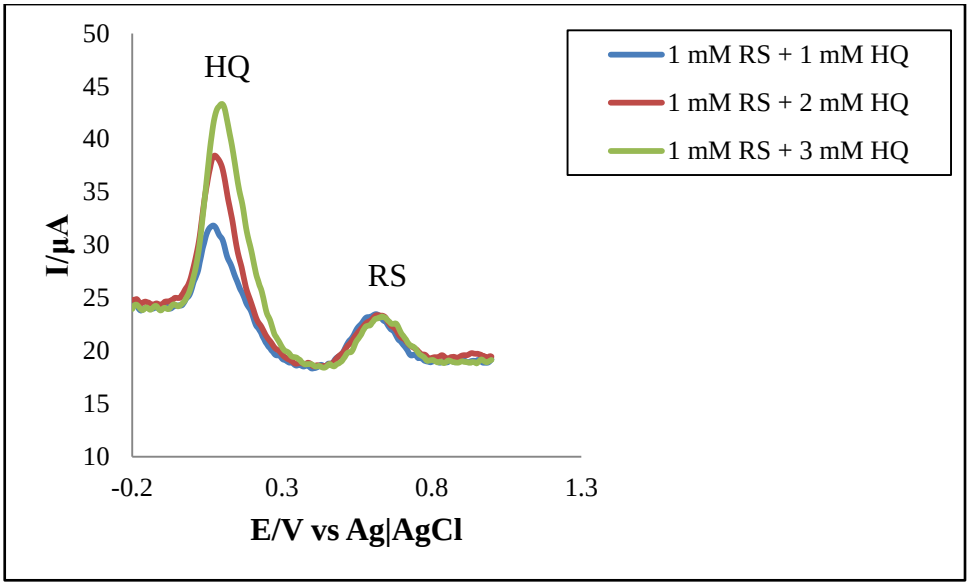

Figure 4.65: DPV for quantitative estimation of HQ in presence of RS at HIL-PGE in PBS.

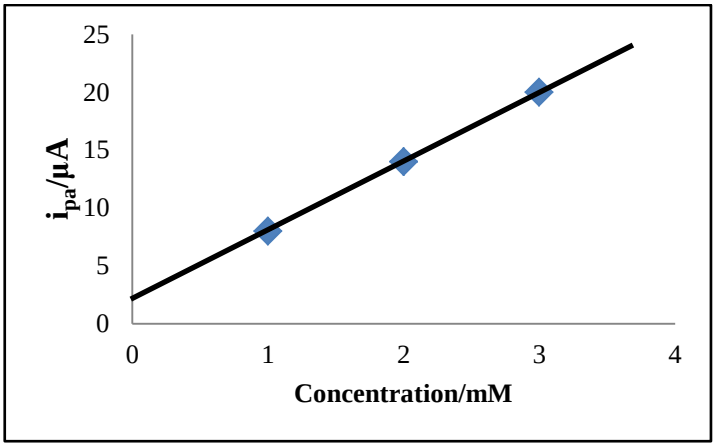

Figure 4.66: Calibration curve for estimation of HQ in presence of RS (current response with variation of concentration).

4.30 Quantitative estimation of HQ in presence of CC in PBS at HIL-PGE

DPV of the binary mixture of HQ, CC at HIL-PGE in the potential range of -200 mV to +1000 mV in PBS was taken. Concentration of CC was kept constant whereas the concentration of HQ was varied successively by added definite amount of solution using a micro pipette. The DPV is shown in Figure 4.67. A calibration curve (Figure 4.68) was drawn for different concentrations of HQ. This calibration curve can be used to determine HQ in presence of CC quantitatively in a binary mixture. In case of HQ the peak current increases approximately 3 µA per mM.

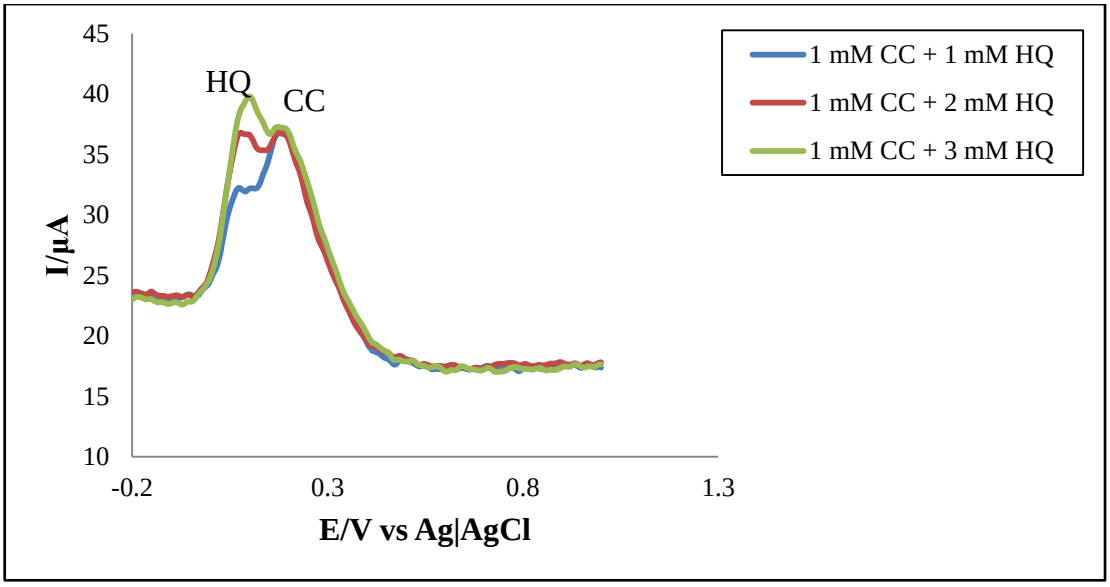

Figure 4.67: DPV for quantitative estimation of HQ in presence of CC at HIL-PGE in PBS.

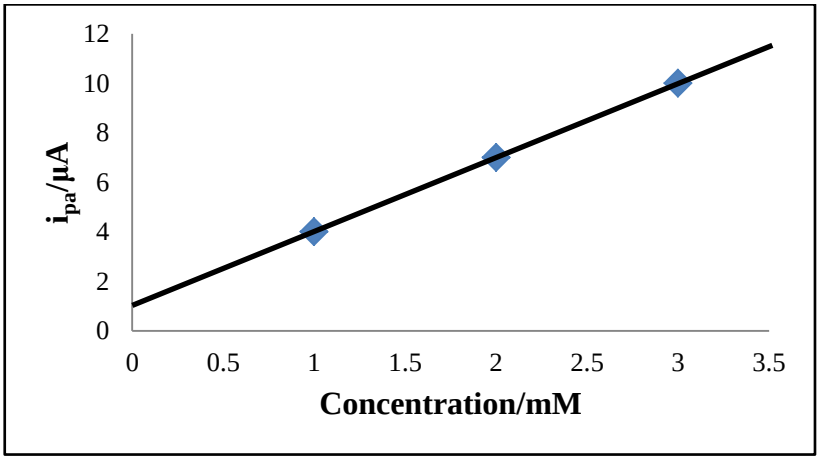

Figure 4.68: Calibration curve for estimation of HQ in presence of CC (current response with variation of concentration).

4.31 Quantitative estimation of RS in presence of HQ in PBS at HIL-PGE

DPV of the binary mixture of HQ, RS at HIL-PGE in the potential range of -200 mV to +1000 mV in PBS was taken. Concentration of HQ was kept constant whereas the concentration of RS was varied successively by added definite amount of solution using a micro pipette. The DPV is shown in Figure 4.69.

A calibration curve (Figure 4.70) was drawn for different concentrations of RS. This calibration curve can be used to determine HQ in presence of RS quantitatively in a binary mixture. In case of RS the peak current increases approximately 3.5 µA per mM.

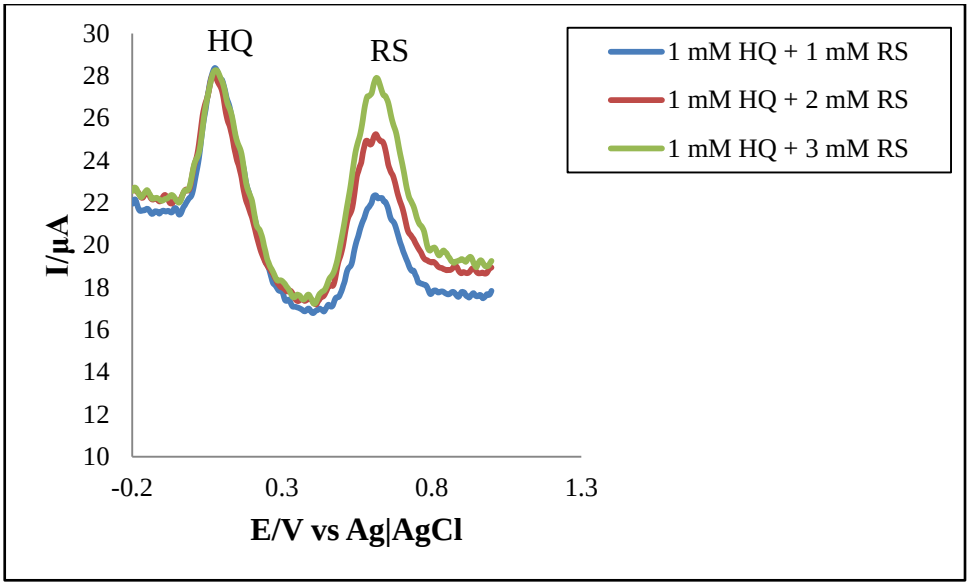

Figure 4.69: DPV for quantitative estimation of RS in presence of HQ at HIL-PGE in PBS.

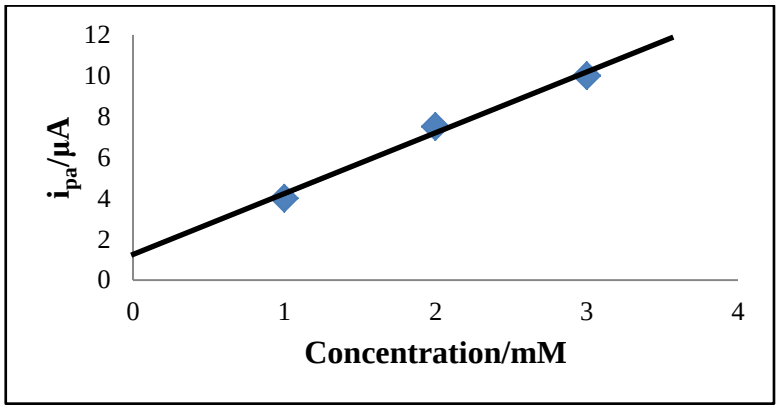

Figure 4.70: Calibration curve for estimation of RS in presence of HQ (current response with variation of concentration).

4.32 Quantitative estimation of RS in presence of CC in PBS at HIL-PGE

DPV of the binary mixture of CC, RS at HIL-PGE in the potential range of -200 mV to +1000 mV in PBS was taken. Concentration of CC was kept constant whereas the concentration of RS was varied successively by added definite amount of solution using a micro pipette. The DPV is shown in Figure 4.71.

A calibration curve (Figure 4.72) was drawn for different concentrations of RS. This calibration curve can be used to determine CC in presence of RS quantitatively in a binary mixture. In case of RS the peak current increases approximately 3 µA per mM.

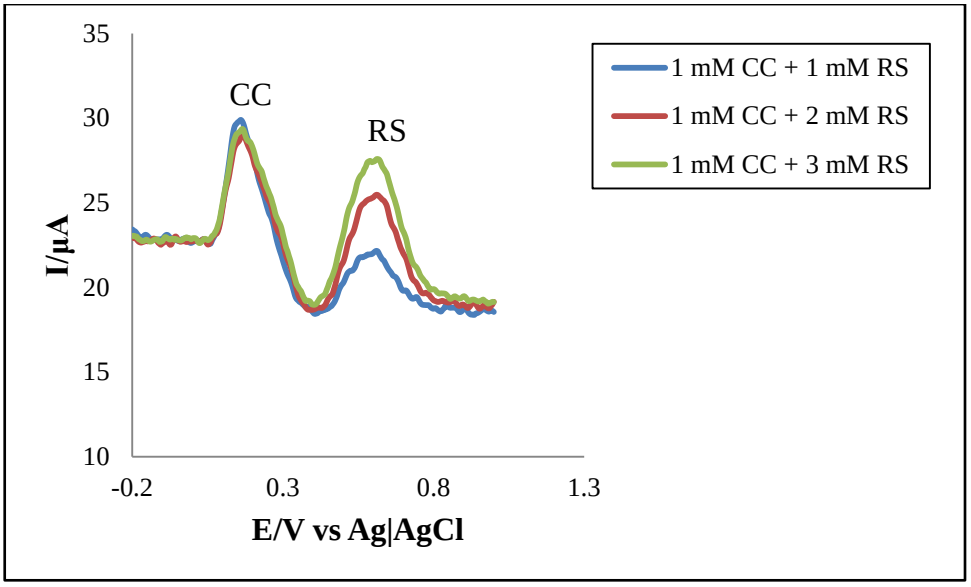

Figure 4.71: DPV for quantitative estimation of RS in presence of CC at HIL-PGE in PBS.

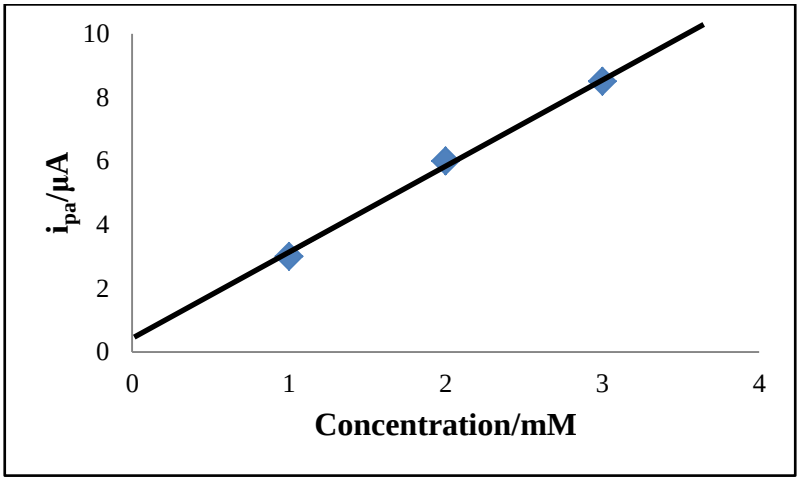

Figure 4.72: Calibration curve for estimation of RS in presence of CC (current response with variation of concentration).

4.33 Simultaneous quantitative estimation of HQ, CC and RS in PBS at HIL-PGE

DPV of the ternary mixture of HQ, CC and RS at ME in the potential range of -200 mV to +1000 mV in PBS was taken. Concentration of HQ, RS and CC was varied successively by added definite amount of solutions using a micro pipette. The DPV is shown in Figure 4.73.

A calibration curve (Figure 4.74) was drawn for different concentrations of CC, HQ and RS. This calibration curve can be used for quantitative estimation of RS, HQ and CC

simultaneously from a ternary mixture. In case of HQ the peak current increases approximately 2.5 µA per mM. In case of CC the peak current increases approximately 3.5 µA per mM. In case of RS the peak current increases approximately 3.5 µA per mM. The limit of detection was calculated by signal-to-noise ratio. The limit of detection (LOD) was calculated by signal-to-noise ratio (S/N=3). The LOD for HQ, CC and RS is 6.38 µM L^{-1}, 4.56 µM L^{-1} and 19.6 µM L^{-1} respectively in simultaneous detection.

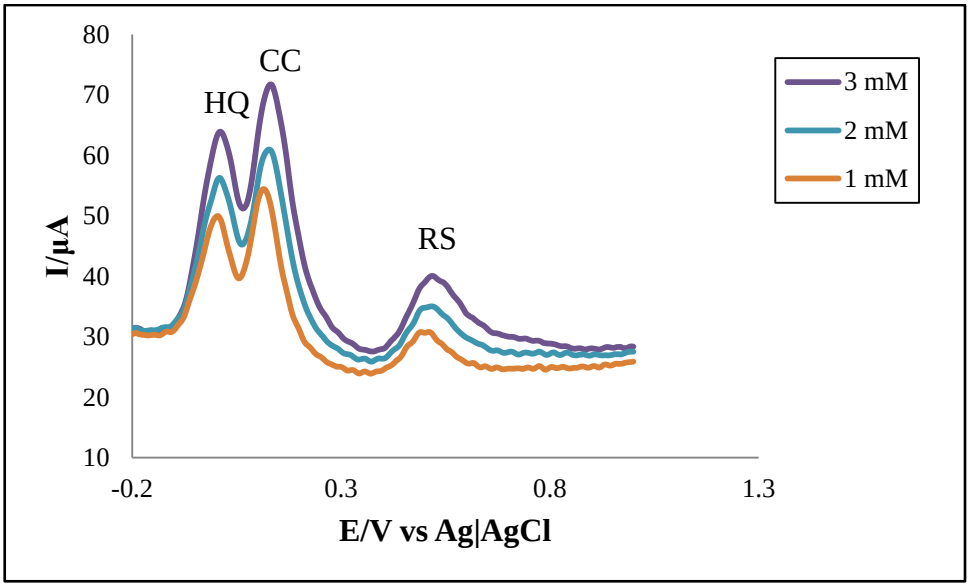

Figure 4.73: DPV for simultaneous quantitative estimation of RS, HQ and CC from a mixture in PBS at HIL-PGE.

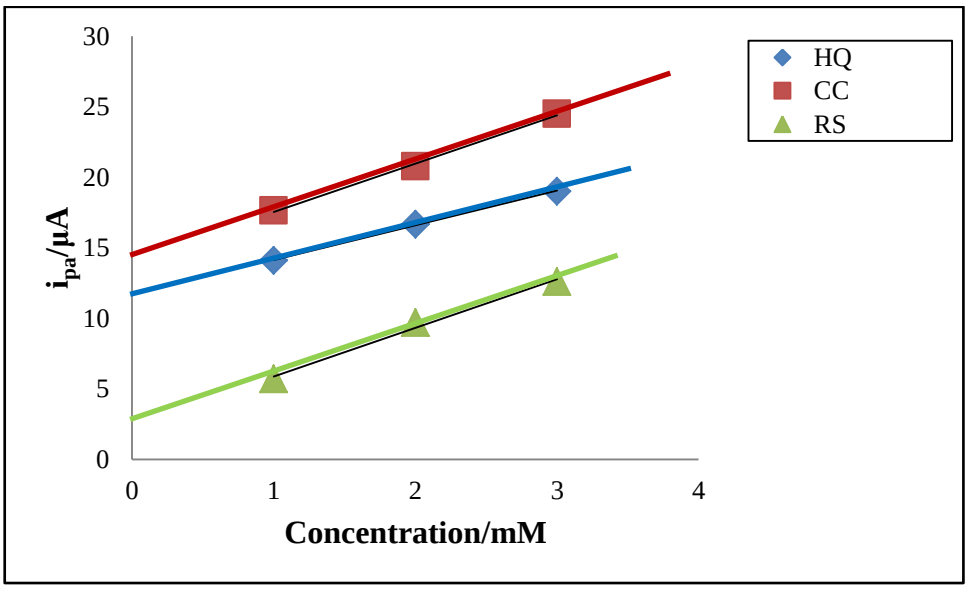

Figure 4.74: Calibration curve for simultaneous estimation of RS, HQ and CC with respect to concentration.

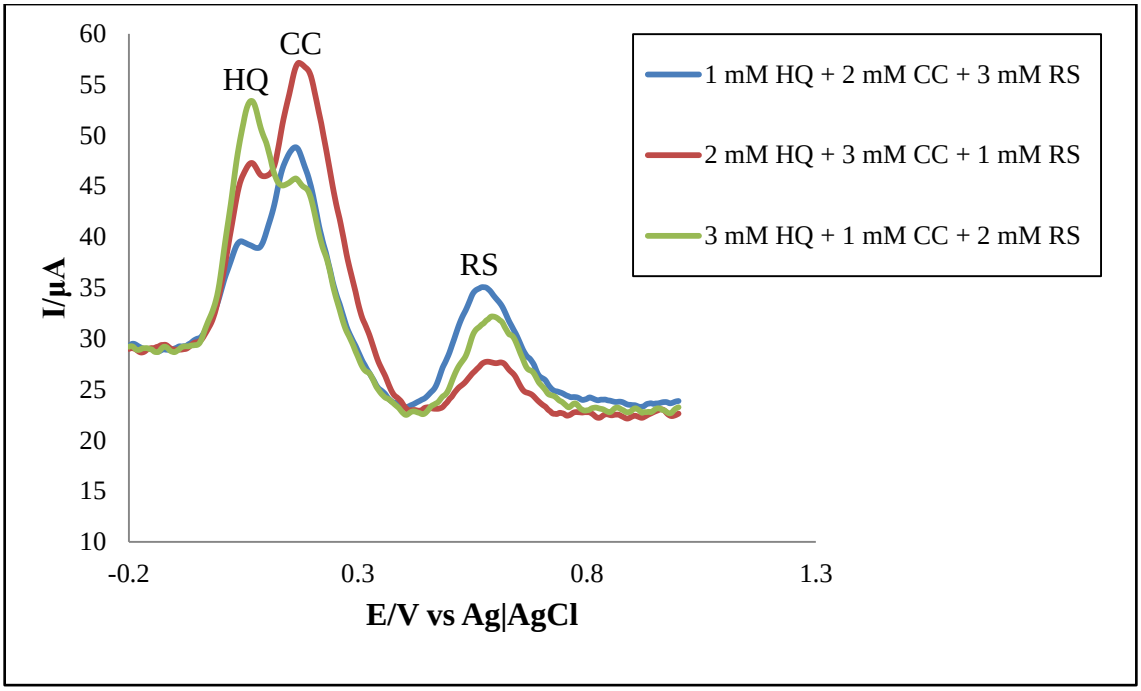

Figure 4.75: DPV for simultaneous estimation of three isomers at different concentrations.

The sensitivity of three isomers was calculated. The sensitivity for HQ is 448.49 µA/mM/cm^2, for CC is 627.35 µA/mM/cm^2 and for RS is 146.10 µA/mM/cm^2 in simultaneous detection. This value of sensitivity is very high. This can be explained by the information of SEM image of the surface of working electrode. There are so many pores and pits, that results increase in surface area of working electrode.

4.34 Simultaneous detection of HQ and CC at BIL-PGE in PBS by DPV

The DPV of HQ, CC and the binary mixture (5mM) of CC and HQ in PBS at BIL-PGE is shown in Figure 4.76. In BIL-PGE, HQ and CC gives two peaks at +0.01 V and +0.125 V with peak currents 48.7 µA and 49.85 µA respectively and for the binary mixture of HQ and CC, there two peaks were seen at +0.01V and +0.13 V with peak currents 18.22 µA and 23.01 µA. The BIL-PGE could separate the peaks of CC and HQ when they are present in a mixture.

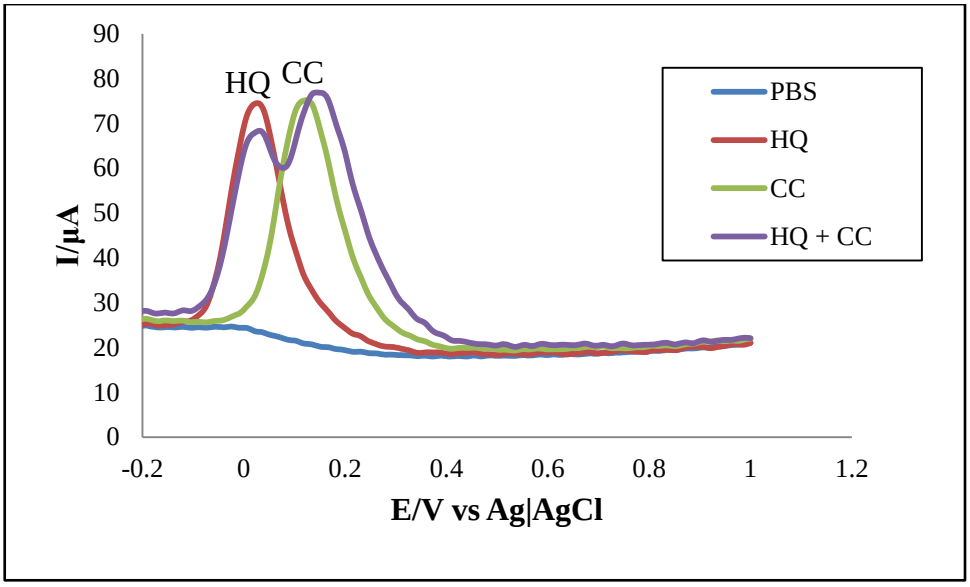

Figure 4.76: DPV of CC, HQ and simultaneous CC+HQ in PBS at BIL-PGE.

4.35 Simultaneous detection of CC and RS at BIL-PGE in PBS by DPV

The DPV of CC, RS and the binary mixture (5mM) of CC and RS in PBS at BIL-PGE is shown in Figure 4.77. In BIL-PGE, CC and RS gives two peaks at +0.125 V and +0.46V with peak currents 49.85 µA and 20.8 µA respectively and for the binary mixture of CC and RS, there two peaks were seen at +0.115 V and +0.525 V with peak currents 45.1 µA and 15.5. The BIL-PGE could separate the peaks of CC and RS when they are present in a mixture.

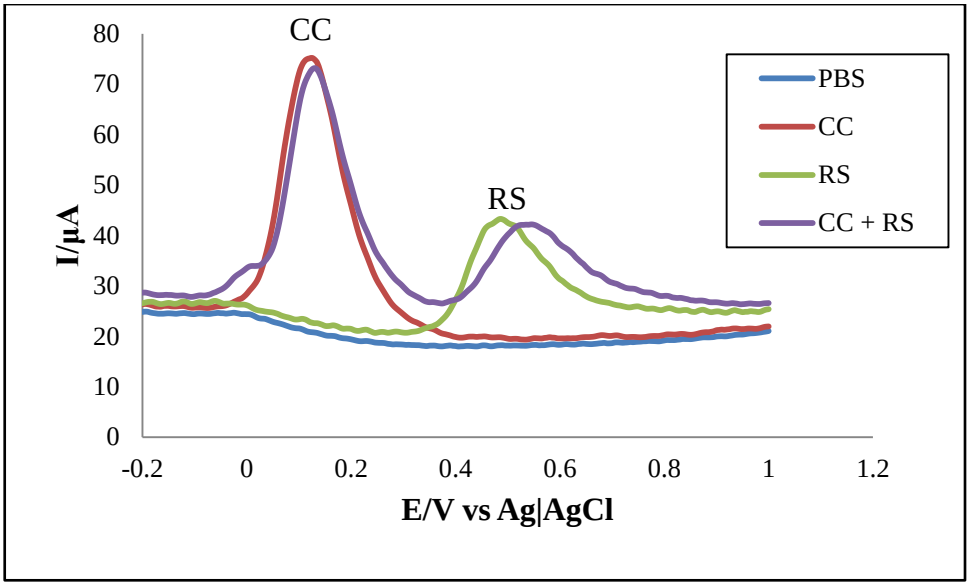

Figure 4.77: DPV of CC, RS and simultaneous CC+RS in PBS at BIL-PGE.

4.36 Simultaneous detection of HQ and RS at BIL-PGE in PBS by DPV

The DPV of HQ, RS and the binary mixture (5mM) of HQ and RS in PBS at BIL-PGE is shown in Figure 4.78. In BIL-PGE, HQ and RS gives two peaks at +0.01 V and +0.46 V with peak currents 48.7 µA and 20.8 µA respectively and for the binary mixture of HQ and RS, there two peaks were seen at +0.005 V and +0.5 V with peak currents 40.14 µA and 20.6 µA. The BIL-PGE could separate the peaks of HQ and RS when they are present in a mixture.

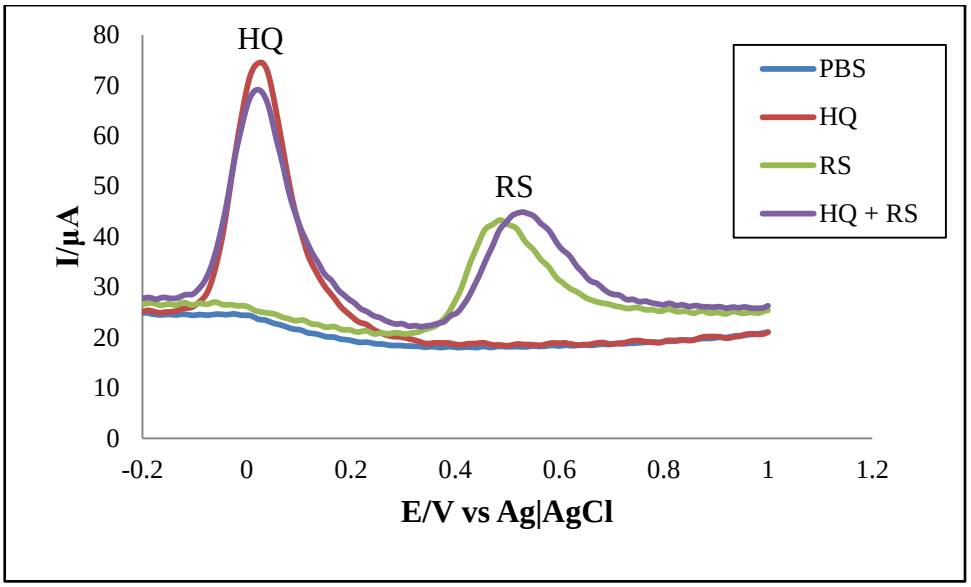

Figure 4.78: DPV of HQ, RS and simultaneous HQ+RS in PBS at BIL-PGE.

4.37 Simultaneous detection of HQ, CC and RS at BIL-PGE in PBS by DPV

The DPV of HQ, CC, RS and the ternary mixture (5mM) of HQ, CC and RS in PBS at BIL-PGE is shown in Figure 4.79. In BIL-PGE, HQ, CC and RS gave three peaks at +0.01 V, +0.125 V and +0.46 V with peak currents 48.7 µA, 49.85 µA and 20.8 µA respectively and for the ternary mixture of HQ, CC and RS, there three peaks were seen at +0.005 V, +0.125 V and +0.515 V with peak currents 20.45 µA, 24.7 µA and 13.4 µA. The BIL-PGE could separate the peaks of CC and HQ when they are present in a mixture.

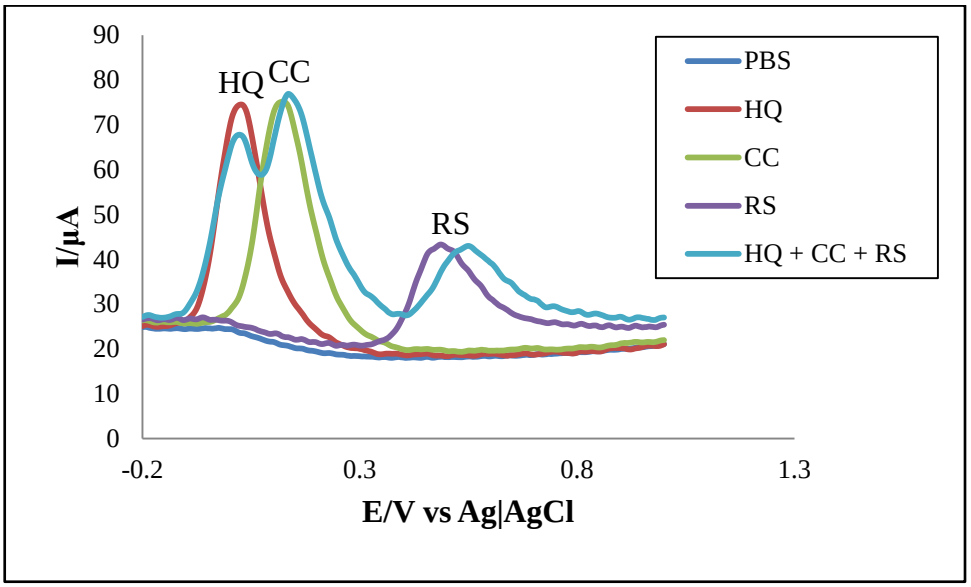

Figure 4.79: DPV of CC, HQ, RS and simultaneous CC+HQ+RS in PBS at BIL-PGE.

4.38 Comparison of the response of HQ, CC and RS at HIL-PGE and BIL-PGE in PBS by DPV

DPVs of three solutions of HQ, CC and RS in PBS all are at HIL-PGE and BIL-PGE are shown in Figure 4.80, Figure 4.81 and Figure 4.82. In HIL-PGE, HQ gives peak at +0.01 V with peak current 31 µA, CC gives peak at +0.105 V with peak current 34 µA and RS gives peak at +0.505 V with peak current 15 µA. But at BIL-PGE the peak intensity is higher than HIL-PGE. In BIL-PGE, HQ gave peak at +0.01 V with peak current 48.7 µA, CC gave peak at +0.125 V with peak current 49.85 µA and RS gives peak at +0.46 V with peak current 20.8 µA. From HIL-PGE to BIL-PGE current increased 17.7 µA for HQ, 15.85 µA for CC and 5.8 µA for RS.

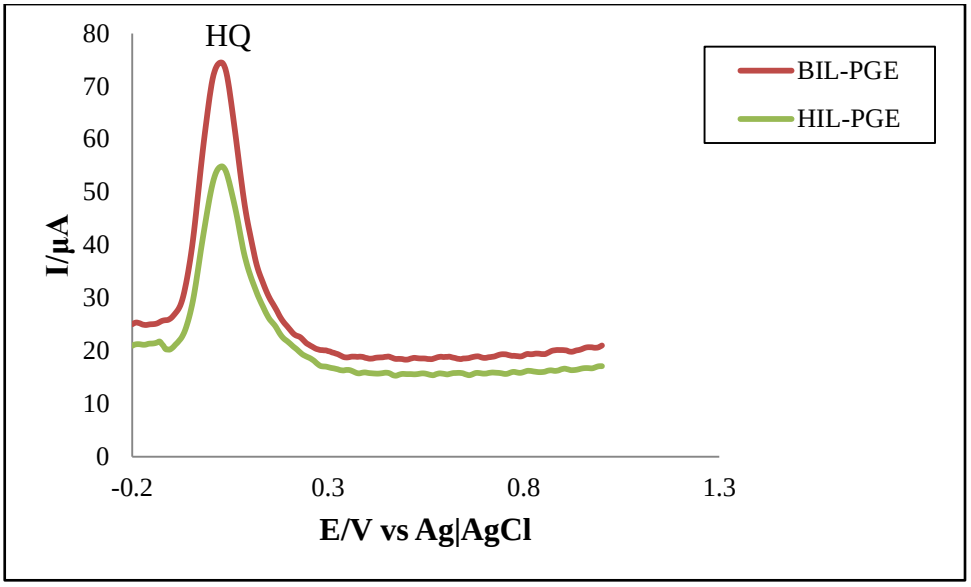

Figure 4.80: Comparison DPV of 5 mM HQ at BIL-PGE and HIL-PGE in PBS at 50 mV/s.

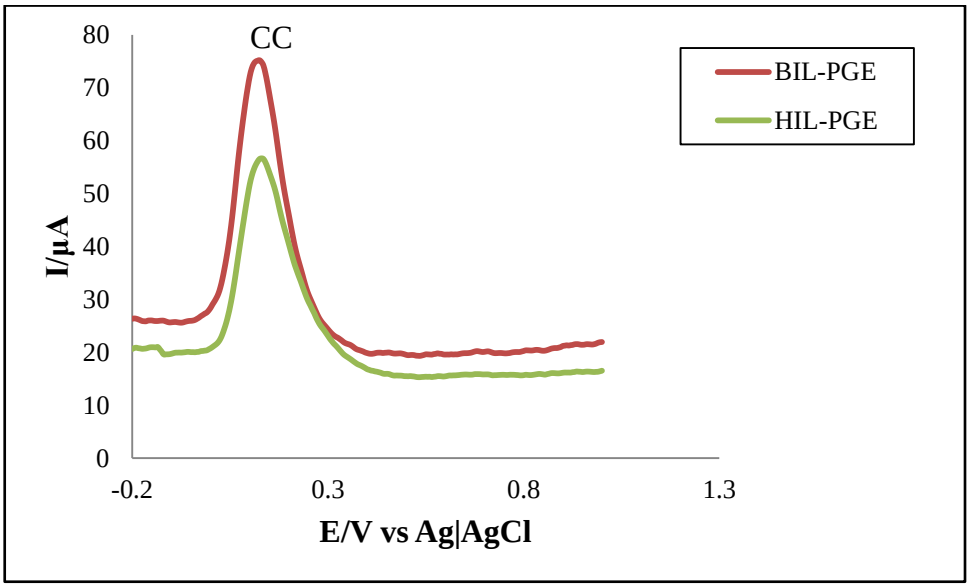

Figure 4.81: Comparison DPV of 5 mM CC at BIL-PGE and HIL-PGE in PBS at 50 mV/s.

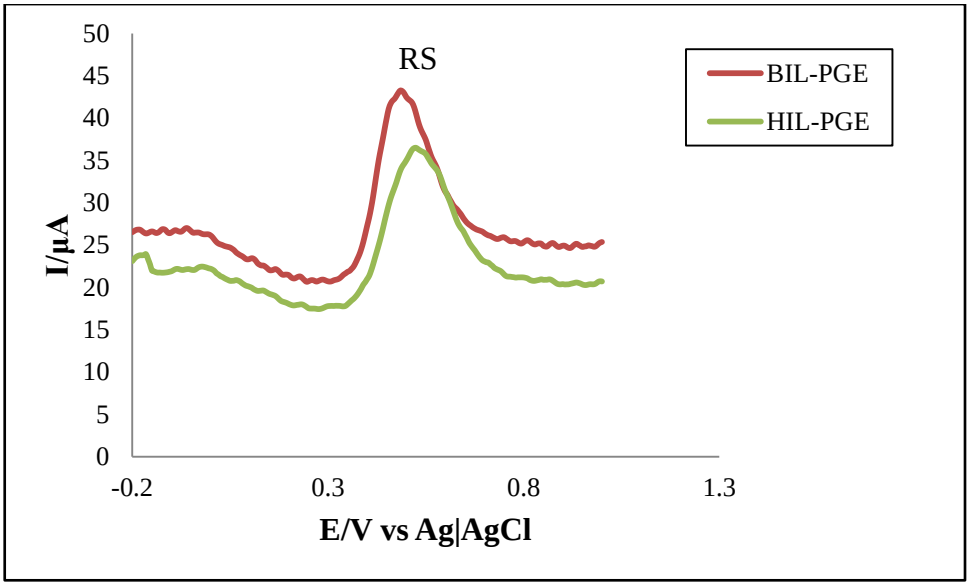

Figure 4.82: Comparison DPV of 5 mM RS BIL-PGE and HIL-PGE in PBS at 50 mV/s.

4.39 Comparison of simultaneous detection of CC and HQ at HIL-PGE and BIL-PGE in PBS by DPV

DPV of a binary mixture of 5 mM of CC and HQ in PBS both at HIL-PGE and BIL-PGE is compared in Figure 4.83. At BIL-PGE the peak current is higher than HIL-PGE. Peak current increased by 3.22 µA for HQ and 3.4 µA for CC.

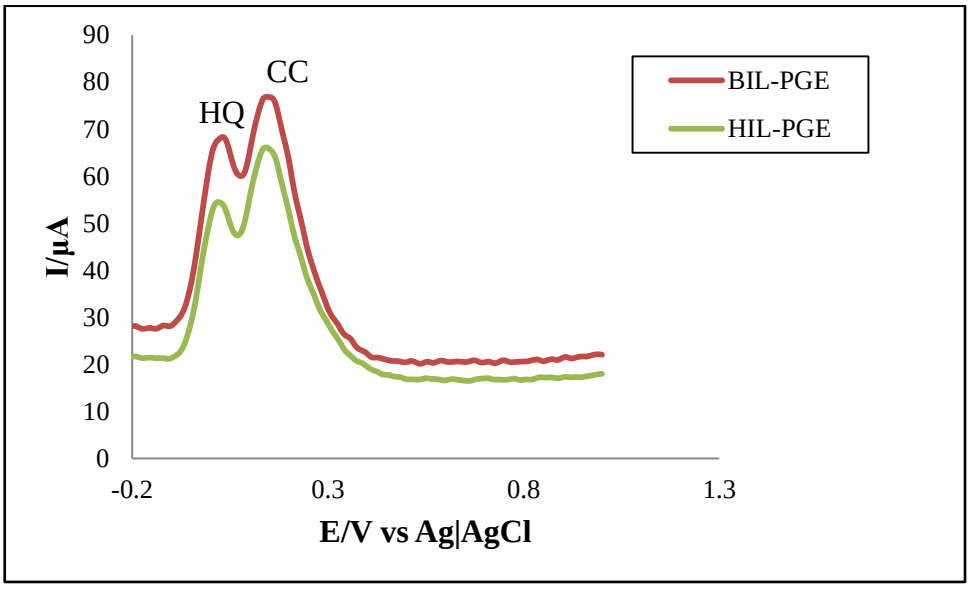

Figure 4.83: Comparison DPV of binary mixture (1:1) of CC and HQ at BIL-PGE and HIL-PGE in PBS at 50 mV/s.

4.40 Comparison of simultaneous detection of CC and RS at HIL-PGE and BIL-PGE in PBS by DPV

DPV of a binary mixture of 5 mM of CC and RS in PBS both at HIL-PGE and BIL-PGE is compared in Figure 4.84. At BIL-PGE the peak current is higher than HIL-PGE. Peak current increased by 15.1 µA for CC and 6.5 µA for RS.

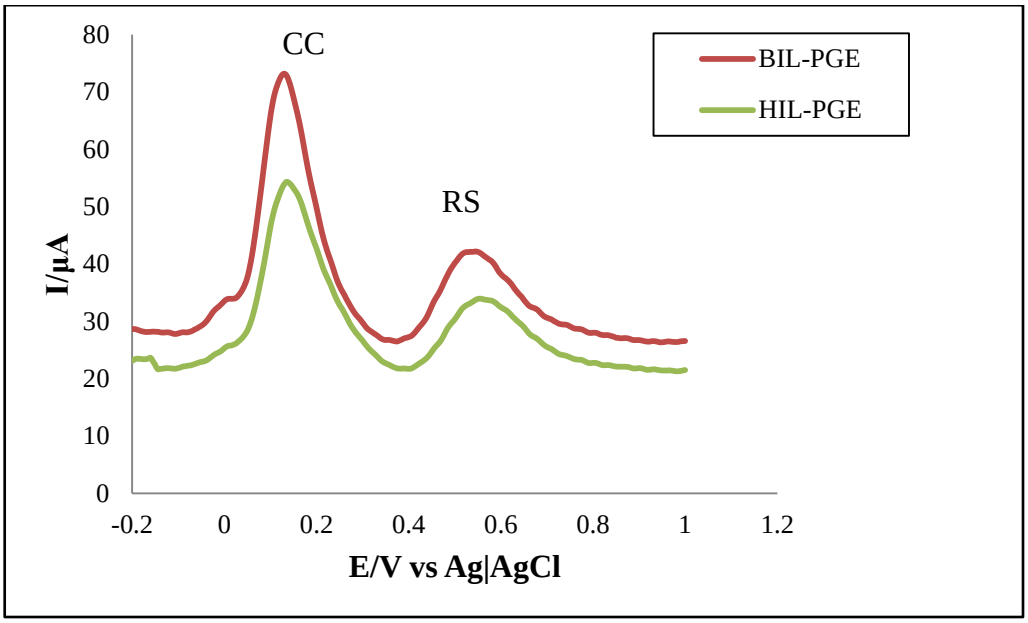

Figure 4.84: Comparison DPV of binary mixture (1:1) of CC and RS at BIL-PGE and HIL-PGE in PBS at 50 mV/s.

4.41 Comparison of simultaneous detection of HQ and RS at HIL-PGE and BIL-PGE in PBS by DPV

DPV of a binary mixture of 5 mM of HQ and RS in PBS both at HIL-PGE and BIL-PGE is compared in Figure 4.85. At BIL-PGE the peak current is higher than HIL-PGE. Peak current increased by 11.14 µA for HQ and 4.6 µA for RS.

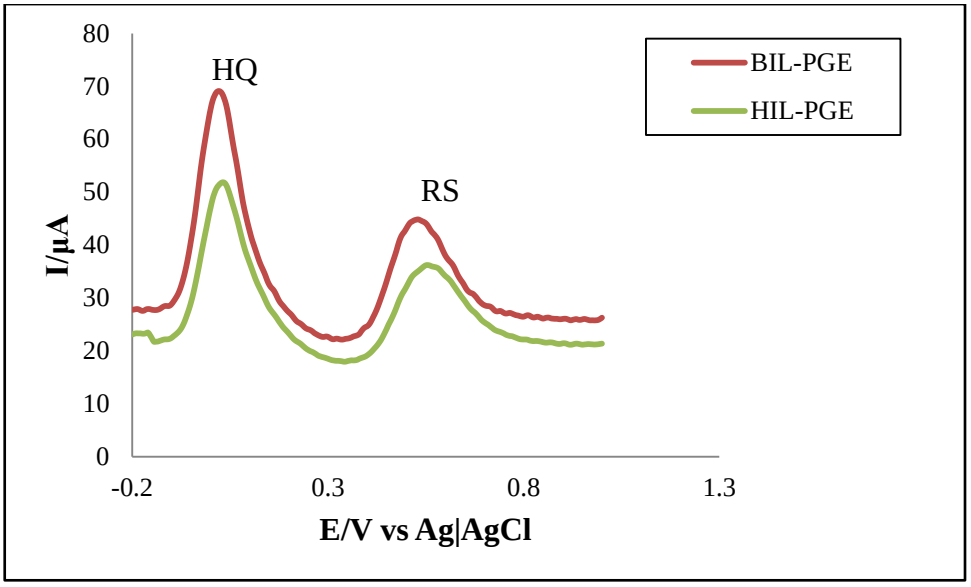

Figure 4.85: Comparison DPV of binary mixture (1:1) of HQ and RS at BIL-PGE and HIL-PGE in PBS at 50 mV/s.

4.42 Comparison of simultaneous detection of CC, HQ and RS at HIL-PGE and BIL-PGE in PBS by DPV

DPV of a ternary mixture of 5 mM of HQ, CC and RS in PBS both at BIL-PGE and HIL-PGE is shown in Figure 4.86. At BIL-PGE the peak current is higher than HIL-PGE. Peak increased 8.45 µA for HQ, 7.7 µA for CC and 5.4 µA for RS.

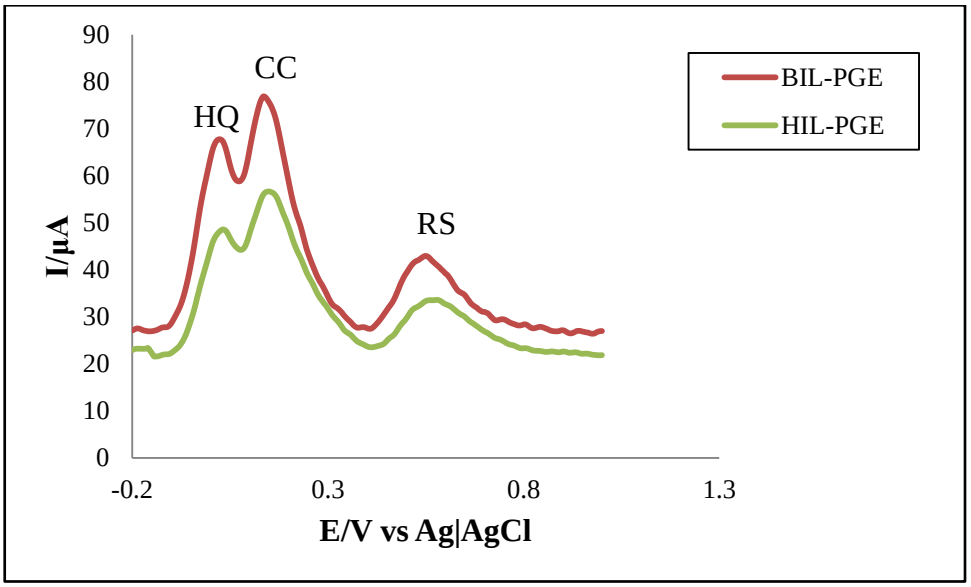

Figure 4.86: Comparison DPV of CC, HQ and RS mixture (1:1:1) at BIL-PGE and HIL-PGE in PBS at 50 mV/s.

4.43 Simultaneous quantitative estimation of RS, HQ and CC in PBS at BIL-PGE

DPV of the ternary mixture of CC, HQ and RS at BIL- PGE in the potential range of -200 mV to +1000 mV in PBS was taken. Concentration of HQ, RS and CC was varied successively by added definite amount of solutions using a micro pipette. The DPV is shown in Figure 4.87. A calibration curve (Figure 4.88) was drawn for different concentrations of CC, HQ and RS. This calibration curve can be used for quantitative estimation of RS, HQ and CC simultaneously from a ternary mixture. In case of HQ the peak current increases approximately +4 μA per mM. In case of CC the peak current increases approximately +5 μA per mM. In case of RS the peak current increases approximately +3.5 μA per mM. The limit of detection (LOD) was calculated by signal-to-noice ratio (S/N=3). The LOD for HQ, CC and RS is 9.09 μML^{-1}, 8.15 $\mu M\ L^{-1}$ and 26.78 $\mu M\ L^{-1}$ respectively in simultaneous detection.

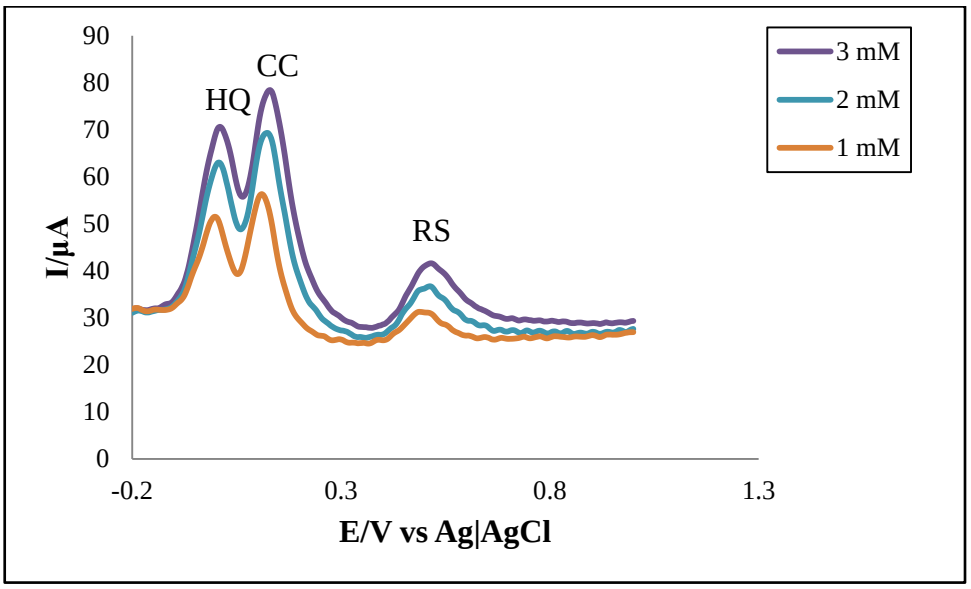

Figure 4.87: DPV for simultaneous quantitative estimation of RS, HQ and CC from a mixture in PBS at BIL-PGE.

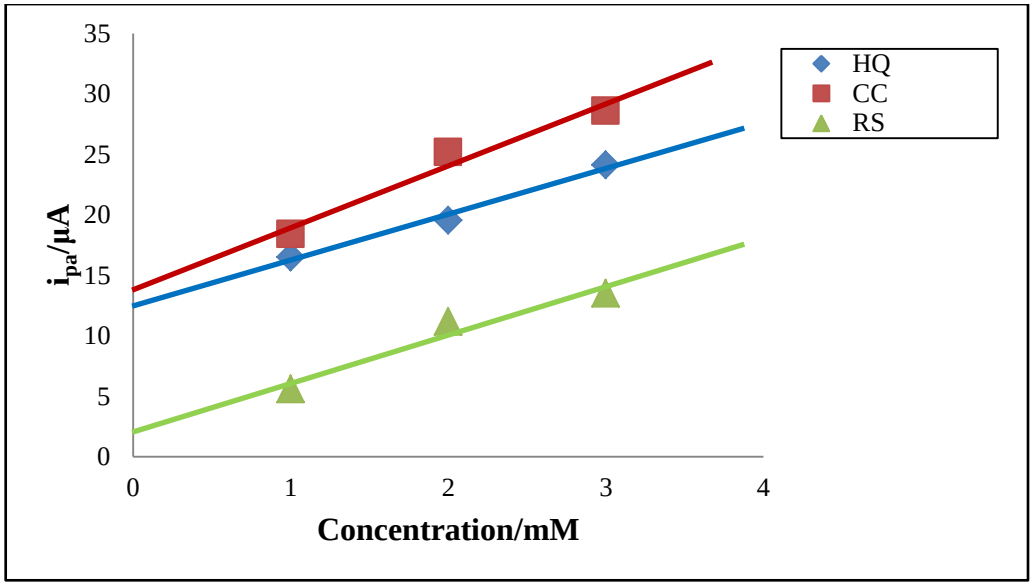

Figure 4.88: Calibration curve for simultaneous estimation of RS, HQ and CC with respect to concentration.

The sensitivity of three isomers was calculated. The sensitivity for HQ is 525.21 µA/mM/cm^2, for CC is 585.68 µA/mM/cm^2 and for RS is 178.0 µA/mM/cm^2 in simultaneous detection. This value of sensitivity is very high. This can be explained by the information of SEM image of the surface of working electrode. There are so many pores and pits, that results increase in surface area of working electrode.

4.44 Price of Conventional electrodes vs PGE

Conventional electrodes, like GCE (15,000/- to 22,000/-), gold electrode (17,000/- to 20,000/-), platinum electrode (17,000/- to 20,000/-), are very expensive and they are not available. Minimum time of getting a mentioned electrode is 3-4 months. Sometimes it needs 6 months even. But PGE is unbelievably cheap (8/- to 10/-) and very available.

4.45 Comparison of HIL-PGE and BIL-PGE

The peak current at BIL-PGE is higher than HIL-PGE but signal-to-noise ratio (S/N=3) at BIL-PGE is higher than HIL-PGE. That's why LOD for HQ, CC and RS is lower at HIL-PGE than BIL-PGE for simultaneous detection. The sensitivity of HQ and RS is higher at BIL-PGE than HIL-PGE and that of CC is higher at HIL-PGE than BIL-PGE.

Chapter V

Conclusions

DHBIs are highly toxic pollutants and coexist in the environment. Simultaneous identification and quantification from their mixture is challenging. UV-Vis spectroscopy, CV and DPV were employed for their simultaneous detection. From the research following conclusions might be pointed out:

UV-Vis spectroscopy couldn't detect and separate DHBIs from the aqueous solution. Facile and cheap technique for the detection of DHBIs was developed. PGE was successfully fabricated from 2B pencil and was characterized by SEM and EDX. Bare PGE couldn't detect or quantify DHBIs unambiguously from their aqueous solutions. Electrochemically modified PGE by IL [HIL or BIL] identified and quantified CC, HQ and RS effectively. HQ, CC and RS showed reversible, quasi-reversible and irreversible behavior respectively at Modified PGE during CV. The anodic peak current versus the concentration of HQ, CC and RS showed a linear relationship and the electrochemical process was diffusion controlled. Positive shift of anodic peak might be due to IR drop in the system. DPV employed more effectual detection and quantification of BHBIs. By using DPV the three peaks of three isomers was detected explicitly in their binary and ternary mixtures. Both HIL-PGE and BIL-PGE could detect DHBIs simultaneously with high sensitivity and considerable detection limit. BIL-PGE gave sharper peaks with more current than HIL-PGE. Modified PGE is at least 2250 times cheaper than conventional GCE.

References

[1] Skoog, D. A. West, D. M., Holler, F. J., and Crouch, S. R., 2014, Fundamentals of Analytical Chemistry, Belmont: Brooks/Cole, Cengage Learning. p. 1. ISBN 0-495-55832-X.

[2] Skoog, D. A. West, D. M., Holler, F. J., and Crouch, S. R., 2007. Principles of Instrumental Analysis. Belmont, CA: Brooks/Cole, Thomson. p. 1. ISBN 0-495-01201-7.

[3] Skoog, D. A. West, D. M. and Holler, F. J., 2014, Fundamentals of Analytical Chemistry, 7th ed^{n}.). Harcourt Brace College Publishers, ISBN 0-03-005938-0.

[4] Kissinger, P., and William R. H., 1996, Laboratory Techniques in Electroanalytical Chemistry, 2nd ed^{n}, Revised and Expanded (2nd ed^{n}.). CRC. ISBN 0-8247-9445-1.

[5] Bard, A. J. and Larry R. F., 2000, Electrochemical Methods: Fundamentals and Applications (2nd ed^{n}.). Wiley. ISBN 0-471-04372-9.

[6] Janata, J., 1989, Principles of Chemical Sensors, Plenum Press, New York, pp. 749.

[7] Kissinger, P. and Heineman, W., 1984, Laboratory Techniques in Electroanalytical Cheistry, Dekker, New York, pp. 749.

[8] Wang, J., 1994, Analytical Electrochemistry, VCH Publishers, New York, pp. 198.

[9] Brett, C. and Brett, A. M. O., 1993, Electrochemistry: Principles, methods and Applications, Oxford University Press, Oxford, pp. 427.

[10] Convington, A. K. (ed^{n}.), 1978, Ion Selective Electrode Methodology, CRC Press, Boca Raton, pp. 150.

[11] Wang, J., and Lu, Z., 1989, "Electrocatalysis and Determination of Hydrazine Compounds at a Glassy Carbon Electrodes Coated with Mixed-Valent Ru (III,II) Cysnide Film", Electroanalysis, Vol. 1, pp. 517.

[12] Gorski, W. and Cox, J., 1994, "Amperometric Determination of N-Nitroamines in Aqueous Solution at an Electrode Coated with a Ru-Based Inorganic Polymer", Anal. Chem., Vol. 66, pp. 2771.

[13] Cai, X., and Kalcher, K., 1994, "Studies on the Electrocatalytic Reduction of Aliphatic Aldehydes on Pd-Modified Carbon Paste Electrodes", Electroanalysis, Vol. 6, pp. 397.

[14] Doherty, A., Forster, R., Smyth, M. and Vos, J., 1991, "Development of a Sensor for the Detection of Nitrite Using a Glassy Carbon Electrode Modified with the Electrocatalyst $[(Os)(bipy)_2(PVP)_{10}Cl]Cl$", Anal. Chim. Acta, Vol. 225, pp. 45.

[15] Fogg, A., Scullion, S., Edmond, T., and Birch, B., 1991, "Direct Reductive Amperoetric Determination of Nitrate at a Copper Electrode Formed In-situ in a Capillary Fill Sensor Device", Analyst, Vol. 116, pp. 573.

[16] Wang, J., Angnes, L., Chen, L. and Evans, O., 1991, "Electrocatalysis and Amperoetric Detection of Organic Peroxides at Modified Carbon Paste Electrodes", Talanta, Vol. 38, pp. 1077.

[17] Gao, Z., Ivaska, A., Pin, L., Kuaizhi, L., and Jianjun, Y., 1992, "Electrocatalysis and Flow Injection Analysis for Hydrogen Peroxide at a Chemically Modified Electrode", Anal. Chem. Acta, Vol. 259, pp. 211.

[18] Baldwin, R., Christensen, J. and Kryger, L., 1986, "Voltammetric Determination of Ni(II) at a Chemically Modified Electrode Based on DMG Containing Carbon Paste", Anal. Chem., Vol. 58, pp. 1790.

[19] Wang, J., and Bonakdar, M., 1998, "Preconcentration and Voltammetric Measureent of Mercury with Crown-Ether Modified Carbon Paste Electrode", Talanta, Vol. 35, pp. 277.

[20] Downward, A., Kipton, H., Powell, J. and Xu, S., 1991, 'Voltammetric Determination of Al using a Chemically Modified Electrode", Alan. Chem, Acta, Vol. 251, pp. 157.

[21] Kalcher, K., 1986, "A New Method for the Voltammetric Deterination of Nitrite", Talanta, Vol. 33, pp. 489.

[22] Cox, J. and Kulesza, P., 1983, "Stripping Voltammetry of Cr(VI) at a Poly(4-vinyl pyridine)-Coated Pt Electrode", Anal. Chem, Acta, Vol. 154, pp. 71.

[23] Ugo, P., Ballarin, B., Daniele, S. and Mazzocchin, A. 1992, "Electrochemical Behavior and Preconcentration of Uranyl(VI) at Nafion-Coated Glassy Carbon Electrodes", J. Electroanal. Chem., Vol. 324, pp. 145.

[24] Gardea, J., Darnall, D., and Wang, J., 1988, "Bioaccumulation and Measurement of Copper at an Alga-Modified Carbon Paste Electrode", Anal. Chem., Vol. 60, pp. 72.

[25] Liu, K., and Abruna, H., 1989, "Electroanalysis of Arometic Aldehydes with Modified Carbon Paste Electrode", Anal. Chem., Vol. 61, pp. 2599.

[26] Sasso, S., Pierce, R., Walla, R., and Yacynych, A., 1990, " Electropolymerized 1,2-Diaminobenzene as a Means to Prevent Interferences and Fouling and to Stabilize Immobilized Enzyme in Electrochemical Biosensor", Anal. Chem., Vol. 62, pp. 1111.

[27] Wang, J., Chen, S., and Lin, M., 1989, "Use of Different Electroploymerization Conditions for Controlling the Size-Exclusion Selectivity at Polyaniline, Polypyrrole and Polyphenol Films", J. Electroanal. Chem., Vol. 273, pp. 231.

[28] Matsue, T., 1993, "Electrochemical Sensors Using Microarray Electrodes", Anal. Chem., Vol. 12, pp. 100.

[29] Bidan, G., 1992, "Electroconducting Polymers: New Sensitive Matrices to Build Up Chemical or Electrocheical Sensors, A Review", Sens. Act. B., Vol. 6, pp. 45.

[30] Ren, W., Luo, H. Q. and Li, N. B., 2006, Biosens. Bioelectron., Vol. 21, pp. 1086.

[31] Ward, T. J., 2002, Anal. Chem., Vol. 74, pp. 2863.

[32] Ding, Y. P., Liu, W. L., Wu, Q. S. and Wang, X. G., 2005, J. Electroanal. Chem., Vol. 575, pp. 275.

[33] De Carvalho, R. M., Mello, C. and Kubota, L. T., 2000, Anal. Chem. Acta, Vol. 420, pp. 109.

[34] Zawisza, I., Bilewicz, R., Luboch, E., and Biernat, J. F., 1999, Electroanal. Chem., Vol. 471, pp. 156.

[35] Wang, X. G., Wu, Q. S. and Ding, Y. P., 2006, Electroanal. Vol. 18, pp. 517.

[36] Duvall, S. H. and McCreery, R. L., 1999, Anal. Chem., Vol. 71, pp. 4594.

[37] Murray, R. W., 1980, Acc. Chem. Res., Vol. 13, pp. 135.

[38] Qi, H. L. and Zhang, C. X., 2005, Electroanal., Vol. 17, pp. 832.

[39] Diab, N., Oni, J. and Schuhmann, W., 2005, Bioelectrochem., Vol. 66, pp. 105.

[40] Deng, C., Li, M., Xie, Q. Liu, M. Tan, Y. Xu, X. and Yao, S., 2006, Anal. Chem. Act., Vol. 557, pp. 85.

[41] Chen, Z., and Zhou, Y., 2006, Surface and Coatings Technology, Vol. 201, pp. 2419.

[42] Pyun, S. and Bae, J. S., 1997, J. Power Sources, Vol. 68, pp. 669.

[43] Sivakumar, C., Nian, J. N. and Teng, H., 2005, J. Power Sources, Vol. 144, pp. 295.

[44] Munoz, E., Heras, M. A., Colina, A. I., Ruiz, V. and Lo'pez-Palacios, J., 2007, Electrochem. Acta, Vol. 52, pp. 4778.

[45] Duvall, S. H. and McCreery, R. L., 1999, Ana. Chem., Vol. 71, pp. 4594.

[46] Urray, R. W., 1980, Acc. Chem. Res., Vol. 13, pp. 135.

[47] Qi, H. L. and Zhanh, C. X., 2005, Electroanal., Vol. 17, pp. 832.

[48] Zawisza, I., Bilewicz, R., Luboch, E. and Biernat, J. Electroanal. Chem., Vol. 471, pp. 156.

[49] Wang, J., Park, J. N., Wei, X. Y. and Lee, C. W., 2003, Chem. Commun., pp. 628.

[50] Russell, I., M. and Burton, S. G., 1999, Anal. Chem. Acta., Vol. 161, pp. 389.

[51] Jagetia, G. C. and Aruma, R., 1997, Toxicol. Lett., Vol. 205, pp. 93.

[52] Schweigert, N., Acero, J. L., Gunten, U. V., Canonica, S., Zehnder, A. J. B. and Eggen, R. I. L., 2000, Environ., Vol. 5, pp. 36.

[53] Irons, R. D., 1985, J. Txicol. Environ. Health., Vol. 16. Pp. 673.

[54] De Carvalho, R. M., Mello, C. and Kubota, L. T., 2000, Anal. Chem. Acta, Vol. 109, pp. 420.

[55] Sun, A., Li, J. and Liu, R., 2006, J. Sep. Sci., Vol. 29, pp. 995.

[56] Qi, H. L. and Zhang, C. X., 2005, Electroanal., Vol. 17, pp. 832.

[57] Bensalah, N., Gadri, A., Canizares, P., Saez, C., Lobato, J. and Rodrigo, M. A., 2005, Environ. Sci. Technol., Vol. 39, pp. 7234.

[58] Xu, Z. A., Chen, X., Qu, X. H. and Dong, S., 2004, Electroanal., Vol. 16, pp. 684.

[59] Carvalho, R. M., Mello, C. L. and Kubota, T., 2000, Anal. Chem. Acta, Vol. 420, pp. 109.

[60] Lunstord, S. K., Ma, Y. L., Galal, A., Striley, C., Zimmer, H. and Mark, Jr. H. B., 1995, Electroanal., Vol. 7, pp. 420.

[61] Zhao, H., Zhang, Y. Z. and Yuan, Z. B., 2002, Electroanal., Vol. 14, pp. 445.

[62] Zhao, H., Zhang, Y. Z. and Yuan, Z. B., 2002, Electroanal., Vol. 14, pp. 1031.

[63] Roy, P. R., saha, M. S., Okajima, T., Park, S. G., Fujishima, A. and Ohsaka, T., 2004, Electroanal., Vol. 16, pp. 1777.

[64] Roy, P. R., Saha, M. S., Okajima, T., and Ohsaka, T., 2004, Electroanal., Vol. 16, pp. 289.

[65] Roy, R. R., Okajima, T. and Ohsaka, T., 2004, J. Electroanal. Chem.,75, pp. 561.

[66] IUPAC Recommendation, 1997, Pure and Appl. Chem., Vol. 69, pp. 132.

[67] Faridbod, F., Ganjali, N. R., Norouzi, P., Riahi, S. and Rashedi, H., (2011), "Application of Room Temperature Ionic Liquids in Electrochemical Sensors and Biosensors, Ionic Liquids: Applications and Perspectives", Prof. Alexander Kokorin (ed^{n}.), ISBN: 978-953-307-248-7.

[68] Singh, V. V., Nigam, A. K., Batra, A., Boopathi, M., Singh, B. and Vijayaraghavan R., 2012, "Applications of Ionic Liquids in Electrochemical Sensors and Biosensors", International Journal of Electrochemistry, Vol. 2012, pp. 1-19.

[69] Holbrey, J.D., and Seddon, K.R. 1999. Ionic liquids. Clean Prod. Proc. 1:223-236.

[70] Rogers, R.D. 2003. Final report: Investigation of room temperature ionic liquids as environmentally benign solvents for industrial separation (TSE99-A). EPA Grant No. R828257. National Center for Environmental Research (NCER), U.S. Environmental Protection Agency (EPA).

[71] Sochor, J., Dobes, J., Krystofova, O., Ruttkay-Nedecky, B., Babula, P., Pohanka, M., Jurikova, T. Zitka, O., Adam, V. and Klejdus, B., 2013, "Electrochemistry as a tool for studying antioxidant properties", Int. J. Electrochem. Sci., Vol. 8, pp. 8464–8489.

[72] Vestergaard, M., Kerman, K. and Tamiya, E, 2005, "An electrochemical approach for detecting copper-chelating properties of flavonoids using disposable pencil graphite electrodes: Possible implications in copper-mediated illnesses", Anal. Chim. Acta,Vol. 538, pp. 273–281.

[73] Briggs, D. E. G., 1999, "Molecular taphonomy of animal and plant cuticles: selective preservation and diagenesis", Philisophical Transactions of the Royal Society B: Biological Sciences, Vol. 354, pp. 7.

[74] Fiegel, H., Voges, H. W., Hamamoto, T., Umemura, S., Iwata, T., Miki, H., Fujita, Y., Buysch, H. J., Gabre, D. and Paulus, W., 2002, "Phenol Derivatives" in Ullmann's Encyclopedia of Industrial Chemistry", Vol. 19, pp. 313.

[75] Barner, B. A., 2004, "Catechol" in Encyclopedia of Reagents for Organic Synthesis (Ed^{n}: L. Paquette), J. Wiley & Sons, New York.

[76] Fahlbusch, K. G., Hammerschidt, F. J. and Panten, J., 2005, "Horst Surburg Flavors and Fragrances" in Ullmann's Encyclopedia of Industrial Chemistry, Wiley-VCH.

[77] Fiegel, H., Voges, H. W., Hamamoto, T., Umemura, S., Iwata, T., 2002, "Phenol Derivatives" in Ullmann's Encyclopedia of Industrial Chemistry", Wiley-VCH.

[78] Joval, E. and Kroger, P. N., 1996, "Hydroquinone: the toxic compound of agaricushondensis", PlantaMedica., Vol. 62, pp. 185.

[79] United States Food and Drug Administration;Skin Bleaching Drug Products for Over-the-Counter Product Use; Proposed Rule, 2006.

[80] Olumide, Y. M., Akinkgbe, A. O., Altraide, D., Mohammad, T. and Ahmefule, N., 2008, International Journal of Dermatology, Vol. 47, pp. 344-53.

[81] Meyer, J., 1897, Ber30, pp. 2569.

[82] Army TM 9-1300-214, pp. 7-12.

[83] Brad, A.J. and Faulkner, L. R., 2001, Electrochemical Methods: Fundaentals and applications, 2nd ed^{n}., John Wiley & Sons, Hobokon, Nj.

[84] Kaifer, A. E. and Gomez, K. M., 1999, Supramolecular Electrochemistry, Wiley-VCH, New York.

[85] Zhang, L. and Lin, X., 2001, Analyst, Vol. 126, pp. 367-370.

[86] Santos, D. P., Fogg, A. G. and Zanoni, B., 2005, Microchem. Acta., Vol. 151, pp. 127-134.

[87] Egerton, F., 2005, Physical Principles of Electron microscopy: An Introduction to TEM, SEM and AEM ray, 1st ed^{n}. Springer.

[88] Yang, P., Wei, W. and Yang, L., 2007, "Simultaneous voltammetric determination of dihydroxybenzene isomers using a poly(acid chrome blue K)/carbon nanotube composite electrode", Microchim Acta, Vol. 157, pp. 229–235.

[89] Wang, L., Huang, P. F., Bai, J. Y., Wang, H. J., Zhang, L. Y. and Zhao, Y. Q., 2007, "Covalent modification of a glassy carbon electrode with penicillamine for simultaneous determination of hydroquinone and catechol", Microchim Acta, Vol. 158, pp. 151–157.

[90] Wang, L., Huang, P. F., Wang, H. J., Bai, J. Y., Zhang, L. Y., Zhao, Y. Q., 2007, "Covalent modification of glassy carbon electrode with aspartic acid for simultaneous determination of hydroquinone and catechol", Annali di Chimica, Vol. 97, pp. 395- 404.

[91] Bai, J., Guo, L., Ndamanisha, J. C. and Qi, B., 2009, "Electrochemical properties and simultaneous determination of dihydroxybenzene isomers at ordered mesoporous carbon-modified electrode", Appl Electrochem, Vol. 39, pp. 2497–2503.

[92] Naranchimeg, O., Kim, S. K. and Jeon, S., 2011, "The Modified Electrode by PEDOP with MWCNTs-Palladium Nanoparticles for the Determination of hydroquinone and Catechol", Bull. Korean Chem. Soc., Vol. 32, No. 8, pp. 2771-2775.

[93] Ahammad, A. J. S., Rahmana, M. M., Xub, G. R., Kim, S. and , Leea, J. J., 2011, "Highly sensitive and simultaneous determination of hydroquinone and catechol at poly(thionine) modified glassy carbon electrode", Electrochimica Acta, Vol. 56, pp. 5266–5271.

[94] Ghoreishi, S. M., Behpour, M., Hajisadeghian, E. and Golestaneh, M., 2012, "Voltammetric determination of resorcinol on the surface of a glassy carbon electrode modified with multi-walled carbon nanotube", Arabian Journal of Chemistry, Vol. 2012, pp. 1-6.

[95] Li, S. J., Xing, Y. and Wang, G. F., 2012, "A graphene-based electrochemical sensor for sensitive and selective determination of hydroquinone", Microchim Acta, Vol. 176, pp. 163–168.

[96] Wang, L., Zhang, Y., Du, Y., Lu, D., Zhang, Y., and Wang, C., 2012, "Simultaneous determination of catechol and hydroquinone based on poly (diallyldimethylammonium chloride) functionalized graphene-modified glassy carbon electrode", Solid State Electrochem, Vol.16, pp. 1323–1331.

[97] Zhou, Y., Ren, X., Sheng, C., Chen, X., Kong, Y., Tao, Y., and Chen, Z., 2012, "Selective determination of hydroquinone in the presence of catechol based on over-oxidized poly(hydroquinone)", Solid State Electrochem, Vol. 16, pp. 3159–3164.

[98] Huang, K. J., Wang, L., Li, J., Yu, M. and Liu, Y. M., 2013, "Electrochemical sensing of catechol using a glassy carbon electrode modified with a composite made from silver nanoparticles, polydopamine, and graphene", Microchim Acta, Vol. 180, pp. 751–757.

[99] Selvakumar, P., Karuppiah, C., Chen, S. M., Yang, C. Y. and Periakaruppan, P., 2014, "Simultaneous and selective electrochemical determination of dihydroxybenzene isomers at a reduced graphene oxide and copper nanoparticles

composite modified glassy carbon electrode", Anal. Methods, Vol. 6, pp. 4271–4278.

[100] Cui, Y. P., Yu Zhu, Y., Li, Y. L., Wang, W. X. and Xu, F., 2014, "Electrochemical behavior of dihydroxybenzene isomers at MWCNTs modified electrode and simultaneous determination in neutral condition", Res Chem Intermed, Vol. 40, pp. 3153–3162.

[101] Liu, W., Wu, L., Zhang, X., and Chen, J., 2014, "Simultaneous electrochemical determination of hydroquinone, catechol and resorcinol at nitrogen doped porous carbon nanopolyhedrons-multiwall carbon nanotubes hybrid materials modified glassy carbon electrode", Bull. Korean Chem. Soc., Vol. 35, pp. 204-210.

[102] Liu, Y., Wang, W., Wei, H., Li, J., Lu, X., and Liu, X., 2014, "Simultaneous determination of dihydroxybenzene isomers based on thionine functionalized multiwall carbon nanotubes modified electrode", Appl. Electrochem, Vol. 44, pp. 667–674.

[103] Li, C., Liu, W., Gu, Y., Hao, S., Yan, X., Zhang, Z. and Yang, M., 2014, "Simultaneous determination of catechol and hydroquinone based on poly(sulfosalicylic acid)/functionalized graphene modified electrode", Appl Electrochem, Vol. 44, pp. 1059–1067.

[104] Wang, J., Shi, Z., Jing, J., Tan, Y., Zhang, S. and Tian, D., "Simultaneous determination of hydroquinone and catechol based on three-dimensionally ordered macroporous polycysteine film modified electrode", Rus. J. Electrochem., Vol. 2015, pp. 1-7.

[105] Alshahrani, L. A., Li, X., Luo, H., Yang, L., Wang, M., Yan, S., Liu, P., Yang, Y. and Li, Q., 2014, "The Simultaneous Electrochemical Detection of Catechol and Hydroquinone with [Cu(Sal-β-Ala)(3,5-DMPz)2]/SWCNTs/GCE", Sensors, Vol. 14, pp. 22274-22284.

[106] Hua, Y. A., Huang, J. Z. , Song, Z. R., Zhang, Y. and Song, L., 2014, "Determination of Hydroquinone and Catechol at a Poly(arginine acid) Modified Electrode", Sens. & Transduce., Vol. 175, pp. 1-5.

[107] Zhang, M., Gan, F. and Cheng, F., 2015, "Preparation of flower-like Pd–graphene composites for simultaneous determination of catechol and hydroquinone", Res Chem Intermed, DOI 10.1007/s11164-015-2056-8.

[108] Foroughi, M. M., Noroozifar, M. and Motlagh, M. K., 2015, "Simultaneous determination of hydroquinone and catechol using a modified glassy carbon electrode by ruthenium red/carbon nanotube", Iran Chem Soc, Vol. 12, pp. 1139–1147.

[109] Zhang, W., Zheng, J., Lin, Z., Zhong, L., Shi, J., Wei, C., Zhang, H., Hao, A. and Hu, S. 2015, "Highly sensitive simultaneous electrochemical determination of hydroquinone, catechol and resorcinol based on carbon dot/reduced grapheme oxide composite modified electrodes", Anal. Methods, Vol. 7, pp. 6089–6094.

[110] Hu, S., Zhang, W., Zheng, J., Shi, J., Lin, Z., Zhong, L., Cai, Wei, C., Zhang, H., and Hao, A., 2015, "One step synthesis cadmium sulphide/reduced graphene oxide sandwichedfilm modified electrode for simultaneous electrochemical determination of hydroquinone, catechol and resorcinol", Anal. Methods, Vol. 5, pp. 18615–18621.

[111] Meng, Z., Zhang, H. and Zheng, J., 2015, "An electrochemical sensor based on titanium oxide– carbon nanotubes nanocomposite for simultaneous determination of hydroquinone and catechol", Res Chem Intermed, Vol. 41, pp. 3135–3146.

[112] Wang, Y., Qu, J., Li, S., Dong, Y. and Qu, J., 2015, "Simultaneous determination of hydroquinone and catechol using a glassy carbon electrode modified with gold nanoparticles, ZnS/NiS@ZnS quantum dots and L-cysteine", Microchim Acta, Vol. 182, pp. 2277–2283.

[113] Wang, X., Xi, M., Guo, M., Sheng, F., Xiao, G., Wu, S. ,Uchiyamab, S. and Matsuurab, H., 2016, "An electrochemically aminated glassy carbon electrode for simultaneous determination of hydroquinone and catechol", Anal. Methods, Vol. 141, pp. 1077–1082.

[114] Hossain, M. U., Rahman, M. T. and Ehsan M. Q., 2015, "Simultaneous Detection and Estimation of Catechol, Hydroquinone, and Resorcinol in Binary and Ternary

Mixtures Using Electrochemical Techniques", Int. J. Anal. Chem., Vol. 2015, pp. 1-8.

[115] Wang, B. and Huang, J. S., 2014, "Using Poly-L-Histidine Modified Glassy Carbon Electrode to Trace Hydroquinone in the Sewage Water", Int. J. Electrochem., Vol. 2014, pp. 1-7.

[116] Xu, G., Tang, B., Jing, S. and Tao, J., 2015, "Simultaneous Determination of Hydroquinone, Catechol and Resorcinol at Poly(3-Thiophenemalonic Acid) Modified Glassy Carbon Electrode", Int. J. Electrochem. Sci., Vol. 10, pp. 10659 – 10667.

[117] Song, Y., Yang, T., Zhou, X., Zheng, H. and Suyeb, S., 2016, "A microsensor for hydroquinone and catechol based on a poly(3,4-ethylenedioxythiophene) modified carbon fiber electrode", Anal. Methods, Vol. 8, pp. 886-892.

[118] Huo, Z., Zhou, Y., Liu, Q., He, X., Liang, Y. and Xu, M., 2011, "Sensitive simultaneous determination of catechol and hydroquinone using a gold electrode modified with carbon nanofibers and gold nanoparticles", Microchim Acta, Vol. 173, pp. 119–125.

[119] Yao, Y., Wen, Y., Xu, J., Zhang, L., Duan, X., Lu, L., and Xia, H., 2014, "Poly(3,4-ethylenedioxythiophene): poly(styrenesulfonate) composite electrode as sensing platform for the simultaneous electrochemical determination of dihydroxybenzene isomers", Monatsh Chem, Vol. 145, pp. 137–146.

[120] Li, S. J., Xing, Y., Deng, D. H., Shi, M. M. and Guan, P. P., 2015, "A comparative study of different types of reduced grapheme oxides as electrochemical sensing platforms for hydroquinone and catechol", Solid State Electrochem, Vol. 19, pp. 861–870.

[121] Wang, S. M., Su, W. Y. and Cheng, S. H., 2010, "A simultaneous and Sensitive Determination of Hydroquinone and Catechol at Anodically Pretreated Screen-Printed CarbonElectrodes", Int. J. Electrochem. Sci., Vol. 5, pp.1649 – 1664.

[122] Yu, Q., Liu, Y., Liu, X., Zeng, X., Luo, S., Wei, W., 2010, "Simultaneous Determination of Dihydroxybenzene Isomers at MWCNTs/b-Cyclodextrin

Modified Carbon Ionic Liquid Electrode in the Presence of Cetylpyridinium Bromide", Electroanal., Vol. 22, No. 9, pp. 1012 – 1018.

[123] She, Y., Tang, Y., Liu, H. and He, P., 2010, "Electrochemical determination of hydroquinone using hydrophobic ionic liquid-type carbon paste electrodes", Chemistry Central Journal, Vol. 4, pp. 1-8.

[124] Sun, X., Hu, S., Li, L., Xiang, J. and Sun, W., 2011, "Sensitive electrochemical detection of hydroquinone with carbon ionogel electrode based on BMIMPF6", J. Electroanal. Chem., Vol. 651, pp. 94–99.

[125] Dong, S., Zhang, P., Yang, Z. and Huang, T., 2012, "Simultaneous determination of catechol and hydroquinone by carbon paste electrode modified with hydrophobic ionic liquid-functionalized SBA-15", Solid State Electrochem, Vol. 16, pp. 3861–3868.

[126] Hu, S., Wang, Y., Wang, X., Xu, L., Xiang, J. and Sun, W., 2012, "Electrochemical detection of hydroquinone with a gold nanoparticle and graphene modified carbon ionic liquid electrode", Sens. and Act. B., Vol. 168, pp. 27– 33.

[127] Ma, L. and Zhao, G. C., 2012, "Simultaneous determination of hydroquinone, catechol and resorcinol at graphene doped carbon ionic liquid electrode", Int. J. Electrochem., Vol. 2012, pp. 1- 8.

[128] Liu, X., Li, Y., Liu, X., Zeng, X., Kong, B., Luo, S. and Wei, W., 2012, "Simple sensor for simultaneous determination of dihydroxybenzene isomers", Solid State Electrochem, Vol. 16, pp. 883–889.

[129] Scientific opinion on the use of resorcinol as a food additive. European Food Safety Authority Journal, 2010, Vol. 8(1), pp. 1411-41.

[130] Skoog, D. A., Holler, F.J. and Nieman, T. A., 2007, Primciples of instrumental analysis. 6th ed^{n}. Thomson Books/Cole, pp. 349-351.

[131] Gooser, Jr. D. K., 1993, Cyclic Voltammetry (Simulation and analysis of reaction mechanisms), Wiely-VCH, Inc.

[132] Hawkridgein, F. M., Kissinger, P. T. and Heieman, W. R. (Eds), 1996, Laboratory Techniques in Electroanalytical chemistry, 2nd ed. Marcel Dekker Inc., New York.

[133] Wang, J., 1994, Analytical Electrochemistry, VCH Publishers Inc, New York.

[134] Brown, E. R. and Large, R. F. in Weissberger, A. and Rossiter, B. (ed^{n}.), 1971, Physical Methods of Chemistry, Vol. 1- Part IIA, Weily-Interscience, New York.

[135] Armada, P. G., Losada, J. and Perez, S. V., 1996, "Cation analysis scheme by differential pulse polarography", Vol. 73, pp. 544-546.

[136] Skoog, D. A., Holler, F. J. and Neiman, T. A., 2007, Principles of Instrumental Analysis, 6th ed^{n}, Thomson Brooks/Cole., pp. 169-173.

[137] Borjesson, J., 2006, Scanning Electron Microscopy.

[138] Agarwal, B.K.,1991, X-ray Spectroscopy, 2nd, ed^{n}, Springer-verlag, Berlin.

[139] Hossain, M. E. and Yousuf, M. A., 2014, "Electrochemical Sensor for Simultaneous Detection and Estimation of Environmental Toxic Pollutants", M. Phil. Thesis, Department of Chemistry, KUET, pp. 65-68, unpublished work.

Appendix I

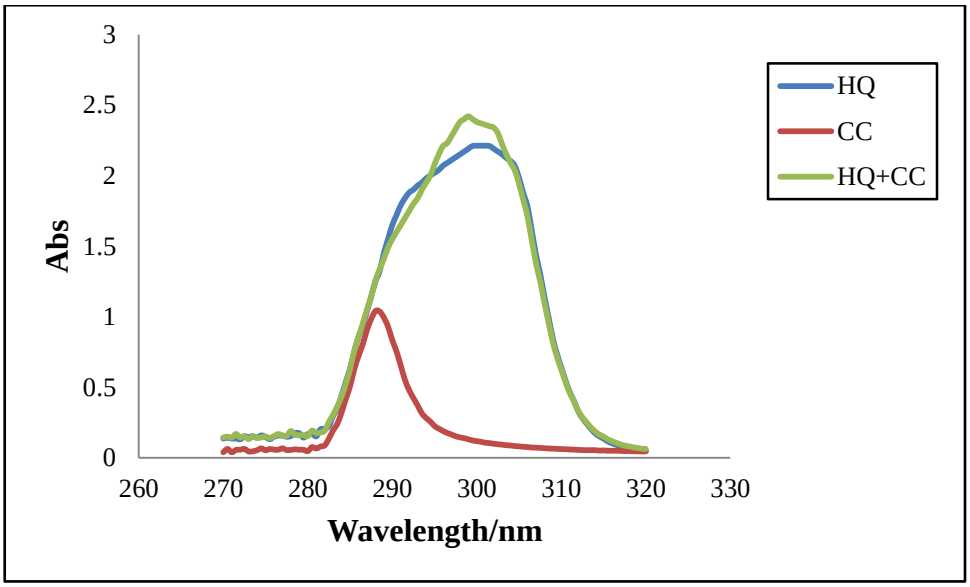

UV-Vis spectra of 10 mM of CC, HQ and binary mixture of CC+HQ in PBS.

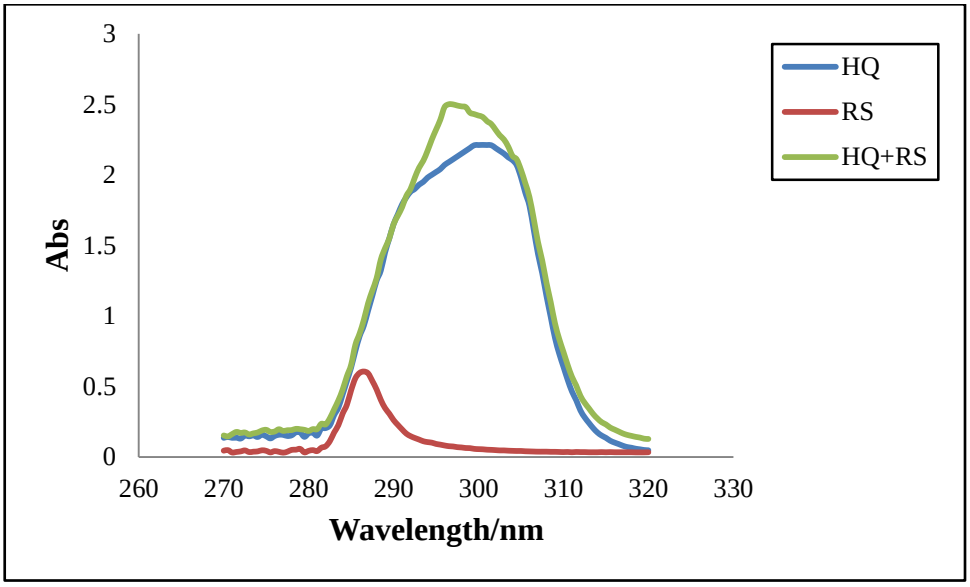

UV-Vis spectra of 10 mM of HQ, RS and binary mixture of HQ+RS in PBS.

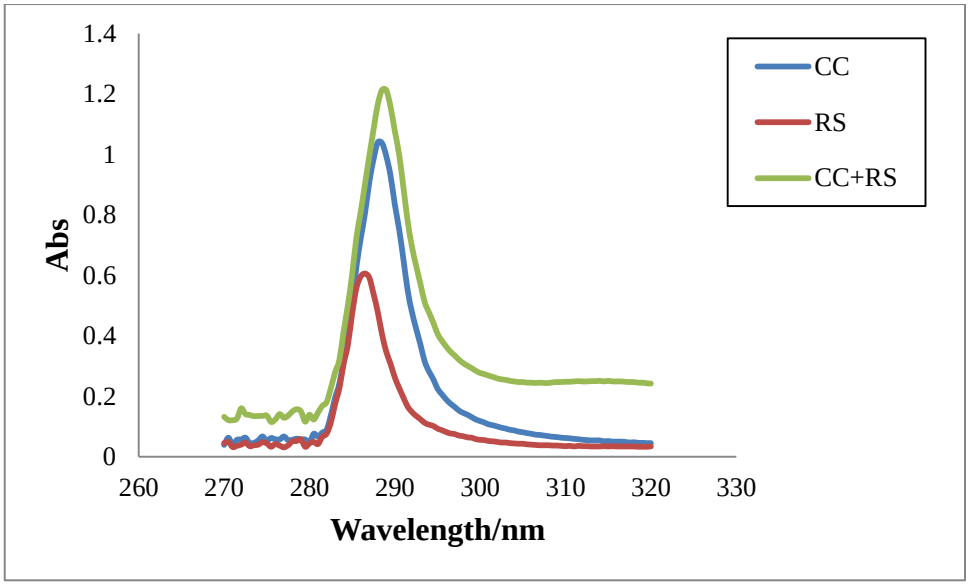

UV-Vis spectra of 10 mM of CC, RS and binary mixture of CC+RS in PBS.

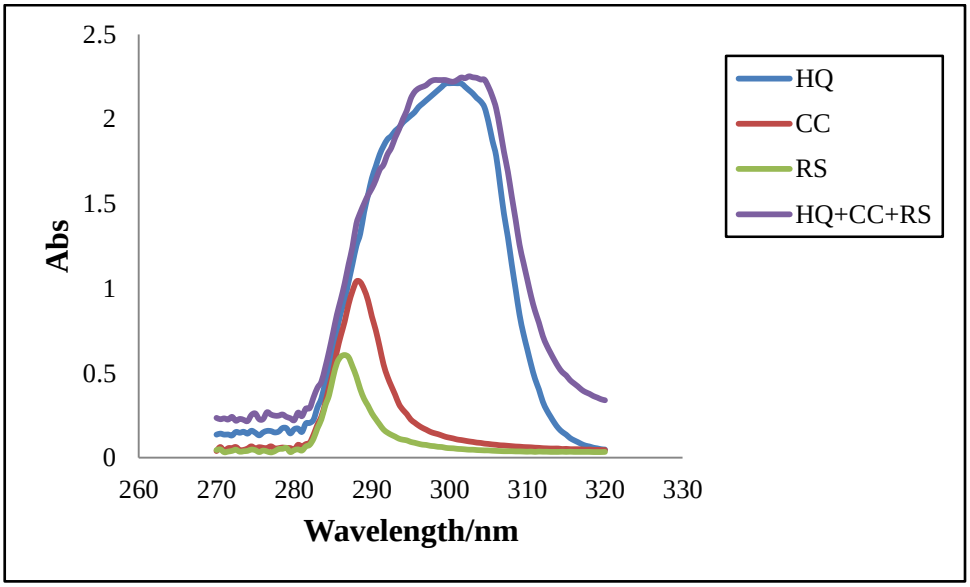

UV-Vis spectra of 10 mM of CC, HQ, RS and mixture of CC+HQ+RS in PBS.